

CCM.FF-K1 for Water Flow

Final Report

Jong S. Paik,¹ Kwang-Bock Lee,¹ Peter Lau,² Rainer Engel,³
Alejandro Loza,⁴ Yoshiya Terao,⁵ Michael Reader-Harris⁶

November, 2006

KRISS

*1 Doryongdong, Yusong Gu, Daejeon 305-340, Korea
jspa@kriss.re.kr*

¹ KRISS, Korea

² SP, Sweden

³ PTB, Germany

⁴ CENAM, Mexico

⁵ NMIJ, Japan

⁶ NEL, U.K.

Table of Content

1	Introduction	2
2	Organization	3
3	Transfer Standard Package (TSP)	4
4	Test Procedure	6
5	Measurement Uncertainty	11
6	Pilot Comparison Tests	12
7	Key Comparison (KC) for Water Flow: CCM.FF-K1	21
7.1.	Description of the TSP for K1	21
7.2.	Technical Protocol	23
8	KC Results	23
8.1.	Reynolds Number Correction	23
8.2.	Results of Participating NMIs	23
8.2.1.	Reproducibility variation	23
8.2.2.	<i>K</i> -factors	26
8.2.3.	Installation effects	26
8.2.4.	KCRVs and NMI-to-KCRV differences	31
8.2.5.	NMI-to-NMI differences	44
9	Summary and Conclusions	74
10	Acknowledgements	75
11	References	75

1 Introduction

In October 1999, the International Committee for Weights and Measures ([CIPM](#)), under authority granted to it by the [Convention of the Metre](#), signed into existence a *Mutual Recognition of National Measurement Standards and of Calibration and Measurement Certificates Issued by National Metrology Institutes* ([CIPM MRA](#)). The goal of the CIPM MRA is to quantify the equivalence of the measurement standards maintained in the world's National Metrology Institutes (NMIs). This quantification is contained in an electronic database, made available through the World Wide Web, which aids in the reduction of measurement-based technical barriers to international trade (see [KCDB](#)).

The strategy of the CIPM MRA is to perform *key comparisons* (KCs) in which participating NMIs can compare their performance through their calibration data [1]. As

a result, the quantification of standards' equivalence, assessed via the routine calibration procedures used by the NMIs, assures buyers and sellers in different countries that the measurements used in their commercial transactions are equivalent within their stated uncertainties. It stands that the economic impact of the quality of the KCs is high and for this reason, the resulting data and the conclusions drawn from it need to be of the highest attainable quality.

This report describes the results obtained during a KC conducted in the area of water flow metrology. This KC, known as [CCM.FF-K1](#), is here described and its results are used to give an indication of the equivalence of the water flow measurement standards maintained by the participating NMIs. In the future, and in accord with the design of the CIPM MRA, these results are to be linked, via additional KCs conducted by the Regional Metrology Organizations (RMOs), so that the equivalence of water flow standards extends to all interested NMIs worldwide. Additionally, CCM.FF-K1 is to be repeated at intervals so that the equivalences are maintained over time.

2 Organization

The Korea Research Institute of Standards and Science ([KRISS](#)), served as pilot laboratory for this KC and five (5) additional NMIs, representing 3 RMOs, participated: for [EUROMET](#): [SP](#) (SE), [PTB](#) (DE), and [NEL](#) (GB); for [SIM](#): [CENAM](#) (MX); and for [APMP](#), [NMIJ](#) (JP) in addition to KRISS (KR).

The comparison was conducted by circulating a *transfer standard package* (TSP) among the participants. As the KC progressed, the TSP traveled from one participant to the next and each NMI was responsible for the customs clearance and delivery of the TSP to the next NMI.

The proposed schedule of CCM.FF-K1 is shown in Table 1, however unexpected circumstances led to a couple of changes. The first change came about when a box containing the TSP's flow meters and pipe pieces was found to be damaged upon arrival to Japan. After visual inspection, the TSP was tested and the resulting data did not show any indication of TSP deterioration. In spite of this, the pilot laboratory decided to perform in-house testing of the TSP before sending it to NEL. The damaged box was replaced by a new one provided by NMIJ prior to sending it to KRISS. This led to a two-week delay and the TSP was shipped to NEL from KRISS on May 3, 2004. The

second change to the schedule occurred when, due to delays in the commissioning of the new water facility at NEL, the comparison was delayed until November, 2004.

3 Transfer Standard Package (TSP)

The aim of CCM.FF-K1 was to compare the national water flow standards as realized in the participating NMIs and this demanded that the KC be conducted at the highest metrological level currently possible. The participants claimed that they could perform water flow measurements with uncertainties of $\pm 0.1\%$ or better. In order to quantify such measurement uncertainties, a stable high precision⁷ TSP and comprehensive KC test procedure were needed. Specifically, the test procedure needed to generate measurements which were statistically sufficient so attain a high confidence level of the desired results.

Table 1. Proposed schedule for CCM.FF-K1.

RMO	NMI	Date	Remark
APMP	KRISS (KR)	16 Sept 03 –15 Oct 03	PILOT Lab
EUROMET	SP (SE)	16 Oct 03 –30 Nov 03	
EUROMET	PTB (DE)	1 Dec 03 –15 Jan 04	
SIM	CENAM (MX)	16 Jan 04 –29 Feb 04	PIVOT Lab
APMP	NMIJ (JP)	1 March 04 –15 Apr 04	
EUROMET	NEL (GB)	16 Apr 04 –31 May 04	PIVOT Lab
APMP	KRISS (KR)	1 June 04 –30 June 04	PILOT Lab
Data Analysis & Report		1 July 04 –15 Aug 04	

To that aim, a TSP comprised of two stable high-precision flow meters was designed so that high confidence could be placed in the results of the KC while allowing the participating NMIs to use their routine capabilities to calibrate the TSP. A third flow meter was included in the package to monitor the flow profile entering the TSP. Figure 1 illustrates the transfer standard package (TSP), which consisted of 3 pipe units of

⁷ **Accuracy of measurement:** closeness of the agreement between the results of a measurement and the true value of the measurand.

NOTES

1 “Accuracy” is a qualitative concept.

2 The term **precision** should not be used for “accuracy”.

Def. 3.5, International Vocabulary of Basic and General Terms in Metrology (VIM), ed. 1993.

0.1016 m in nominal diameter (schedule 40, ANSI 150 lb raised face), 3 flow meters, associated instrumentation and data acquisition system, with a total length of 3.36 m. In this configuration, the 3 flow meters were: (1) ultrasonic flow meter (Changmin Tech, UR-1000), (2) coriolis meter (Endress+Hauser, Promass 83), and (3) turbine meter (Exact Flow, EFM64DR-W-C-T1-B-X0). The coriolis flow meter and the turbine meter were separated by a flow conditioner.

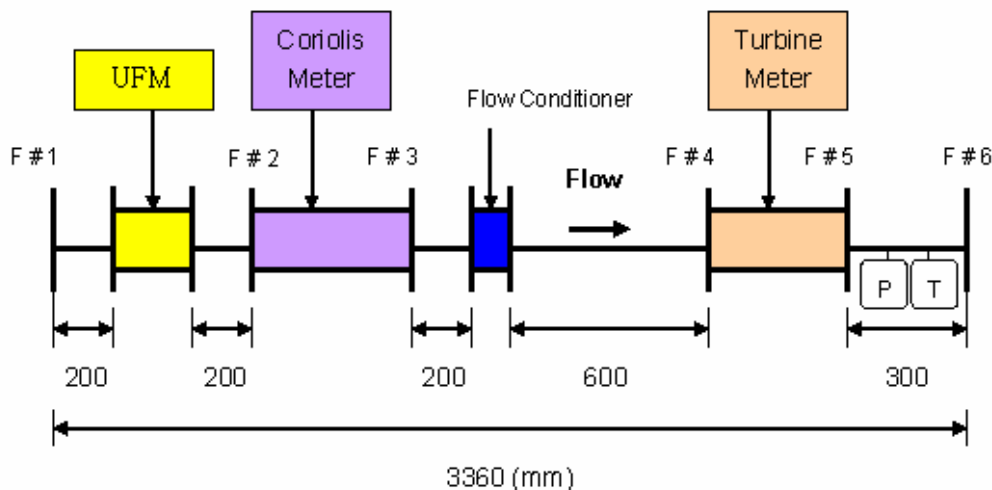


Figure 1. Design of the Transfer Standard Package.

The data acquisition system included with the TSP was only used to set the test flows and monitor the TSP; it was not used by the participating NMI to aid perform any aspect of the calibration. The data acquisition system (data logger and notebook computer) monitored the transfer standard by collecting flow signals from the flow meters, and pressure and temperature transmitters in the TSP.

The KC test procedure was designed to enable the quantification of the TSP performance characteristics [*i.e.*, hysteresis,⁸ repeatability,⁹ reproducibility¹⁰ (turn-on-

⁸ **Hysteresis:** maximum difference between the upscale and downscale readings on the same artifact during a full range traverse in each direction. The standard uncertainty for hysteresis is

$$s_{\text{hysteresis}} = \max |Y_{\text{upscale}} - Y_{\text{downscale}}| / \sqrt{3}.$$

Determining and Reporting Measurement Uncertainties, National Conference of Standards Laboratories RP-12, ed. 1994.

⁹ **Repeatability (of results of measurements):** closeness of the agreement between the results of successive measurements of the same measurand carried out under the same conditions of measurement. *Def. 3.6, International Vocabulary of Basic and General Terms in Metrology (VIM), ed. 1993.*

turn-off and take-out-put-back)] and their separation from those of the NMI calibration system. The NMIs were asked to use their routine procedures, personnel, instruments, software, etc. to calibrate the TSP at the specified test conditions. Details of the test procedure are provided in the next section.

4 Test Procedure

The test procedure for CCM.FF-K1 was designed to yield laboratory comparison results having the lowest reasonably attainable level of uncertainty, because at low levels of uncertainty, the laboratory differences are more clearly quantifiable. This way, not only will the participants be able to understand and agree with the results of the comparison, but also the users of the results (i.e., the international traders) will be able to clearly see and use the conclusions, efficiently and effectively.

To conduct this test in the highly stable way desired, the (TSP) was calibrated according to the same procedure at each participating laboratory using their routine flow meter calibration methods. The two meters in tandem provided redundancy that contributed to the confidence that can be placed on the results obtained. However, flow laboratories do not typically calibrate flow meters in tandem. Thus, in what follows, emphasis is placed on the results obtained from upstream meter since those results are more typical of the data normally obtained in the participating laboratories.

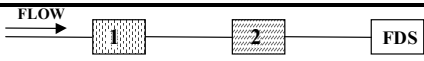
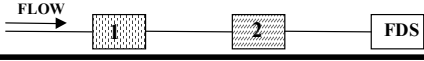
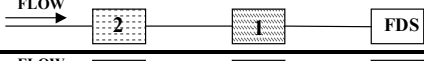
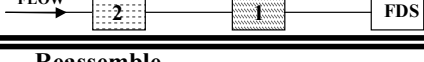
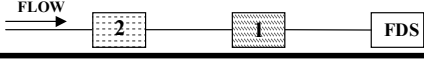
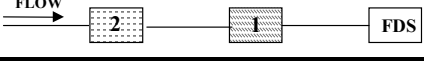
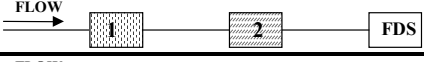
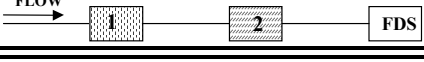
To best compare the participating laboratories, the routine calibration method used at each laboratory was replicated several times according to statistical recommendations. The replications enabled the quantification of the TSP's repeatability⁹ (including hysteresis⁸) and reproducibility¹⁰ under *turn-off-turn-on* (TOTO) conditions. The replications also yielded knowledge pertinent to flow meter performance under changing flow conditions –including cessation of flow– which is pertinent to the use of these instruments in field applications.

During the KC testing, we thought also important to consider an additional type of reproducibility that is not typically considered: the *take-out-put-back* (TOPB) reproducibility. This type of reproducibility accounts for the change in measurement

¹⁰ **Reproducibility (of results of measurements):** closeness of the agreement between the results of successive measurements of the same measurand carried out under changed conditions of measurement. *Def. 3.7, International Vocabulary of Basic and General Terms in Metrology (VIM), ed. 1993.*

conditions that result from the removal of the TSP from the pipeline at the end of each NMI test. In a KC like this one, this type of reproducibility could be significant as the TSP is installed and removed from the calibration pipeline numerous times, each time leading to a slightly different measurement system. If not evaluated, this variation, which is intrinsically contained in the KC data, could then be misinterpreted as NMI-to-NMI variation when it is really a KC feature.

Statistically Sufficient (Swapped) Multiple-Meter Transfer Standard Tests

DAY	Cfg/Tests	FLOWS *	METERING ARRANGEMENT
1	1/A-H&L	ON/ H-L/OFF	
1	1/B-L&H	ON/ L-H/OFF	
1	2/C-L&H	ON/ L-H/OFF	
1	2/D-H&L	ON/ H-L/OFF	
	Disassemble	and	Reassemble
2	2/E-H&L	ON/H-L/OFF	
2	2/F-L&H	ON/L-H/OFF	
2	1/G-L&H	ON/L-H/OFF	
2	1/H-H&L	ON/H-L/OFF	

*At each flow (Re No.), 5 “FDS runs” are done to produce “factors” for meters #1 & #2; “H” and “L” refer to the selected hi and lo test flows; these flows are Cardinal test conditions.

Figure 2. Test procedure.

To quantify the previously mentioned aspects of KC testing, a test procedure was designed (see Figure 2). In this procedure, each of the two flow meters was tested in 4 groups of 5 measurements each at two different flows, on two different days. As a result, this two-day test procedure yields 80 measurements from each flow meter. In our estimation, the four individual sets of 20 measurements (each flow meter tested at the *upstream* or *downstream* positions while operating at *high* or *low* flow) were considered sufficient to adequately estimate the flow meter’s repeatability (including hysteresis), and the TOTO and TOPB reproducibility. As far as the routine laboratory methods of testing was concerned (consider only the flow meter in the upstream position), measurements were obtained using the coriolis flow meter at both flows (1AH, 1AL, 1BL, and 1BH on Day 1) with cessation of flow between them (useful in determining

the TOTO reproducibility). Similar data was also obtained on Day 2 (1GH, 1GL, 1HL, and 1HH) and used to determining the TOPB reproducibility.

Based on the reported characteristics of the flow facilities of the participating NMIs, it was anticipated that the TSP would be tested over a wide range of water temperatures. In fact, several of these NMIs have outdoor facilities that experience temperatures fluctuations from 10 °C to 35 °C, depending on prevailing weather. One way of reducing the effects of such large test temperature differences on KC by setting the flow at the specified Reynolds number,

$$\text{Re} = \frac{D \cdot V}{\nu} \quad (1)$$

where V is the mean flow velocity in the TSP, D is the internal diameter of the TSP, and ν is the kinematic viscosity of the water flowing through the TSP. In (1) we assume the diameter, D , to expand with temperature, T , according to

$$D = D_0 [1 + \alpha(T - T_0)] \quad (2)$$

where α is the linear thermal expansion coefficient, and the subscript 0 refers to a reference condition. In this analysis we selected to neglect the diametric variation of the TSP with pressure.

In spite of the use of this approach for setting testing flows (also known as *cardinal test points*), the temperature fluctuations could affect the measurement principle of the flow meters themselves and appear as NMI to NMI differences in the results of the KC. To avoid that, we selected flow meters having measurement principles known to have low temperature dependency.

At each cardinal test point, the NMIs were asked to determine, using their normal flow meter calibration procedures, the K -factors for the two flow meters. That is,

$$K_V = N/V \quad (3)$$

for the turbine meter and,

$$K_M = N/m \quad (4)$$

for the coriolis meter. In (3) and (4), V and m are the volume and mass of water which passed through the flow meters, respectively, in the time required for the flow meters to

generate N pulses (note that N for the turbine meter may be different from N for the coriolis meter).

The cardinal test points used for this KC were selected to reside in the relatively flat regions of the performance curves for these flow meters (*i.e.*, portions of the response curve of the meters where the K -factor does not significantly change as a function of the Reynolds number). This selection reduced the need to perfectly match the Reynolds number between laboratories. However, we found during testing that the equilibrated flow conditions slightly deviated from the target Reynolds number and to correct for these deviations, the measurements from each NMI were used to produce an estimate of the slope of the response curve of the meters, thus enabling the projection of the measurements to the cardinal test points. This method enhanced both the averaged results for K -factors and reduced the scatter of results due to “off cardinal test points” tests. Thus adjusted results for both meters, in both positions, are hereafter used.

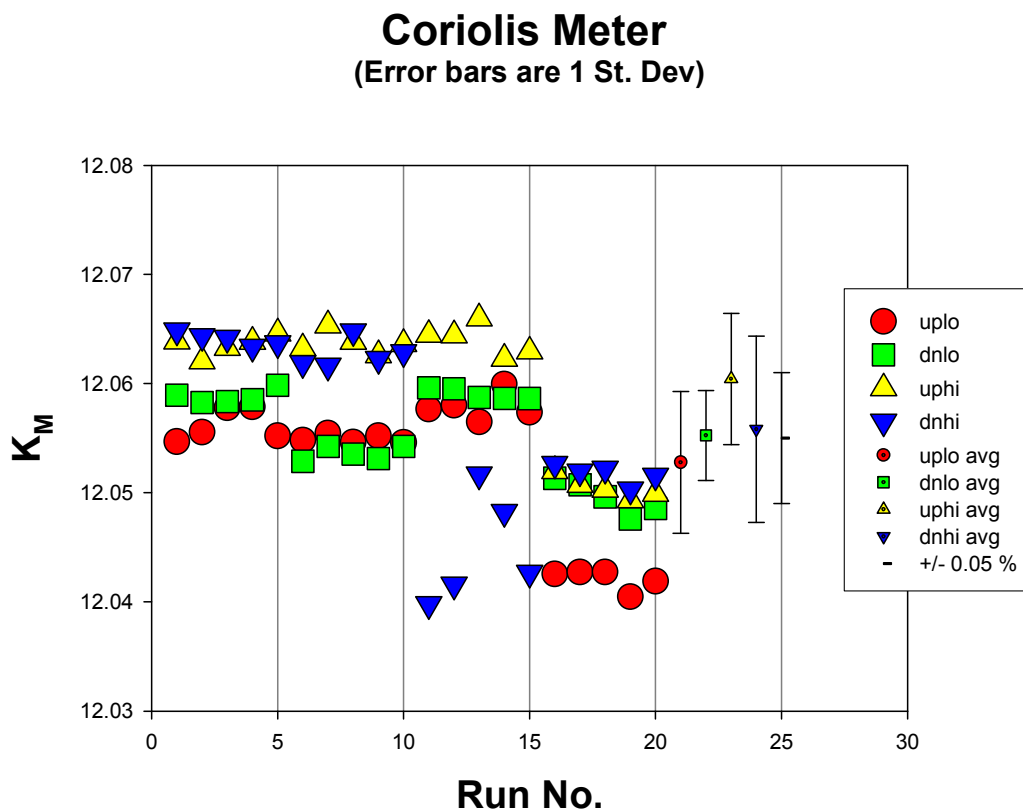


Figure 3. Reproducibilities of coriolis meter in 4 flow conditions. Data taken at KRISS. *uplo*: meter in the upstream position while operating at low flow conditions; *dnlo*: downstream-low flow; *uphi*: upstream-high flow; *dnhi*: downstream-high flow.

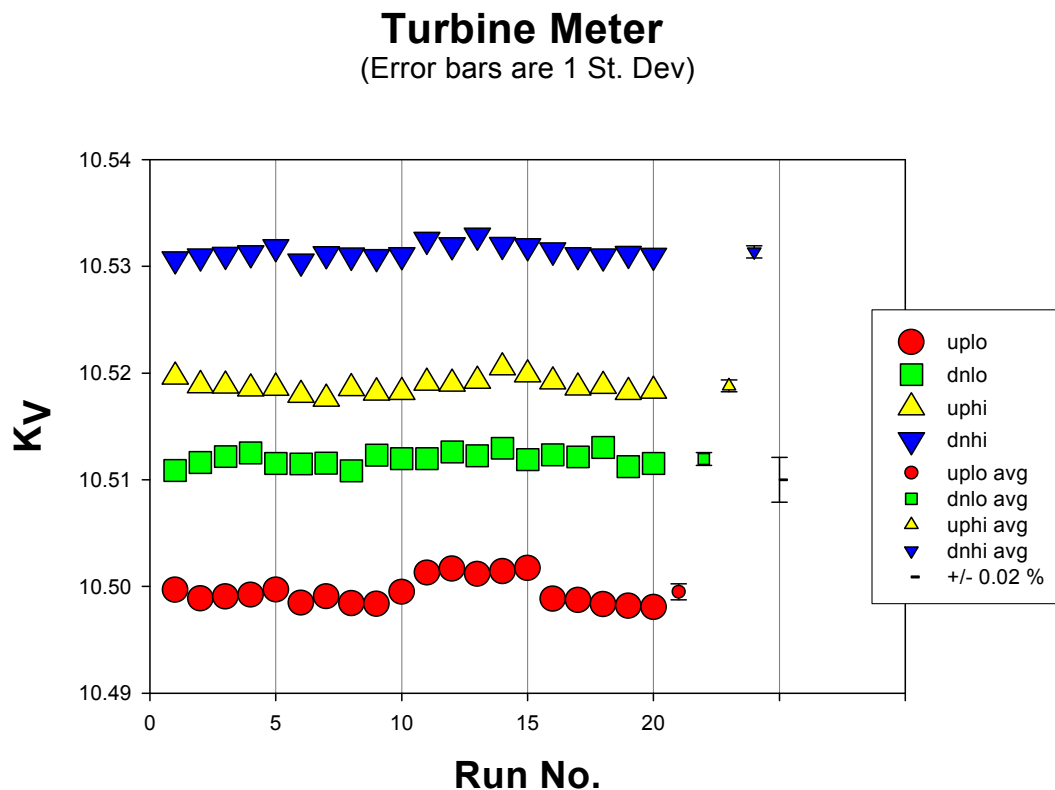


Figure 4. Reproducibilities of turbine meter in 4 flow conditions. Data taken at KRISS. *uplo*: meter in the upstream position while operating at low flow conditions; *dnlo*: downstream-low flow; *uphi*: upstream-high flow; *dnhi*: downstream-high flow.

Results obtained at the pilot laboratory for the test produce described above are shown in Figure 3 and Figure 4. In these figures, the K -factor is shown in the ordinate and the number of the measurement is shown in the abscissa. The results can be used to obtain four independent determinations of the repeatability of the flow meters (each using groups of 5 measurements, *i.e.*, 1-5, 6-10, 11-15, and 16-20), two independent determinations of the TOTO reproducibility (using measurements 1-10 and 11-20), and a determination of the TOPB reproducibility (using measurements 1-20). Averaged values for the 20 measurements (with 1 standard deviation error bars) are shown in the right-hand-side of both figures and $\pm 0.05\%$ (Figure 3) or $\pm 0.02\%$ (Figure 4) scatter are shown.

Figure 3 shows that the repeatability (with hysteresis) of the coriolis meter is relatively low as compared to its TOTO and TOPB reproducibility. In Figure 4 we can see that the repeatability and reproducibility of the turbine meter are far better than those obtained from the coriolis flow meter, which are shown in Figure 3.

5 Measurement Uncertainty

The uncertainties of the K -factors, $u(K_j)$, ($j=1$ for the coriolis meter and $j=2$ for the turbine meter respectively), may be expressed as equations (5) and (6).

$$u(K_1) = u(K_M) = \left[\left(\frac{\partial K_M}{\partial m} \right)^2 u^2(m) + \left(\frac{\partial K_M}{\partial N} \right)^2 u^2(N) \right]^{1/2} \quad (5)$$

$$u(K_2) = u(K_V) = \left[\left(\frac{\partial K_V}{\partial V} \right)^2 u^2(V) + \left(\frac{\partial K_V}{\partial N} \right)^2 u^2(N) \right]^{1/2} \quad (6)$$

in which m and V are mass and volume of water passing through flow meters respectively, and N is the number of pulses generated from the meters (not necessarily the same number for both flow meters). The uncertainty values of K -factors are obtained from uncertainty budgets of participating NMIs.

During testing, when a single flow meter was calibrated using the flow standard at a particular NMI, the replications at each test condition enabled calculations of standard deviations and variances. These standard deviations and variances include contributions from the “meter” being calibrated and from the standard, or the “system”, and it should be noted that these two contributions cannot be separated. However, when the two meters were calibrated simultaneously in tandem – as described above – it is then feasible to separate the variance contributions from “meter” and “system”, using the following numerical technique.

After the K -factors from each of the simultaneously calibrated flow meters are averaged as follows:

$$\bar{K}_j = \frac{\sum_{i=1}^N K_{1j}}{N} \quad (7)$$

the variances are give by:

$$s^2(K_j) = \left[\frac{1}{N-1} \sum_{i=1}^N (K_{ji} - \bar{K}_j)^2 \right] \quad \text{in which } j = 1, \text{ and } 2 \quad (8)$$

and the correlation coefficient for the simultaneously determined meter factors are given by:

$$r_{12} = \frac{\sum_{i=1}^N (K_{1i} - \bar{K}_1)(K_{2i} - \bar{K}_2)}{\left\{ \left[\sum_{i=1}^N (K_{1i} - \bar{K}_1)^2 \right] \left[\sum_{i=1}^N (K_{2i} - \bar{K}_2)^2 \right] \right\}^{1/2}} \quad (9)$$

where the variances of means of K -factors are estimated by,

$$s^2(\bar{K}_j) = s^2(K_j) / 20 \text{ in which } j = 1 \text{ and } 2 \quad (10)$$

Since the coriolis meter and the turbine meter were tested in tandem, the meter factors of these flow meters are correlated. As the variance, $s^2(\bar{K}_j)$, is sum of the meter variance and the system variance, then if correlated portion can be attributed to the common source to both flow meters, *i.e.*, the “system”, then the following is true:

$$r_{1,2} = s^2(\bar{K}_j)_{system} / s^2(\bar{K}_j) \quad (11)$$

$$s(\bar{K}_j)_{system} = \pm \sqrt{|r_{1,2}| \cdot s^2(\bar{K}_j)} \quad (12)$$

$$s(\bar{K}_j)_{meter} = \pm \sqrt{(1 - |r_{1,2}|) \cdot s^2(\bar{K}_j)} \quad (13)$$

It follows that the combined uncertainty for the meter factor, $u_c(K_j)$, of the measurement is given by,

$$u_c(K_j) = \left[u^2(K_j) + u^2(K_j)_{system} \right]^{1/2} \quad (14)$$

6 Pilot Comparison Tests

The pilot comparison performed among the pilot laboratory (KRISS-Korea) and pivot laboratories (CENAM-Mexico and NEL-UK), provided information on the multi-lab reproducibility of the measurement system (*i.e.*, the TSP and the test procedure). During these tests, the flow meters were: (i) a coriolis meter manufactured by Endress+Hauser (model Promass 80FD1600), and (ii) a turbine meter manufactured by Exact Flow (model EFM64DR-W-C-T1-B-X0 1007).

Any changes in flow meter performance associated with transportation of the TSP during travel in between laboratories were an important concern to this key comparison

and were considered as part of the pilot comparison tests. In order to check the change in flow meter performance due to travel, a final set of tests was performed at the pilot laboratory after the tests at NEL; hereafter these results are labeled as KRISS-Check.

The mean test temperatures of the initial test performed at KRISS, as well as of the KRISS-Check tests, were 20.4 °C and 26.5 °C respectively. The average coriolis meter K_M (mass flow rate base K -factor) and the average turbine meter K_V (volume flow rate base K -factor) for 4 different flow conditions for each NMI are shown in Table 2 and Table 3 with their corresponding uncertainties; the same data is illustrated in Figure 5 through Figure 12. In what follows, the medians of the average K_M and K_V were chosen as reference values. In the figures, the red dashed lines indicate $\pm 0.07\%$ uncertainty limits from the median. It can be seen that the average K_M and K_V values of participating NMIs at different flow conditions did not deviate from the median values by more than $\pm 0.07\%$. Also shown in the data are the test temperatures, which ranged from 14 °C to 27 °C, but their effects appear not significant in the results.

Table 2. Pilot comparison results, K_M and K_V , of meters in upstream.

NMI	cuphi ¹¹		tuphi ¹²	
	x_{cuphi} , [1/kg]	$U(x_{\text{cuphi}})$, [1/kg]	x_{tuphi} , [1/L]	$U(x_{\text{tuphi}})$, [1/L]
KRISS	12.0606	0.0064	10.5192	0.0075
CENAM	12.0452	0.0025	10.5125	0.0055
NEL	12.0434	0.0052	10.5176	0.0059
KRISS-Check	12.0601	0.0066	10.5210	0.0075
	cuplo ¹³		tuplo ¹⁴	
	x_{cupho} , [1/kg]	$U(x_{\text{cupho}})$, [1/kg]	x_{tupho} , [1/L]	$U(x_{\text{tupho}})$, [1/L]
KRISS	12.0528	0.0039	10.4996	0.0058
CENAM	12.0457	0.0021	10.4939	0.0056
NEL	12.0528	0.0030	10.4944	0.0059
KRISS-Check	12.0551	0.0043	10.5011	0.0062

¹¹ Coriolis meter in upstream at the high cardinal Reynolds number.

¹² Turbine meter in upstream at the high cardinal Reynolds number.

¹³ Coriolis meter in upstream at the low cardinal Reynolds number.

¹⁴ Turbine meter in upstream at the low cardinal Reynolds number.

Table 3. Pilot comparison results, K_M and K_V , of meters in downstream.

NMI	cdnhi ¹⁵		tdnhi ¹⁶	
	x_{cdnhi} , [1/kg]	$U(x_{\text{cdnhi}})$, [1/kg]	x_{tdnhi} , [1/L]	$U(x_{\text{tdnhi}})$, [1/L]
KRISS	12.0558	0.0064	10.5318	0.0079
CENAM	12.0488	0.0018	10.5228	0.0056
NEL	12.0539	0.0036	10.5252	0.0059
KRISS-Check	12.0616	0.0060	10.5327	0.0075
	cdnlo ¹⁷		tdnlo ¹⁸	
	x_{cdnho} , [1/kg]	$U(x_{\text{cdnho}})$, [1/kg]	x_{tdnho} , [1/L]	$U(x_{\text{tdnho}})$, [1/L]
KRISS	12.0553	0.0040	10.5121	0.0060
CENAM	12.0467	0.0019	10.5045	0.0056
NEL	12.0444	0.0030	10.5006	0.0059
KRISS-Check	12.0575	0.0040	10.5121	0.0063

¹⁵ Coriolis meter in downstream at the high cardinal Reynolds number.

¹⁶ Turbine meter in downstream at the high cardinal Reynolds number.

¹⁷ Coriolis meter in downstream at the low cardinal Reynolds number.

¹⁸ Turbine meter in downstream at the low cardinal Reynolds number.

Coriolis Meter Upstream @ High Flow Rate

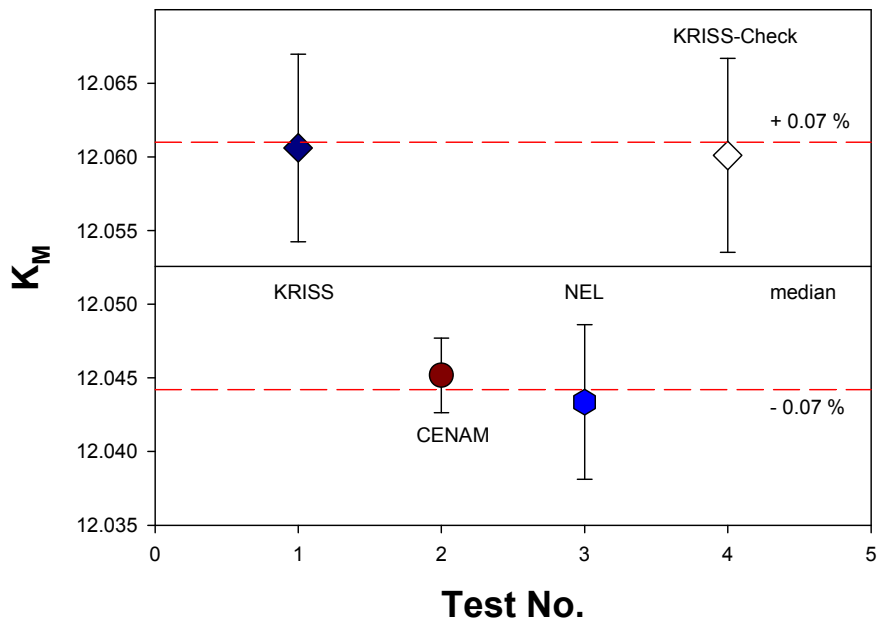


Figure 5. Averaged values of K_M for of the coriolis meter in the upstream position at high flow.

Coriolis Meter Upstream @ Low Flow Rate

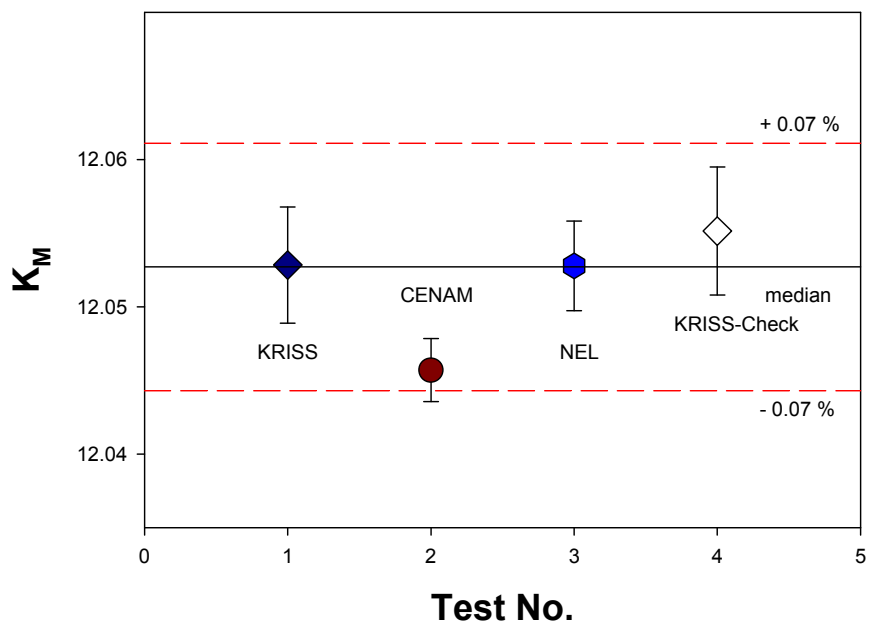


Figure 6. Averaged values of K_M for the coriolis meter in upstream position at low flow.

Turbine Meter Upstream @ High Flow Rate

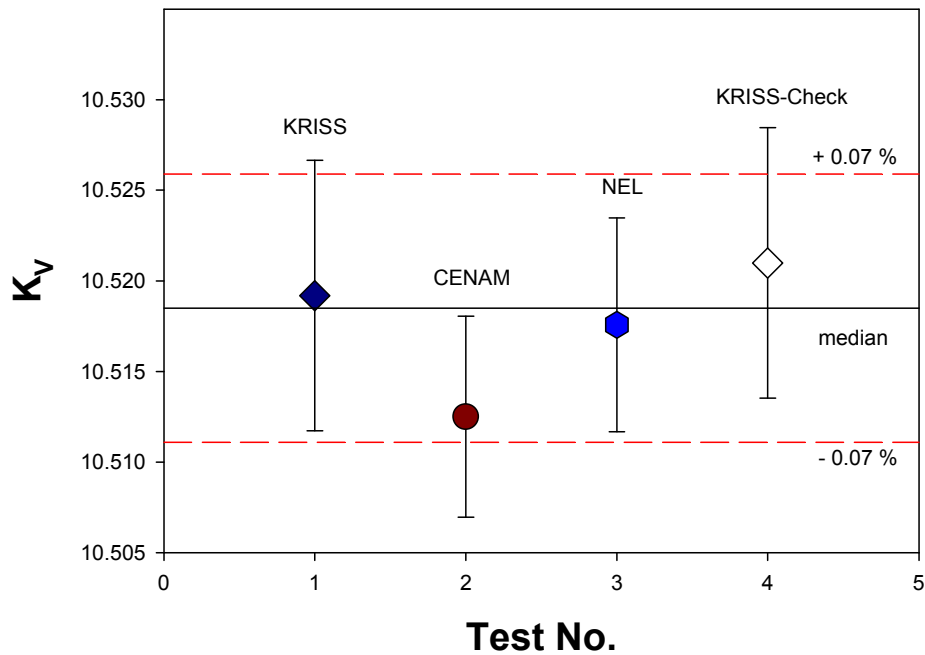


Figure 7. Averaged values of K_V for the turbine meter in upstream position at high flow.

Turbine Meter Upstream @ Low Flow Rate

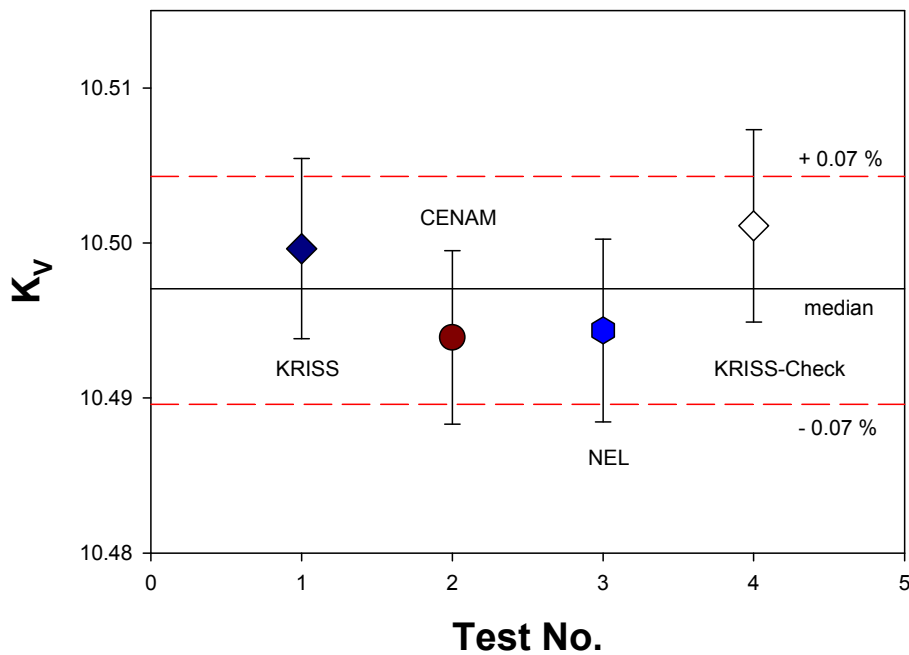


Figure 8. Averaged value of K_V for the turbine meter in upstream position at low flow.

Coriolis Meter Downstream @ High Flow Rate

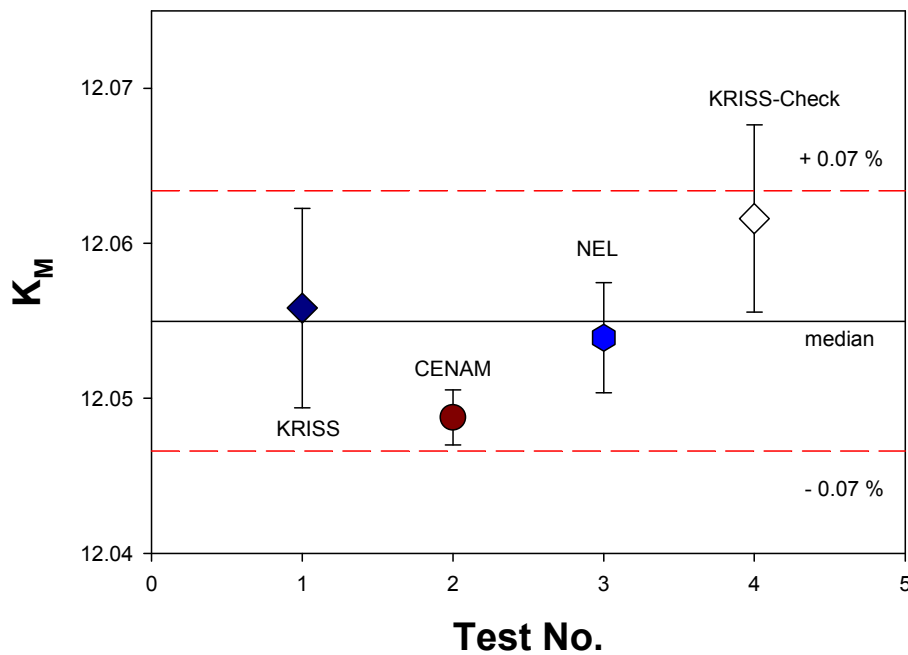


Figure 9. Averaged values of K_M for the coriolis meter in downstream position at high flow.

Coriolis Meter Downstream @ Low Flow Rate

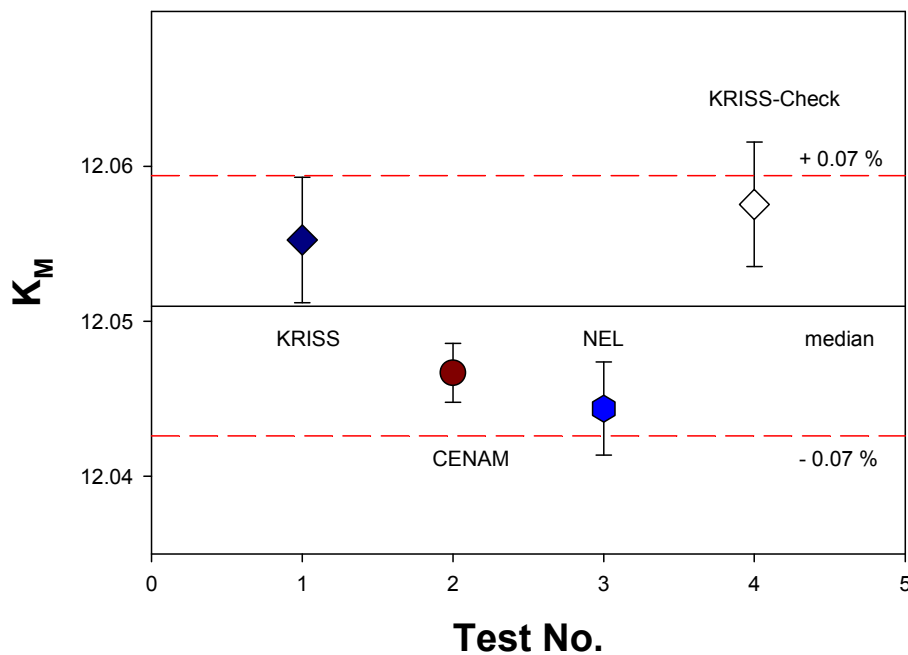


Figure 10. Averaged values of K_M for the coriolis meter in downstream position at low flow.

Turbine Meter Downstream @ High Flow Rate

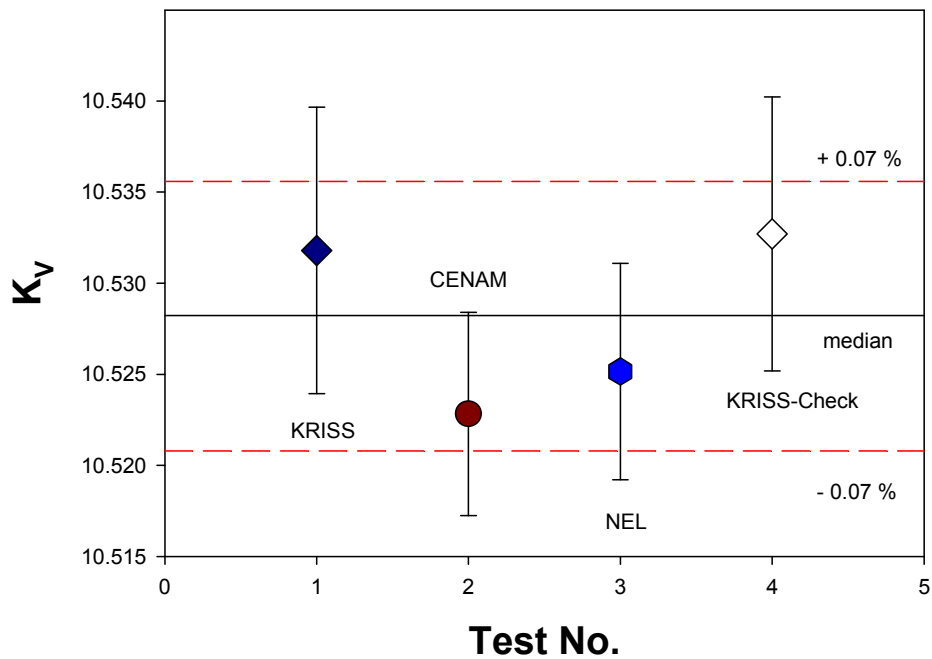


Figure 11. Averaged values of K_V for the turbine meter in downstream position at high flow.

Turbine Meter Downstream @ Low Flow Rate

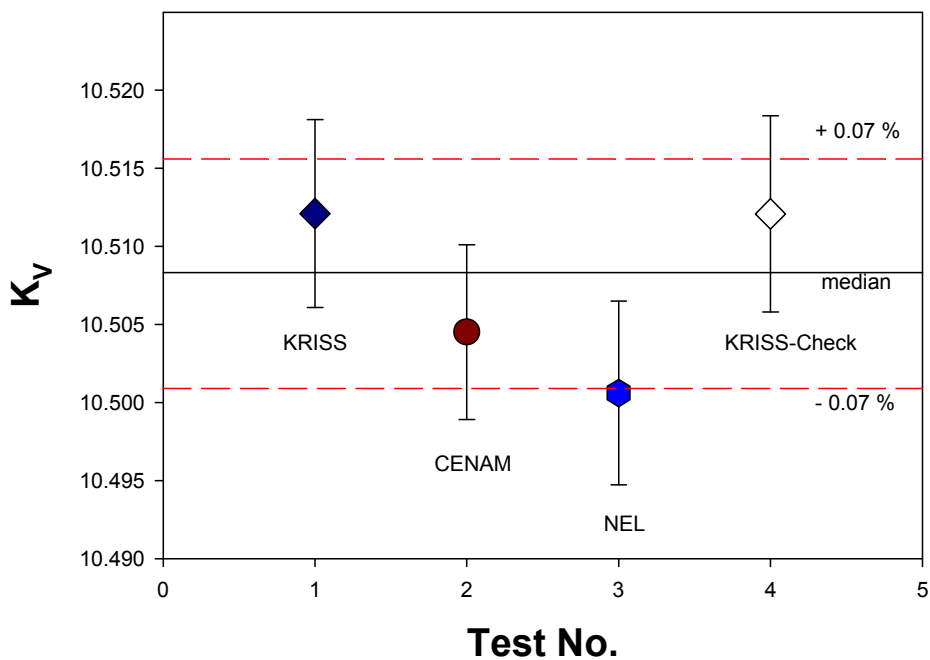


Figure 12. Averaged values of K_V for the turbine meter in downstream position at low flow.

The variation in the reproducibility of the coriolis and turbine meter during the pilot comparison are shown in Figure 13 through Figure 16. These values (here given in 1-standard deviation) were determined according to (13). For the turbine meter, the reproducibility did not exceed 0.03 %, but for the coriolis meter, the values reached about 0.2 % when the meter was in the upstream position at the high flow. Outliers among the coriolis meter data at NEL in upstream position at high flow yielded about four times larger reproducibility than those seen in the other laboratories. But, in the absence of outliers, the reproducibility of the coriolis meter was less than 0.08 % for all four flow conditions.

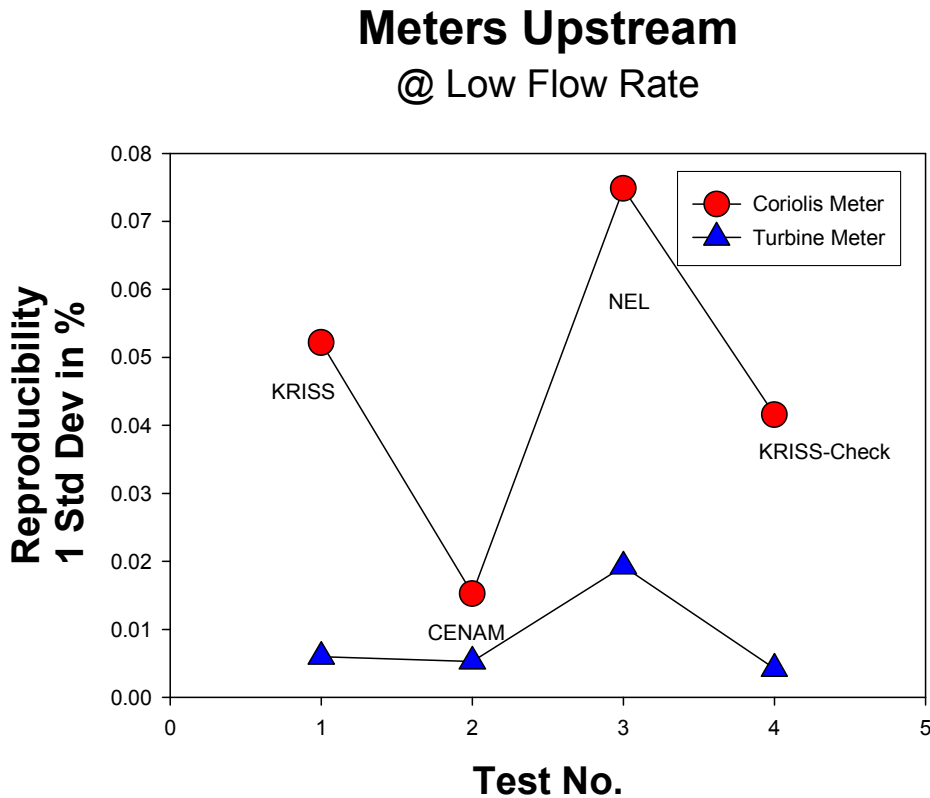


Figure 13. Reproducibility variation of flow meters upstream at low flow.

Meters Upstream @ High Flow Rate

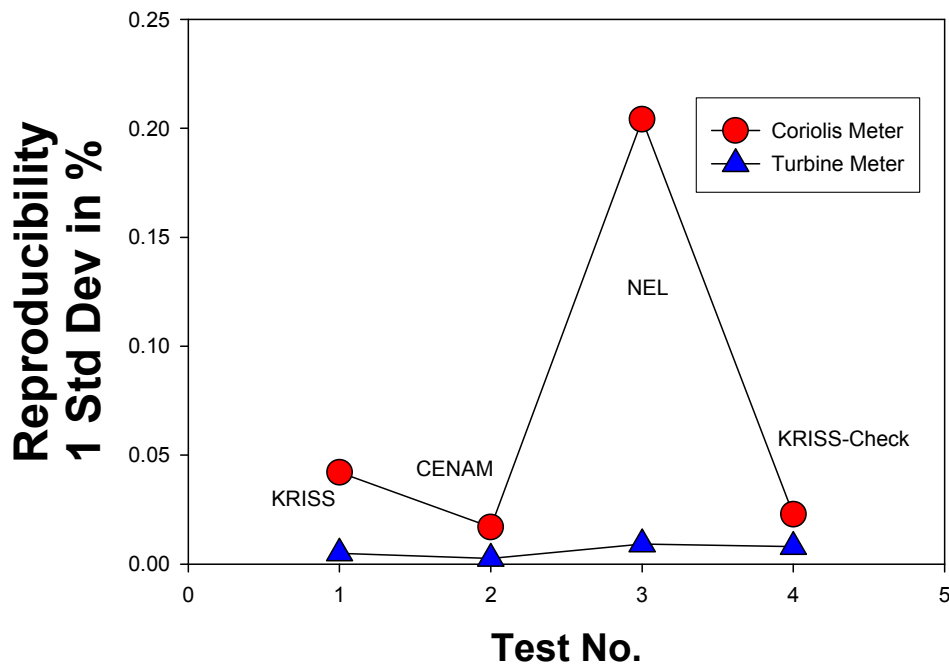


Figure 14. Reproducibility variation of flow meters upstream at high flow.

Meters Downstream @ Low Flow Rate

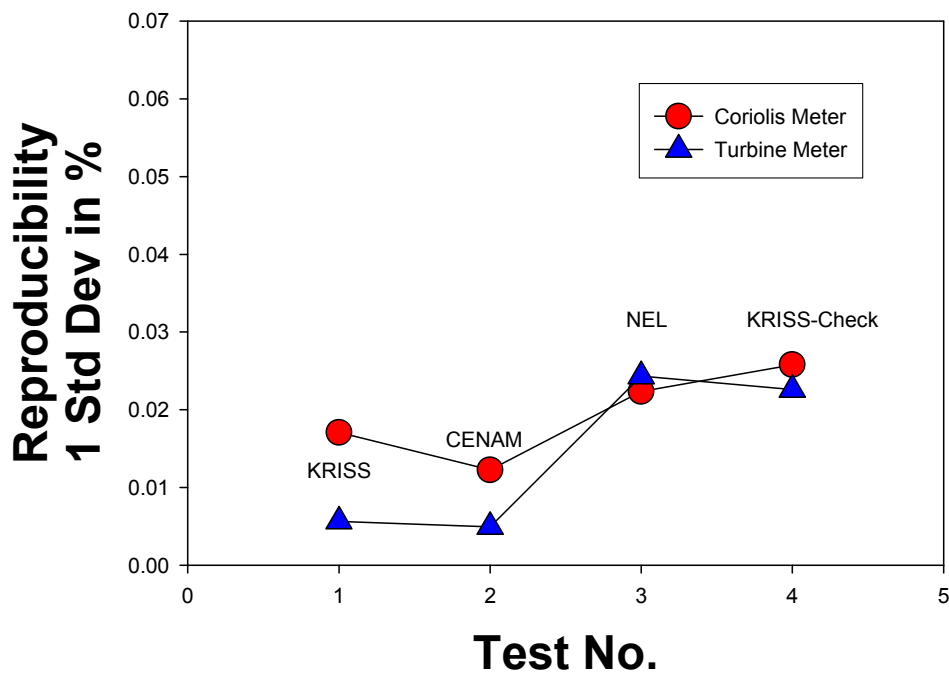


Figure 15. Reproducibility variation of flow meters downstream at low flow.

Meters Downstream @ High Flow Rate

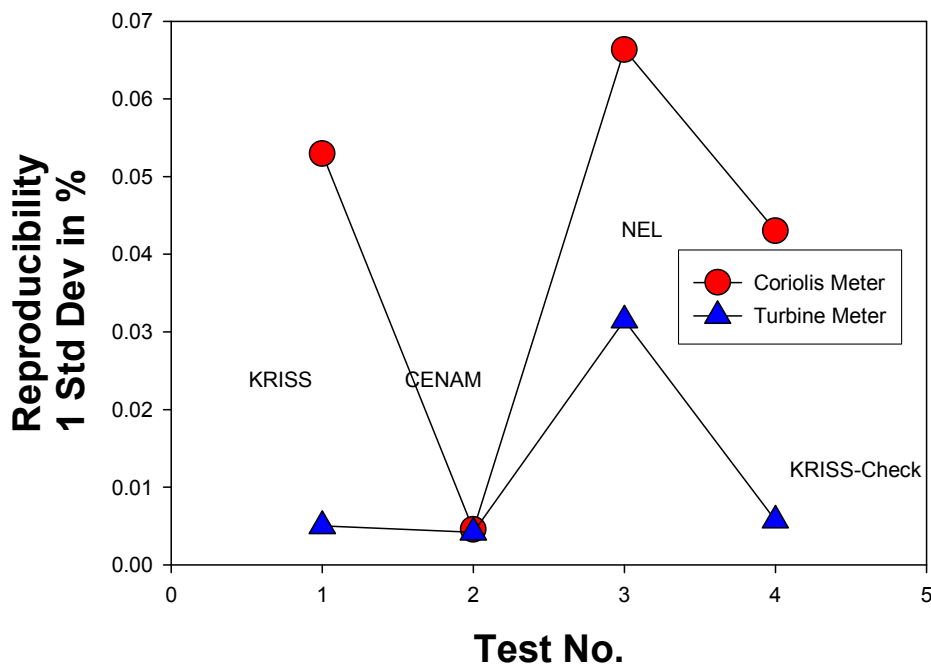


Figure 16. Reproducibility variation of flow meters downstream at high flow.

Based on the data above, we felt that the coriolis flow meter (E&H, Promass 80), which had a reproducibility of about 0.08 %, needed to be replaced by a model of better reproducibility in order to compare NMIs who claimed uncertainties of better than 0.1 %. We contacted Endress+Hauser Flowtec AG and three new coriolis meters of improved flow characteristics (Promass 83 F model) were provided. Test results of these new coriolis flow meters at the Pilot Lab yielded much improved reproducibilities at the level of about +/-0.05 %.

7 Key Comparison (KC) for Water Flow: CCM.FF-K1

7.1. Description of the TSP for K1

The TSP used in CCM.FF-K1 was similar in design to that used during the pilot comparison multi-lab reproducibility tests. However, for the better reproducibility, a new coriolis meter of improved performance (E&H, model Promass 83 F D7) was used and its flow characteristics are shown in Figure 17. The turbine meter used was an Exact Flow model 1005 and its flow characteristics are shown in Figure 18.

Coriolis Meter (E&H Promass 83F D7)

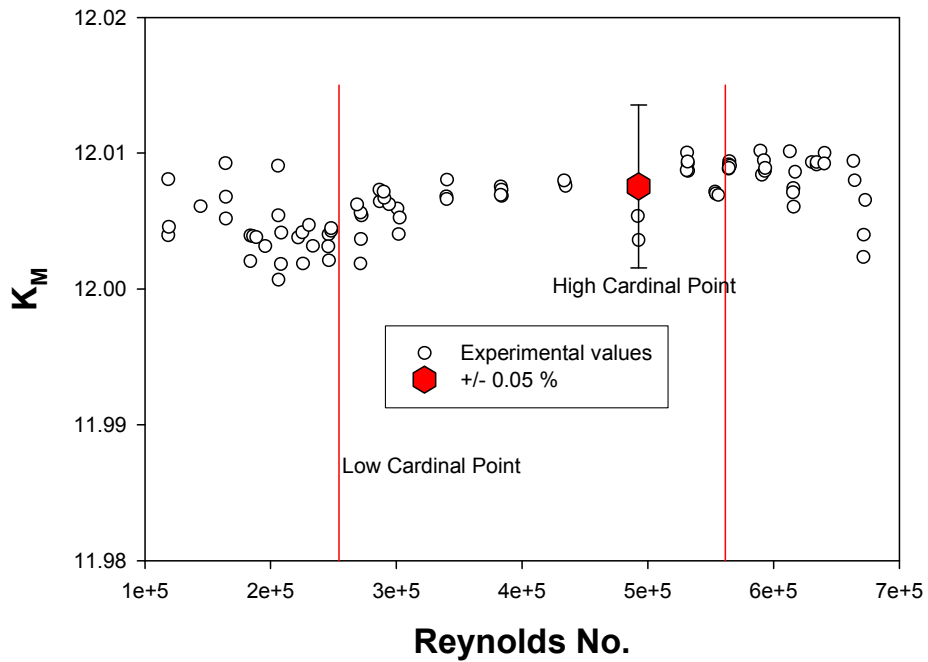


Figure 17. Flow characteristics of the coriolis meter.

Exact Flow Turbine Meter 1005

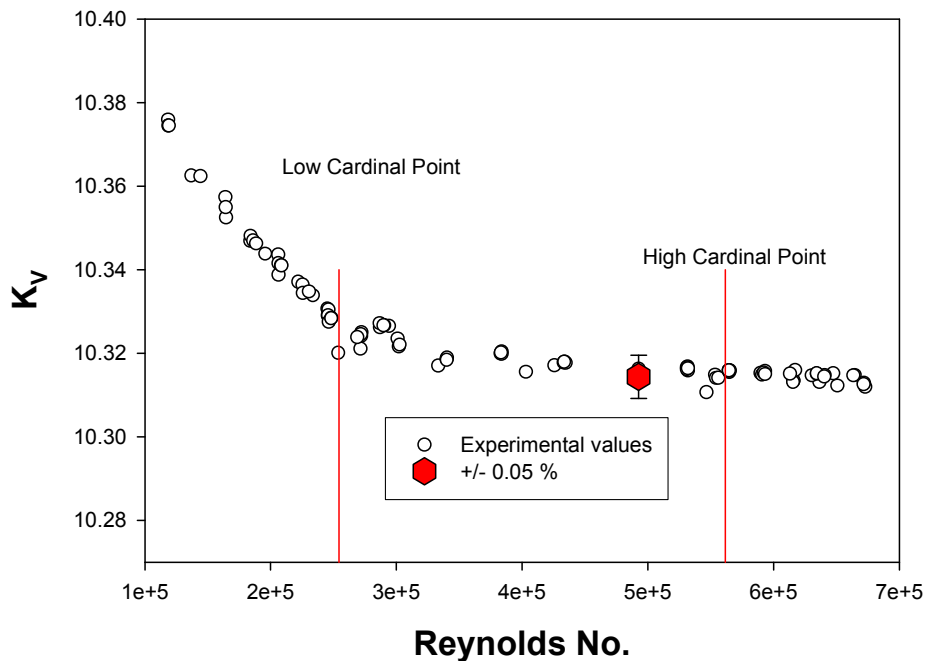


Figure 18. Flow characteristics of the turbine meter.

7.2. Technical Protocol

Based on the test procedure in Figure 2 and the pilot comparison experience, the technical protocol for CCM.FF-K1 was drafted and modified based on comments from the participating NMIs before being approved by the CCM.

8 KC Results

8.1. Reynolds Number Correction

The flow meter factors reported by participating NMIs were spread over a range of Reynolds numbers anchored by the cardinal Reynolds numbers presented in Table 4.

Table 4. Cardinal flow points.

	Cardinal Reynolds No.	Flow Rate (m ³ /h)
High Flow	561569	154
Low Flow	254269	70

As shown in Figure 17 and Figure 18, both the coriolis and turbine flow meter have fairly linear flow characteristics over the range of Reynolds numbers from 250000 to 580000. The reported 40 K -factors from each participating NMI (K_M or K_V values of respective meters at high and low Re numbers in the same configuration) were fitted linearly in order to relate the reported meter factors to their corresponding cardinal Re numbers. This procedure was accomplished by linearly fitting the results using the measured Reynolds numbers and then determining the “effective” K -factor at each cardinal point using the resulting slopes at each configuration. At each flow condition (*i.e.*, the same configuration and flow) the average of 20 corrected K -factors, for each meter, is hereafter presented as the result of the corresponding NMI.

8.2. Results of Participating NMIs

8.2.1. Reproducibility variation

When the TSP returned to the pilot lab it was found to be severely contaminated by fine rust particles and we decided to clean ultrasonically the turbine meter before the final check test was performed. However, we decided not to clean the coriolis meter and no zero point adjustment was needed.

Figure 19 through Figure 22 show the reproducibilities of the coriolis and turbine flow meters at each NMI (single lab reproducibility). As seen, there were no significant changes in reproducibility of the instruments due to contamination of the coriolis meter or due to the cleaning of the turbine meter. The reproducibility results obtained during the final tests at the pilot lab for the coriolis meter without cleaning and the turbine meter after cleaning are labeled in the figures as KRISS-Check.

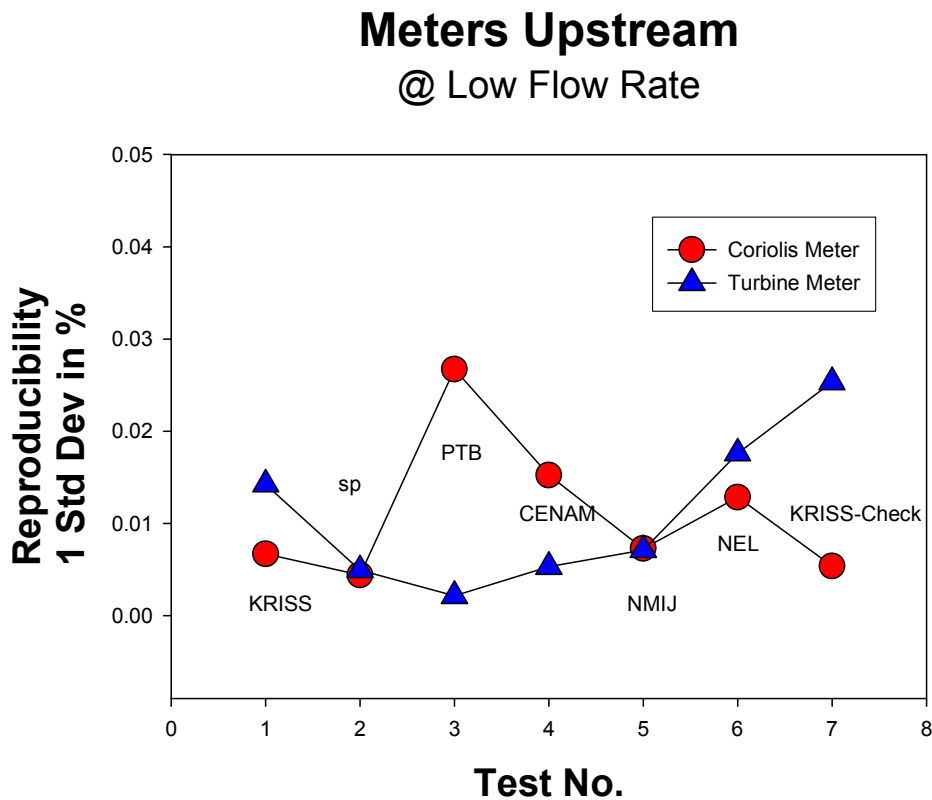


Figure 19. Reproducibility variation of flow meters upstream at low flow.

Meters Upstream @ High Flow Rate

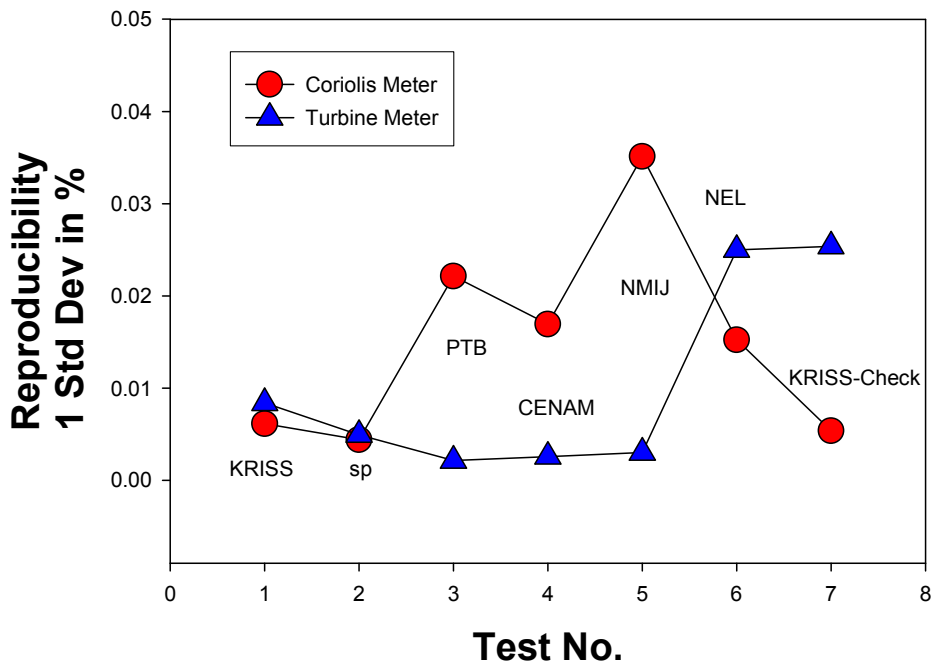


Figure 20. Reproducibility variation of flow meters upstream at high flow.

Meters Downstream @ Low Flow Rate

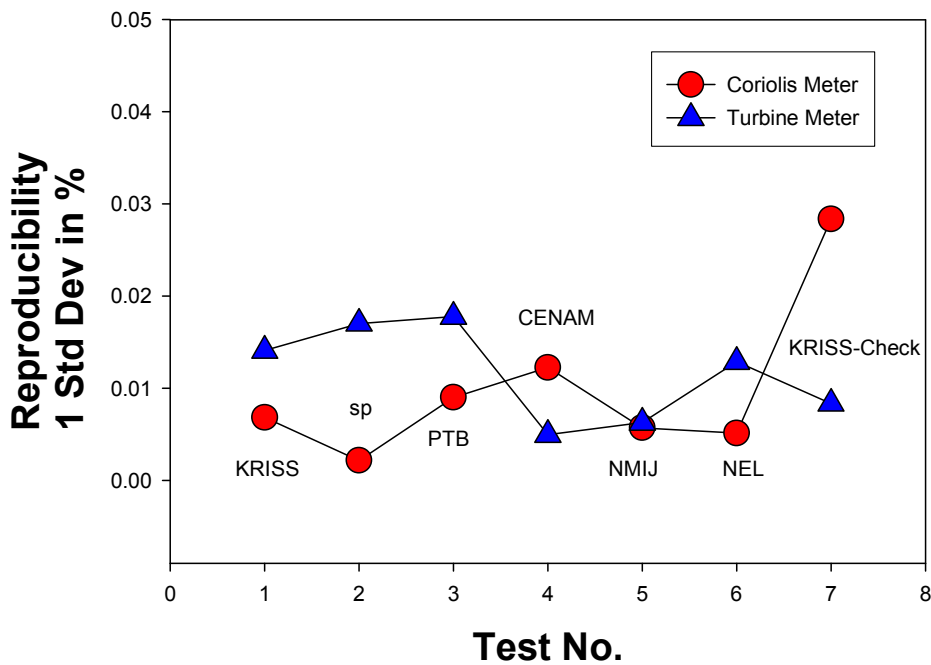


Figure 21. Reproducibility variation of flow meters downstream at low flow.

Meters Downstream @ High Flow Rate

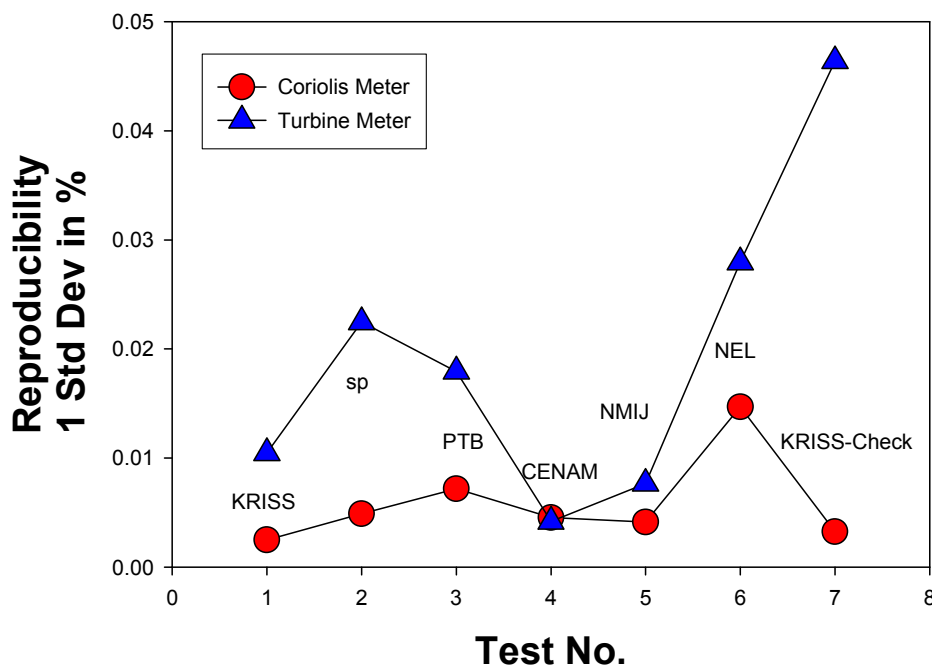


Figure 22. Reproducibility variation of flow meters downstream at high flow.

8.2.2. K -factors

The averaged K_M for the coriolis meter and K_V for the turbine meter, in upstream positions at high and low cardinal conditions, are shown in Table 5 and Table 6 for each of the NMIs with their claimed uncertainties; the average K_M and K_V values in downstream positions are presented in Table 4. In these tables, the uncertainties were estimated using the uncertainty budgets submitted by participating NMIs. As mentioned before, the data labeled KRIS-Check was obtained during the final test at the pilot laboratory.

8.2.3. Installation effects

In the tandem flow meter arrangement used in this key comparison, the upstream meter was always exposed to the typical flow condition seeing at each participating NMI during a normal calibration. However, because the upstream meter and the flow conditioner filtered the flow profile entering the downstream meter, its data showed to be less influenced by any distortions present in the flow profile of the testing NMIs (*i.e.*, installation effects). In Figure 23 and Figure 24, the K_M values of the coriolis flow meter in upstream position from each NMI are compared with results for the same flow

meter in downstream position (both, at high and low flow). As it can be seen, with the exception of the data from CENAM, the participating NMIs show very similar K_M values whether the coriolis meter was located in the upstream or downstream position. This could indicate that the coriolis meter is fairly insensitive to installation effects influencing its response.

Table 5. Comparison results: K_M and K_V , of meters in upstream position, $k = 2$.

NMI	cuphi ¹¹		tuphi ¹²	
	x_{cuphi} , [1/kg]	$U(x_{\text{cuphi}})$, [1/kg]	x_{tuphi} , [1/L]	$U(x_{\text{tuphi}})$, [1/L]
KRISS	12.0121	0.0059	10.3160	0.0074
SP	12.0047	0.0061	10.3047	0.0066
PTB	12.0150	0.0036	10.3099	0.0030
CENAM	12.0040	0.0025	10.3040	0.0070
NMIJ	12.0135	0.0057	10.3083	0.0062
NEL	12.0172	0.0033	10.3126	0.0043
KRISS-Check	12.0179	0.0065	10.3060	0.0078
NMI	cuplo ¹³		tuplo ¹⁴	
	x_{cupho} , [1/kg]	$U(x_{\text{cupho}})$, [1/kg]	x_{tupho} , [1/L]	$U(x_{\text{tupho}})$, [1/L]
KRISS	12.0086	0.0038	10.3297	0.0057
SP	12.0039	0.0070	10.3229	0.0054
PTB	12.0116	0.0036	10.3278	0.0030
CENAM	12.0084	0.0027	10.3188	0.0070
NMIJ	12.0153	0.0057	10.3266	0.0062
NEL	12.0122	0.0033	10.3323	0.0046
KRISS-Check	12.0164	0.0041	10.3273	0.0057

However, as indicated by the results shown in Figure 25 and Figure 26, the K_V values of the turbine meter in upstream position are different from those obtained in downstream position, with the upstream values being lower than those obtained in downstream position. These results lead us to conclude that the turbine meter results could have been influenced by installation effects during testing.

Table 6. Comparison results, K_M and K_V , of meters in downstream position, $k = 2$.

NMI	cdnhi ¹⁵		tdnhi ¹⁶	
	x_{cdnhi} , [1/kg]	$U(x_{\text{cdnhi}})$, [1/kg]	x_{tdnhi} , [1/L]	$U(x_{\text{tdnhi}})$, [1/L]
KRISS	12.0109	0.0057	10.3253	0.0074
SP	12.0024	0.0060	10.3216	0.0100
PTB	12.0154	0.0035	10.3212	0.0030
CENAM	12.0136	0.0024	10.3169	0.0070
NMIJ	12.0158	0.0058	10.3204	0.0062
NEL	12.0199	0.0058	10.3257	0.0044
KRISS-Check	12.0168	0.0064	10.3113	0.0076
NMI	cdnlo ¹⁷		tdnlo ¹⁸	
	x_{cdnho} , [1/kg]	$U(x_{\text{cdnho}})$, [1/kg]	x_{tdnho} , [1/L]	$U(x_{\text{tdnho}})$, [1/L]
KRISS	12.0078	0.0036	10.3412	0.0060
SP	12.0021	0.0068	10.3392	0.0091
PTB	12.0141	0.0035	10.3398	0.0031
CENAM	12.0156	0.0024	10.3319	0.0070
NMIJ	12.0115	0.0057	10.3369	0.0062
NEL	12.0141	0.0033	10.3441	0.0043
KRISS-Check	12.0135	0.0041	10.3338	0.0060

Installation Effects Coriolis Meter @ High Flow rate

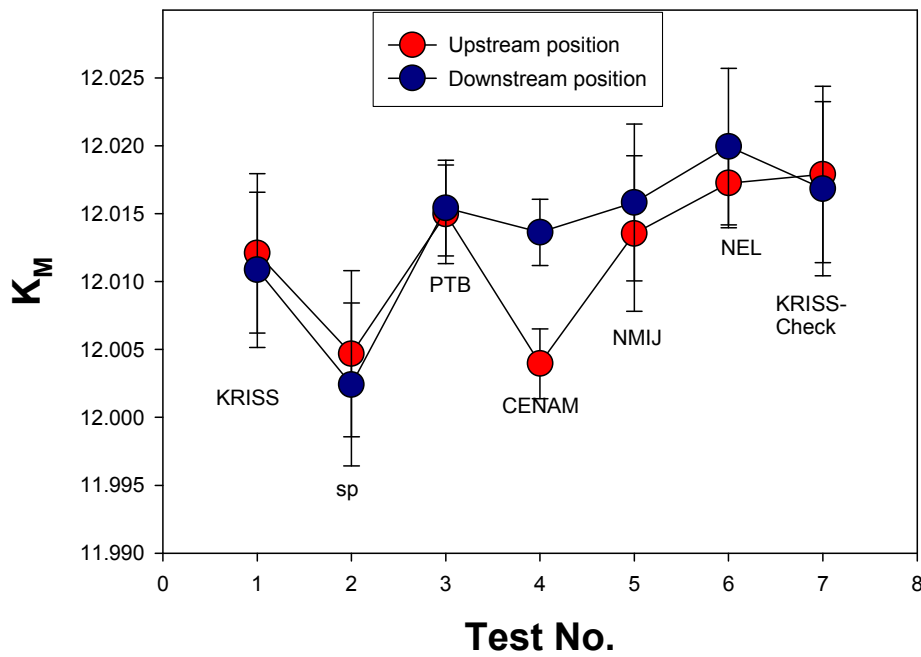


Figure 23. K_M values of the coriolis meter at high flow.

Installation Effects Coriolis Meter @ Low Flow Rate

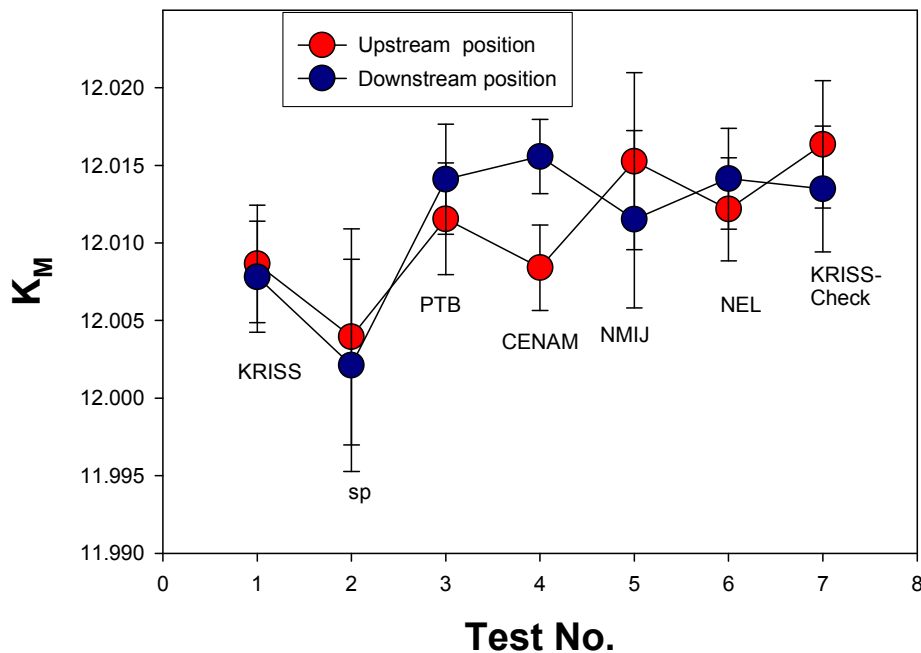


Figure 24. K_M values of the coriolis meter at low flow.

Installation Effects Turbine Meter @ High Flow Rate

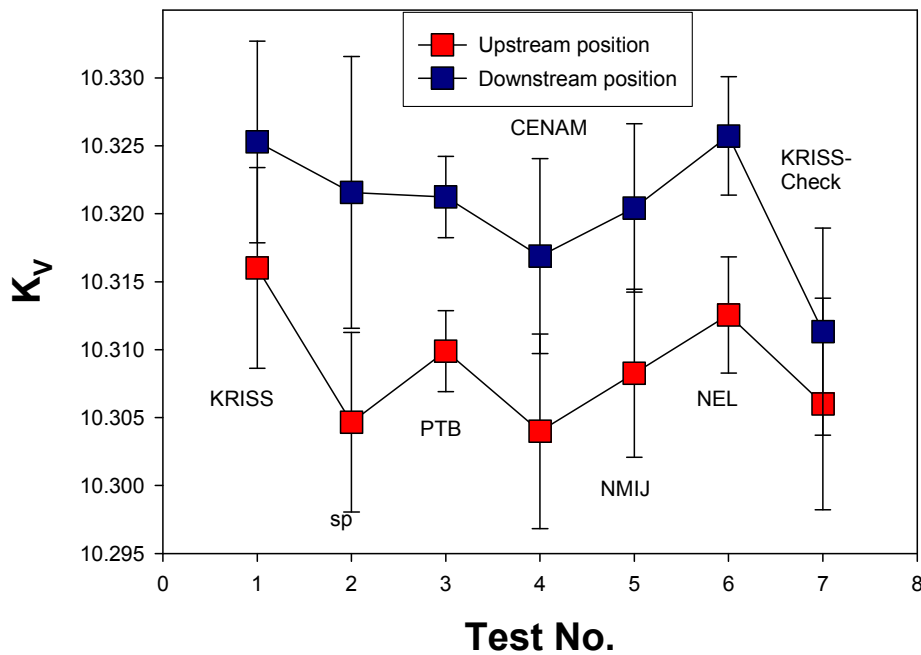


Figure 25. K_V values of the Turbine meter at high flow.

Installation Effects Turbine Meter @ Low Flow Rate

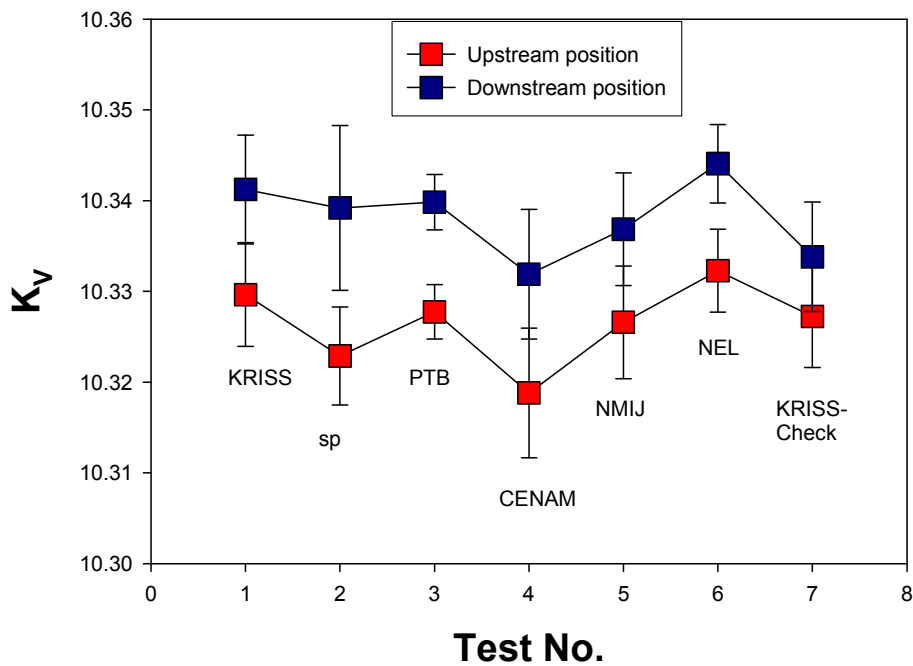


Figure 26. K_V values of the Turbine meter at low flow.

8.2.4. KCRVs and NMI-to-KCRV differences

In what follows, emphasis will be placed on the upstream flow meter results since these results are more typical of the data produced in each participating NMI.

As recommended by Cox [2, 3] a chi-squared test was performed to ascertain the consistency of the results in order to determine whether or not the weighted means of the data could be used in this key comparison. Unfortunately, the consistency test failed, and as recommended in such eventuality, the medians of the Coriolis meter K_M values and of the turbine meter K_V values from the participating NMIs were used in the determination of the Key Comparison Reference Values (KCRVs). Table 7 shows the KCRVs, standard uncertainties and the high and low end values of 95 % confidence intervals for the results of the comparison. These values were estimated by Monte Carlo simulations according to the procedure B recommended by Cox [2, 3]. In their estimation, the KRIS-Check results were excluded.

Table 7. KCRVs of K_M [1/kg] and K_V [1/L] values for meters in the upstream positions (values derived from medians).

	x_{median}	$U(x_{median})$	95 % confidence interval	
			$x_{median, H}$	$x_{median, L}$
cuphi ¹¹	12.0123	0.0017	12.0155	12.0090
tuphi ¹²	10.3093	0.0014	10.3120	10.3066
cuplo ¹³	12.0101	0.0010	12.0121	12.0082
tuplo ¹⁴	10.3270	0.0014	10.3297	10.3242

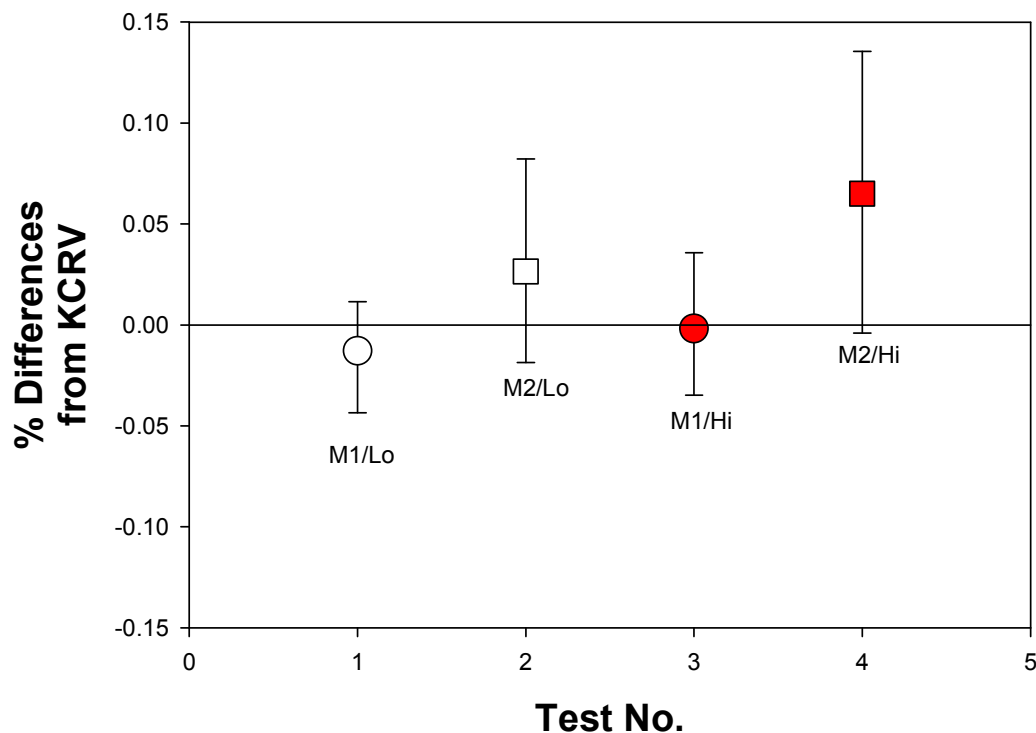
The relative differences of the test results from the relevant KCRVs have been estimated (in percentage terms) by Monte Carlo simulation. For this process we used the test results in Table 5 with their corresponding KCRVs in Table 7. In Table 8 through Table 13, simulation results are presented with associated standard uncertainties, high and low end values of 95 % confidence intervals, and En values. Figure 27 through Figure 38 are graphical presentation of NMI-to-KCRV differences and En values.

In accordance with Cox [2, 3], $En = 0$ designates complete agreement among participants, while values of $En > 1$ designate them as discrepant at the 5 % level of significance. In what follows, En_{total} is the geometric mean of individual En values in

different flow conditions describing the degree of equivalence between a NMI and the KCRV and thus, it shows degree of equivalence between a NMI and the KCRV.

$$En_i = \frac{Abs(d_i)}{2u(d_i)}, \quad En_{total} = \left(\prod_{i=1}^4 En_i\right)^{1/4} \quad (15)$$

KRISS-to-KCRV Differences Meters Upstream



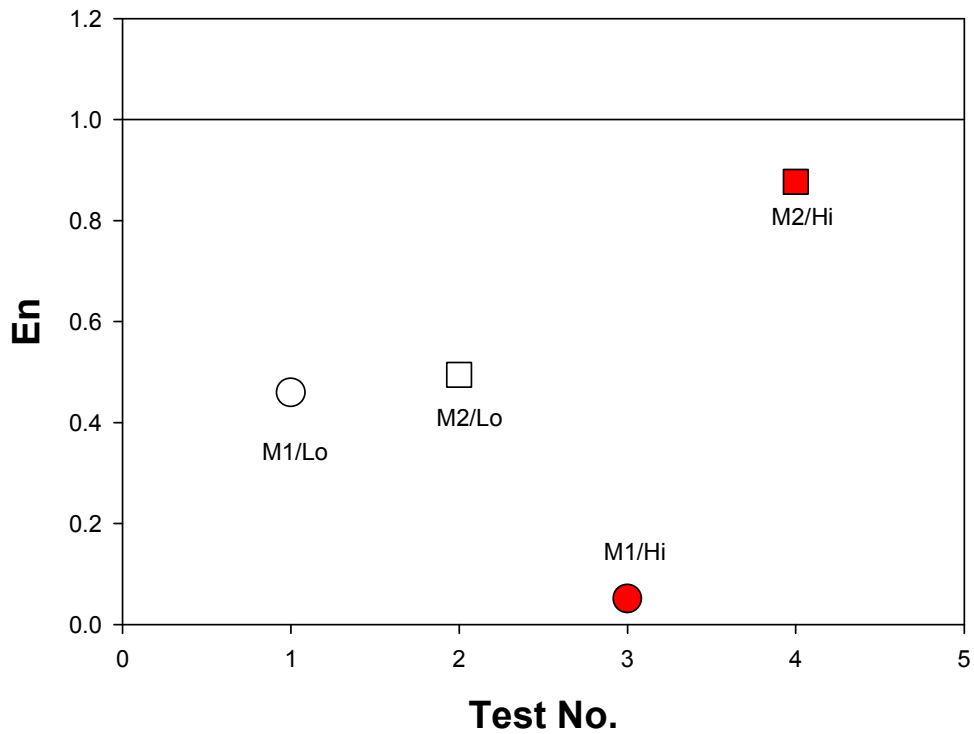
M1/Lo: Coriolis Meter @ Low flow rate, M2/Lo: Turbine Meter @ Low flow rate
M1/Hi: Coriolis Meter @ High flow rate, M2/Hi: Turbine Meter @ High flow rate

Figure 27. KRISS-to-KCRV differences.

Table 8. KRISS-to-KCRV differences in %.

	d_i	$u(d_i)$	95 % confidence interval		En_i
			$U(d_i, H)$	$U(d_i, L)$	
cuphi ¹¹	-0.0018	0.0176	0.038	-0.033	0.05
tuphi ¹²	0.0650	0.0371	0.070	-0.069	0.88
cuplo ¹³	-0.0129	0.0140	0.024	-0.031	0.46
tuplo ¹⁴	0.0264	0.0267	0.056	-0.045	0.49
En_{total}					0.32

KRISS-to-KCRV

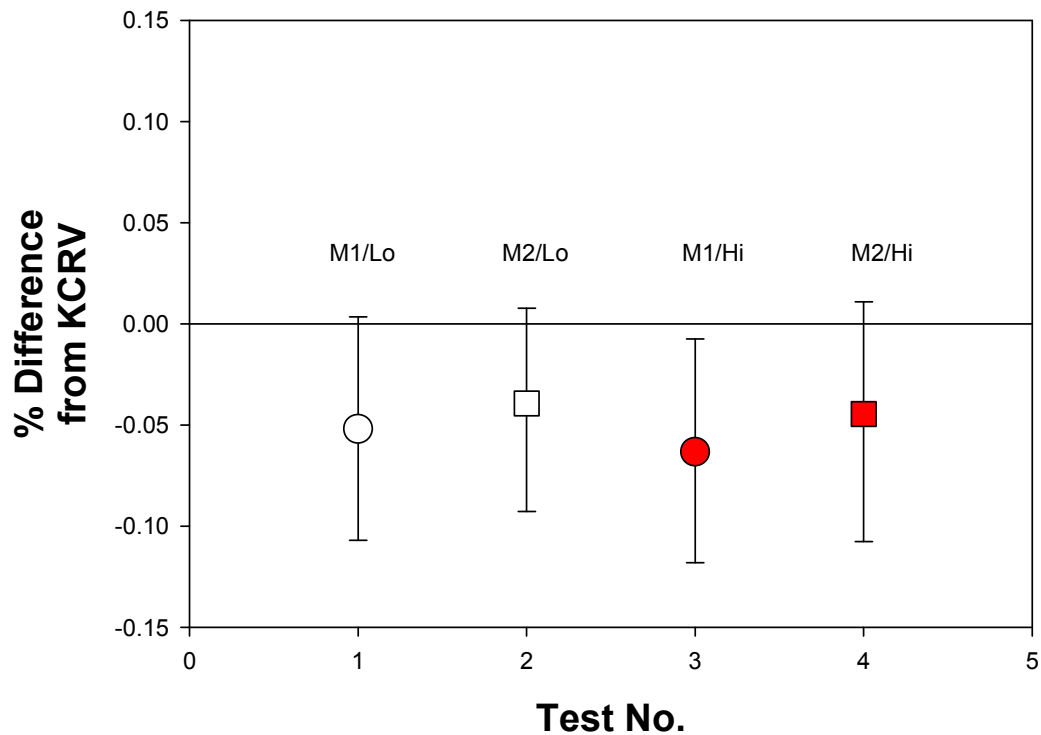


M1/Lo: Coriolis Meter @ Low flow rate, M2/Lo: Turbine Meter @ Low flow rate
M1/Hi: Coriolis Meter @ High flow rate, M2/Hi: Turbine Meter @ High flow rate

Figure 28. *En* values of KRISS of two flow meters at two different flows.

SP-to-KCRV Differences

Meters Upstream



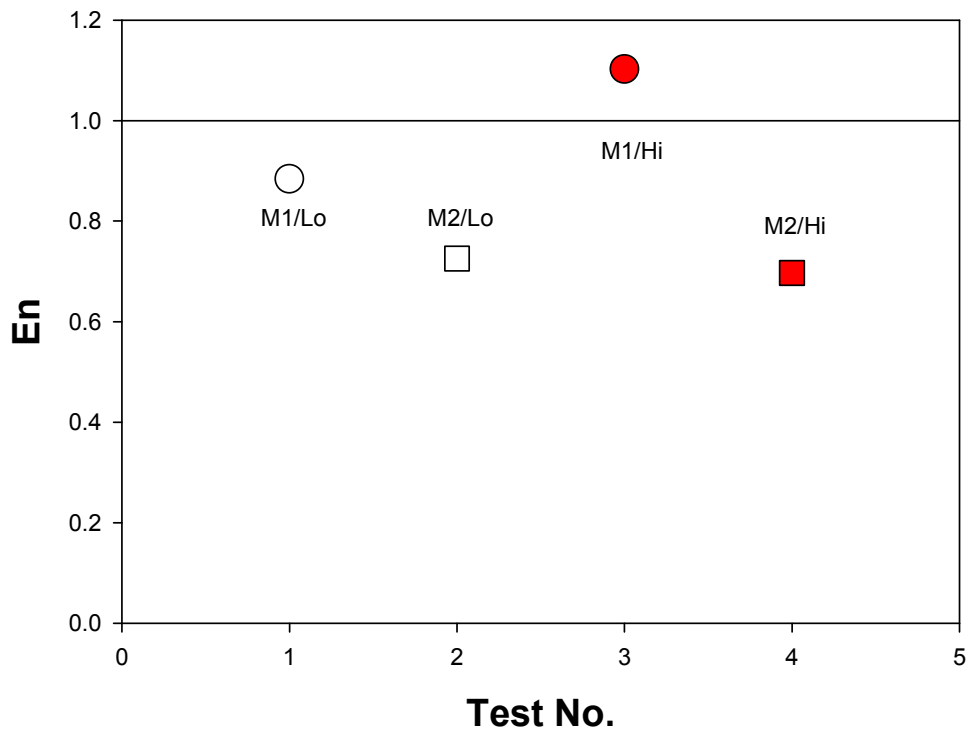
M1/Lo: Coriolis Meter @ Low flow rate, M2/Lo: Turbine Meter @ Low flow rate
M1/Hi: Coriolis Meter @ High flow rate, M2/Hi: Turbine Meter @ High flow rate

Figure 29. SP-to-KCRV differences.

Table 9. SP-to-KCRV differences in %.

	d_i	$u(d_i)$	95 % confidence interval		En_i
			$U(d_i, H)$	$U(d_i, L)$	
cuphi ¹¹	-0.063	0.029	0.056	-0.055	1.10
tuphi ¹²	-0.044	0.032	0.055	-0.063	0.70
cuplo ¹³	-0.052	0.029	0.055	-0.055	0.88
tuplo ¹⁴	-0.039	0.027	0.047	-0.053	0.73
En_{total}					0.84

SP-to-KCRV

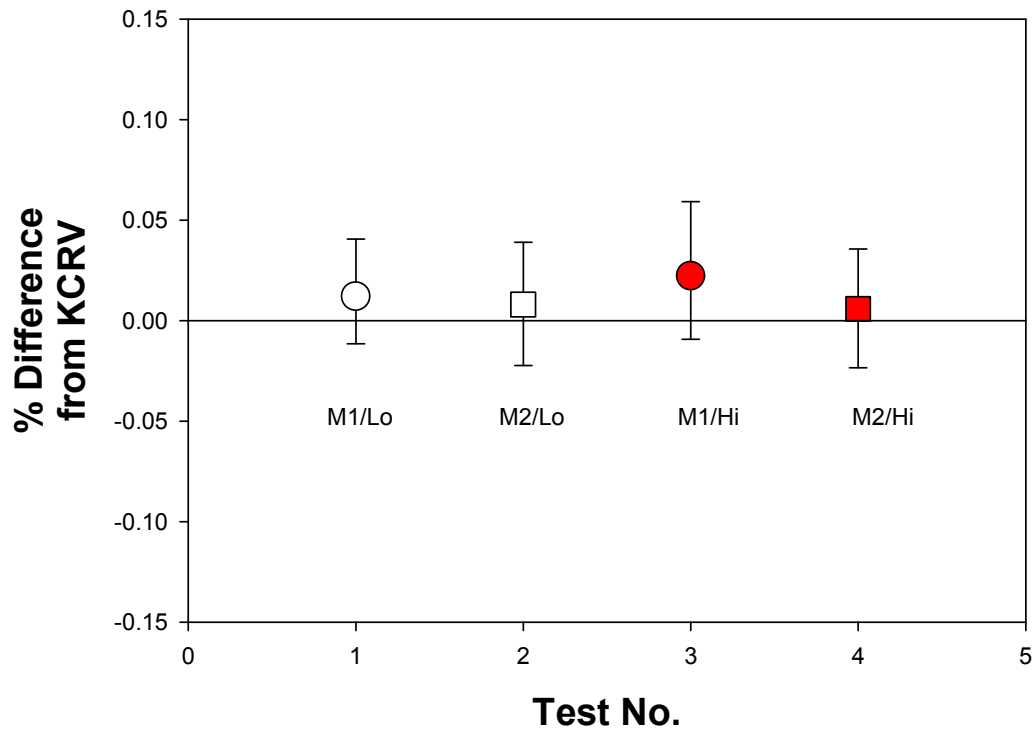


M1/Lo: Coriolis Meter @ Low flow rate, M2/Lo: Turbine Meter @ Low flow rate
M1/Hi: Coriolis Meter @ High flow rate, M2/Hi: Turbine Meter @ High flow rate

Figure 30. En values of SP of two flow meters at two different flows.

PTB-to-KCRV Differences

Meters Upstream



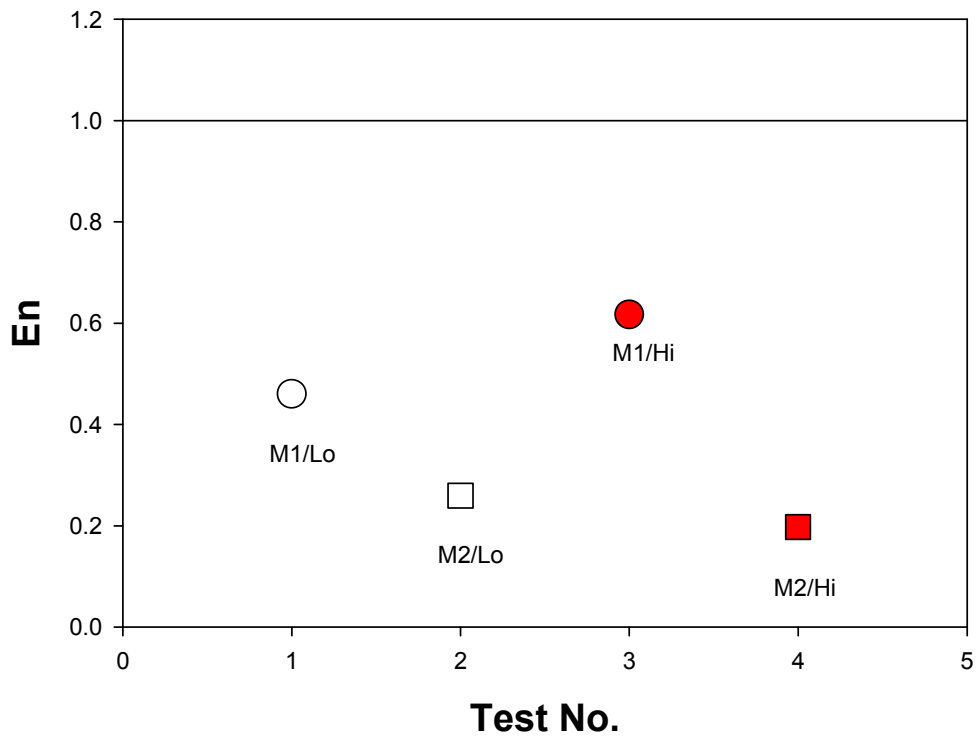
M1/Lo: Coriolis Meter @ Low flow rate, M2/Lo: Turbine Meter @ Low flow rate
M1/Hi: Coriolis Meter @ High flow rate, M2/Hi: Turbine Meter @ High flow rate

Figure 31. PTB-to-KCRV differences.

Table 10. PTB-to-KCRV differences in %.

	d_i	$u(d_i)$	95 % confidence interval		En_i
			$U(d_i, H)$	$U(d_i, L)$	
cuphi ¹¹	0.022	0.018	0.037	-0.032	0.62
tuphi ¹²	0.006	0.015	0.030	-0.029	0.20
cuplo ¹³	0.012	0.013	0.029	-0.023	0.46
tuplo ¹⁴	0.008	0.015	0.031	-0.030	0.26
En_{total}					0.35

PTB-to-KCRV

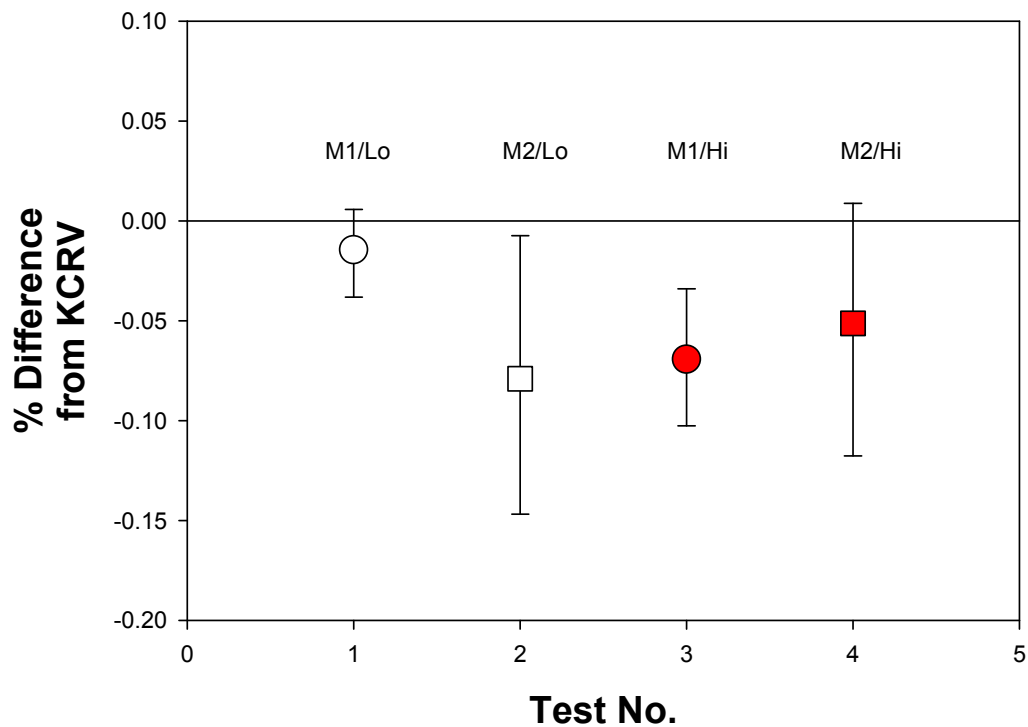


M1/Lo: Coriolis Meter @ Low flow rate, M2/Lo: Turbine Meter @ Low flow rate
M1/Hi: Coriolis Meter @ High flow rate, M2/Hi: Turbine Meter @ High flow rate

Figure 32. *En* values of PTB of two flow meters at two different flow.

CENAM-to-KCRV Differences

Meters Upstream



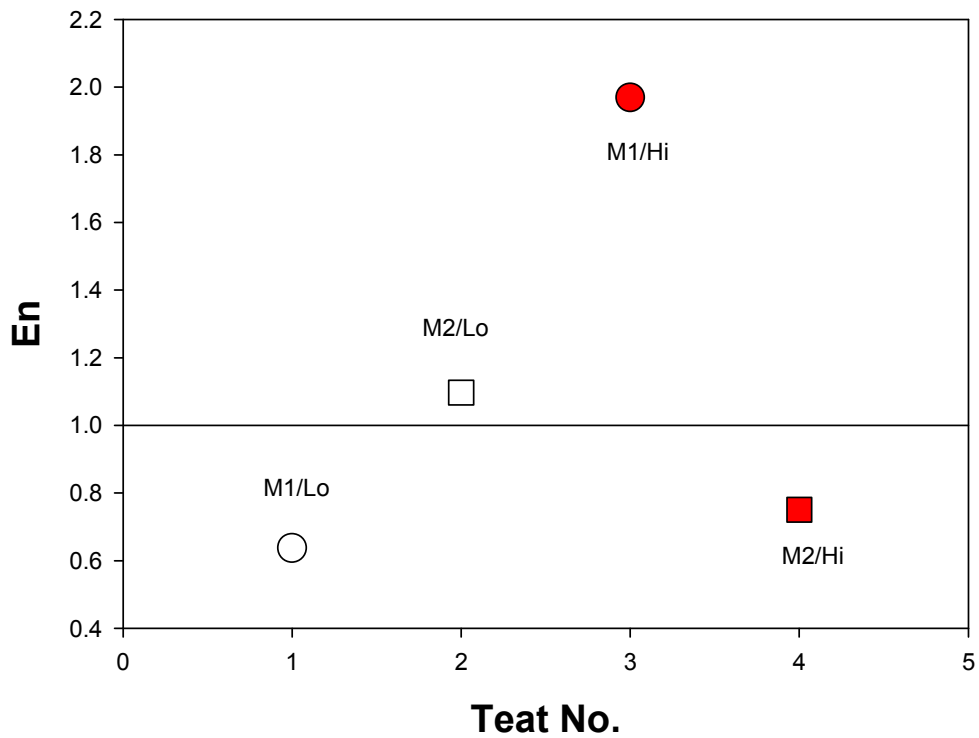
M1/Lo: Coriolis Meter @ Low flow rate, M2/Lo: Turbine Meter @ Low flow rate
M1/Hi: Coriolis Meter @ High flow rate, M2/Hi: Turbine Meter @ High flow rate

Figure 33. CENAM-to-KCRV differences.

Table 11. CENAM-to-KCRV differences in %.

	d_i	$u(d_i)$	95 % confidence interval		En_i
			$U(d_i, H)$	$U(d_i, L)$	
cuphi ¹¹	-0.069	0.018	0.035	-0.033	1.97
tuphi ¹²	-0.051	0.034	0.060	-0.066	0.75
cuplo ¹³	-0.015	0.011	0.020	-0.024	0.64
tuplo ¹⁴	-0.079	0.036	0.072	-0.068	1.10
En_{total}					1.01

CENAM-to-KCRV

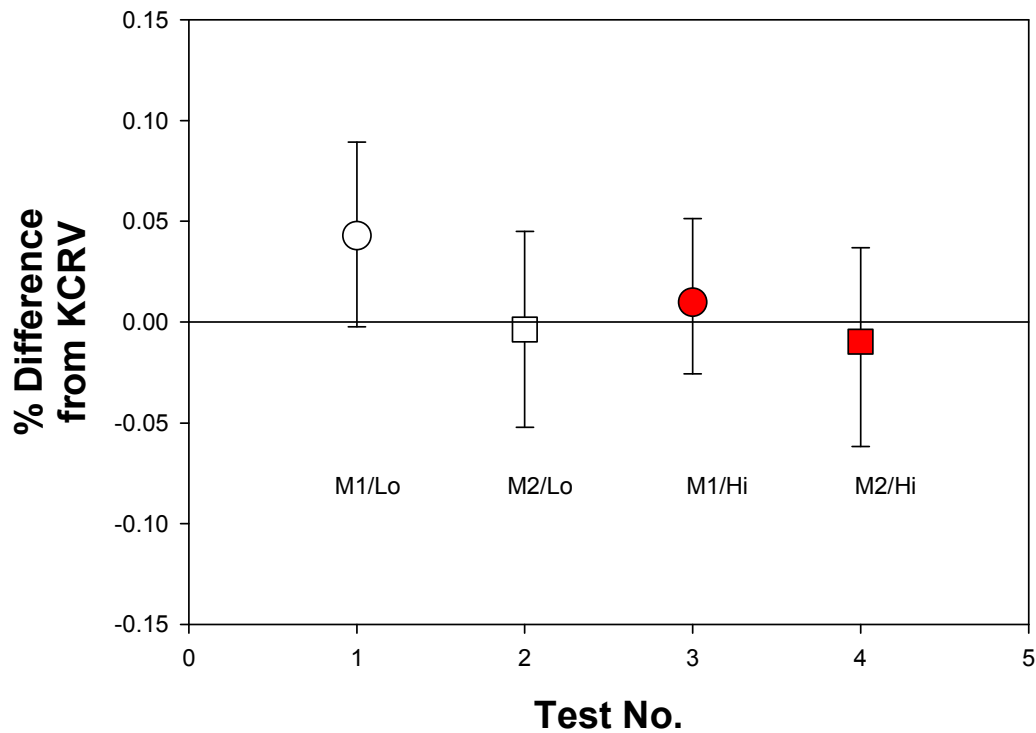


M1/Lo: Coriolis Meter @ Low flow rate, M2/Lo: Turbine Meter @ Low flow rate
M1/Hi: Coriolis Meter @ High flow rate, M2/Hi: Turbine Meter @ High flow rate

Figure 34. *En* values of CENAM of two flow meters at two different flows.

NMIJ-to-KCRV Differences

Meters Upstream



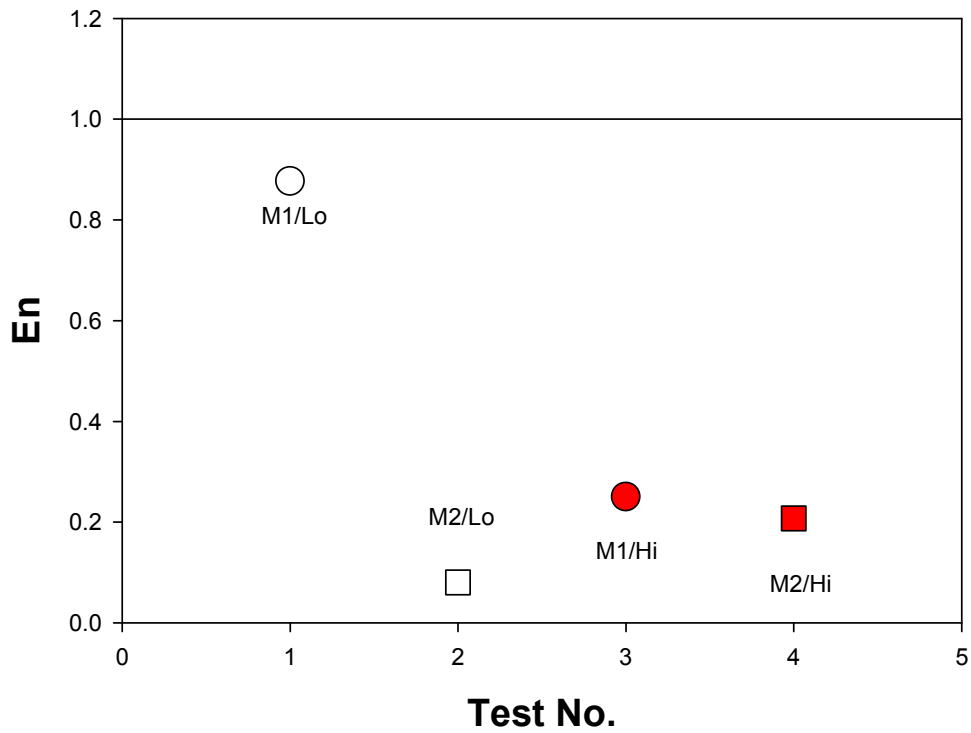
M1/Lo: Coriolis Meter @ Low flow rate, M2/Lo: Turbine Meter @ Low flow rate
M1/Hi: Coriolis Meter @ High flow rate, M2/Hi: Turbine Meter @ High flow rate

Figure 35. NMIJ-to-KCRV differences.

Table 12. NMIJ-to-KCRV differences in %.

	d_i	$u(d_i)$	95 % confidence interval		En_i
			$U(d_i, H)$	$U(d_i, L)$	
cuphi ¹¹	0.010	0.020	0.042	-0.035	0.25
tuphi ¹²	-0.010	0.023	0.047	-0.052	0.21
cuplo ¹³	0.043	0.024	0.046	-0.045	0.88
tuplo ¹⁴	-0.004	0.023	0.049	-0.049	0.08
En_{total}					0.25

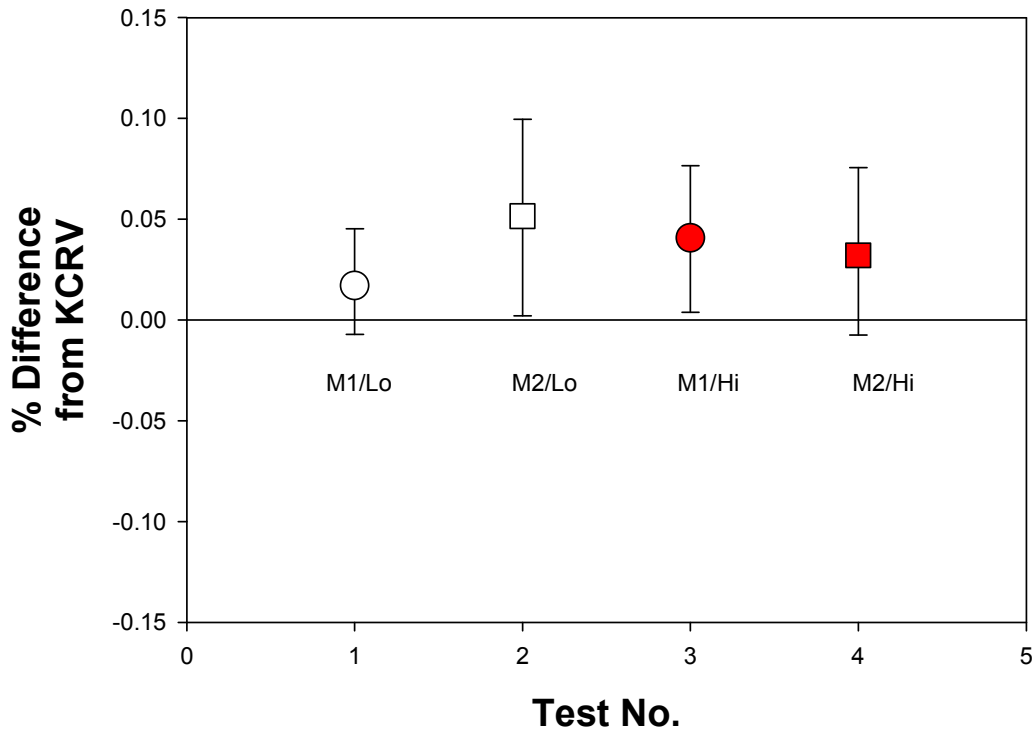
NMIJ-to-KCRV



M1/Lo: Coriolis Meter @ Low flow rate, M2/Lo: Turbine Meter @ Low flow rate
M1/Hi: Coriolis Meter @ High flow rate, M2/Hi: Turbine Meter @ High flow rate

Figure 36. E_n values of NMIJ of two flow meters at two different flows.

NEL-to-KCRV Differences Meters Upstream



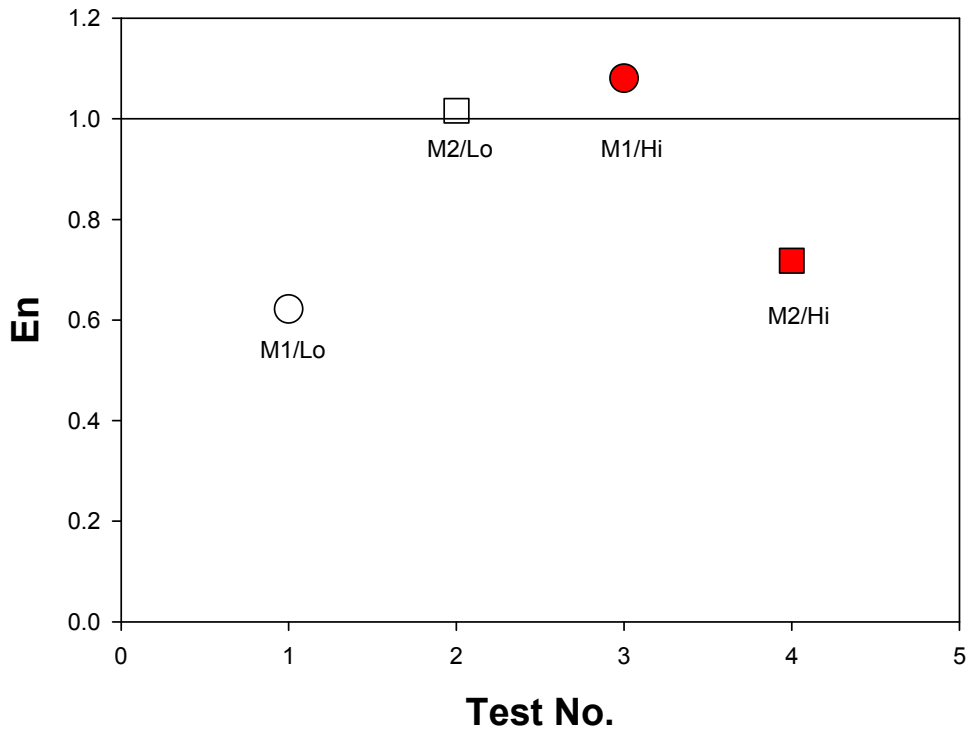
M1/Lo: Coriolis Meter @ Low flow rate, M2/Lo: Turbine Meter @ Low flow rate
 M1/Hi: Coriolis Meter @ High flow rate, M2/Hi: Turbine Meter @ High flow rate

Figure 37. NEL-to-KCRV differences.

Table 13. NEL-to-KCRV differences in %.

	d_i	$u(d_i)$	95 % confidence interval		En_i
			$U(d_i, H)$	$U(d_i, L)$	
cuphi ¹¹	0.041	0.019	0.036	-0.037	1.08
tuphi ¹²	0.032	0.022	0.044	-0.040	0.72
cuplo ¹³	0.017	0.014	0.028	-0.024	0.62
tuplo ¹⁴	0.052	0.025	0.048	-0.049	1.02
En_{total}					0.84

NEL-to-KCRV

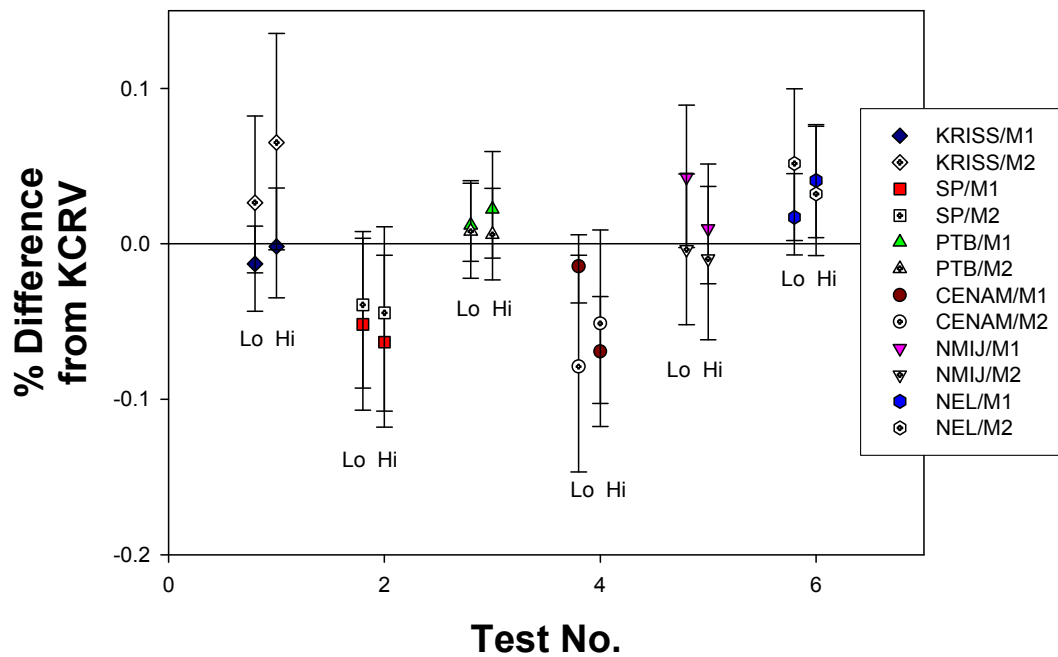


M1/Lo: Coriolis Meter @ Low flow rate, M2/Lo:Turbine Meter @ Low flow rate
M1/Lo: Coriolis Meter @ High flow rate, M2/Lo:Turbine Meter @ High flow rate

Figure 38. *En* values of NEL of two flow meters at two different flows.

The overall differences between key comparison values of participating NMIs in Table 5 and KCRVs are presented in Figure 39.

NMI-to-KCRV Differences Meters Upstream



M1: Coriolis Meter, M2: Turbine Meter
Lo: Low Cardinal Reynolds number
Hi: High Cardinal Reynolds number

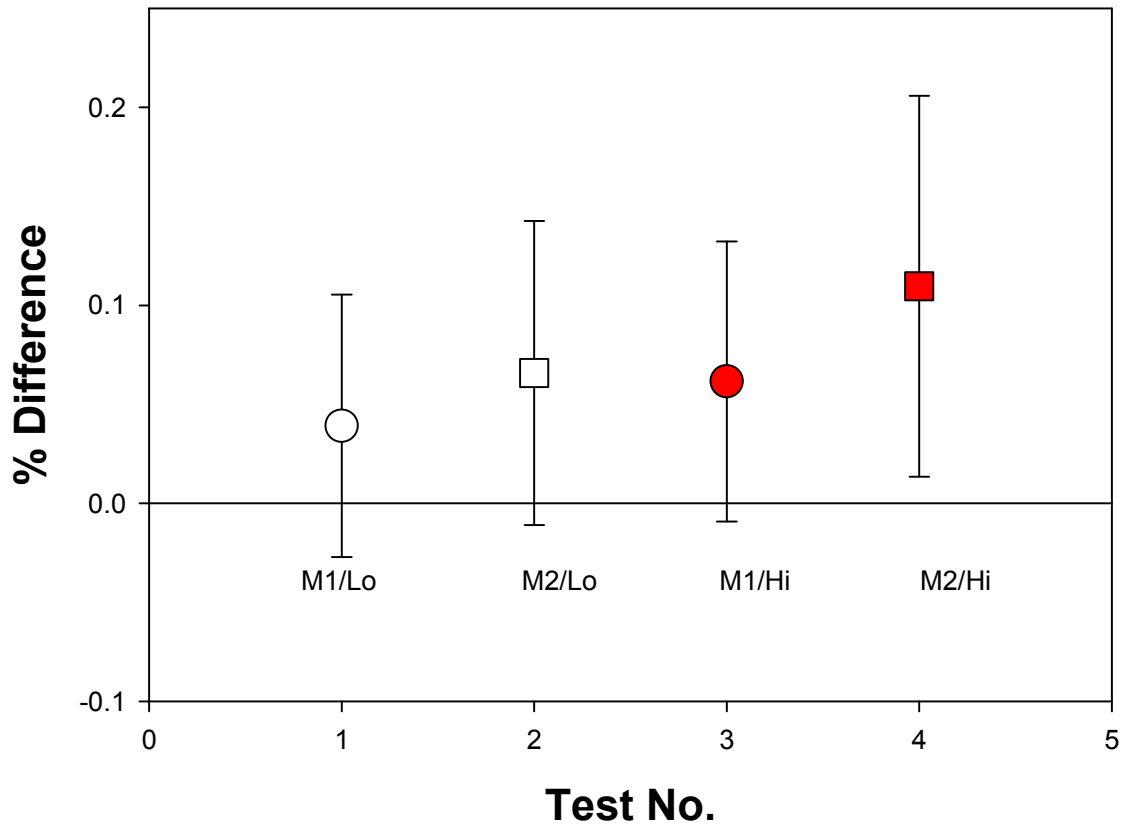
Figure 39. Differences between KC values and KCRVs.

8.2.5. NMI-to-NMI differences

Using the values in Table 3, differences of KC results between NMIs at the same flow condition were estimated. In order to make the differences relative, relevant KCRVs were used as scaling factors. These results are illustrated in Figure 39 through Figure 69 and summarized in Table 14 through Table 28 in terms of En values. As mentioned before, the En_{total} is the geometric mean of the individual En values in different flow conditions and describes the degree of equivalence between NMIs.

KRISS/SP Differences

Meters Upstream



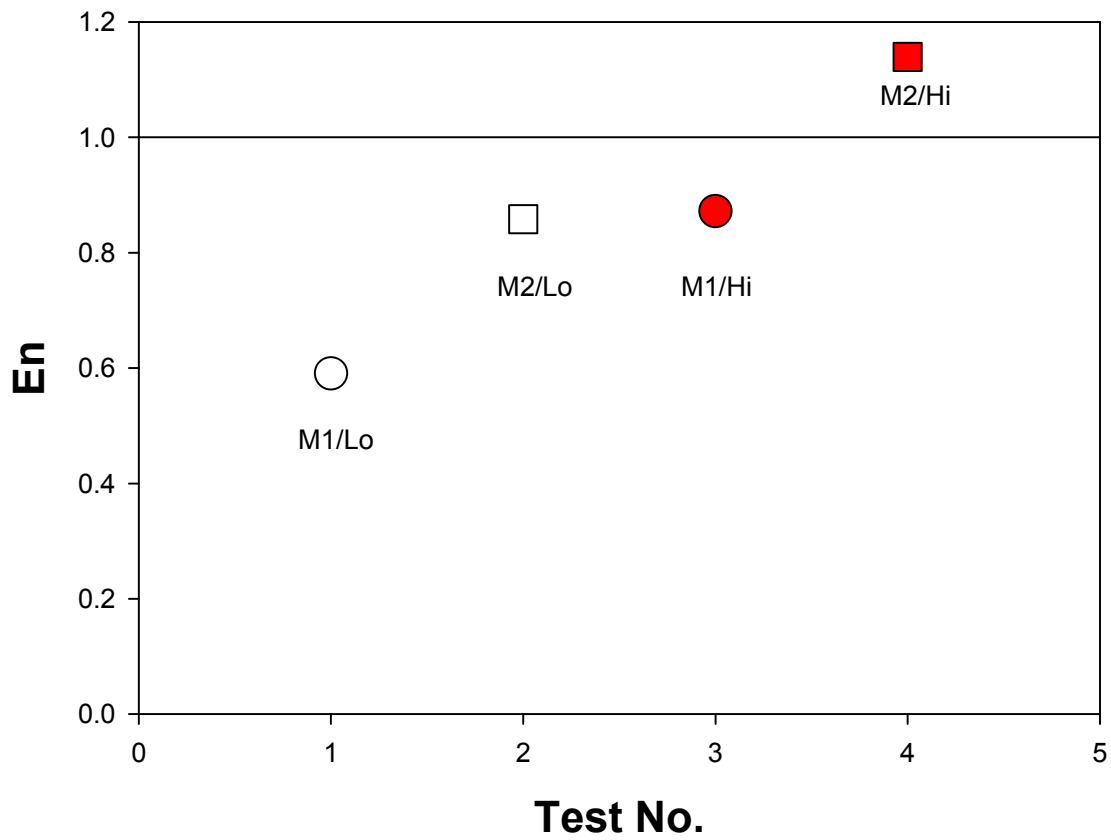
M1/Lo: Coriolis Meter @ Low flow rate, M2/Lo: Turbine Meter @ Low flow rate
M1/Hi: Coriolis Meter @ High flow rate, M2/Hi: Turbine Meter @ High flow rate

Figure 40. Differences between KRISS and SP.

Table 14. KRISS/SP differences in %.

	d_{ij}	$U(d_{ij})$	En_i
cuphi ¹¹	0.062	0.071	0.87
tuphi ¹²	0.110	0.096	1.14
cuplo ¹³	0.039	0.066	0.59
tuplo ¹⁴	0.066	0.077	0.86
En_{total}			0.84

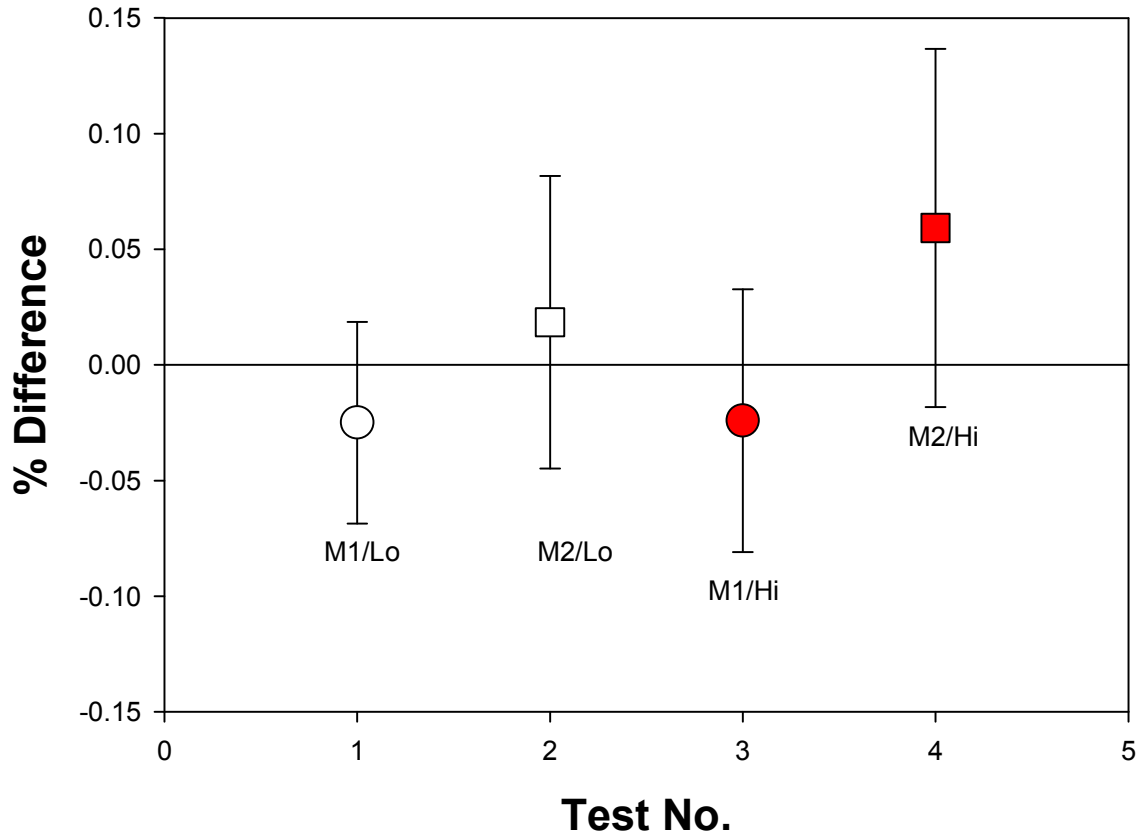
KRISS-to-SP



M1/Lo: Coriolis Meter @ Low flow rate, M2/Lo: Turbine Meter @ Low flow rate
M1/Hi: Coriolis Meter @ High flow rate, M2/Hi: Turbine Meter @ High flow rate

Figure 41. *En* values of KRISS/SP differences.

KRISS/PTB Differences Meters Upstream



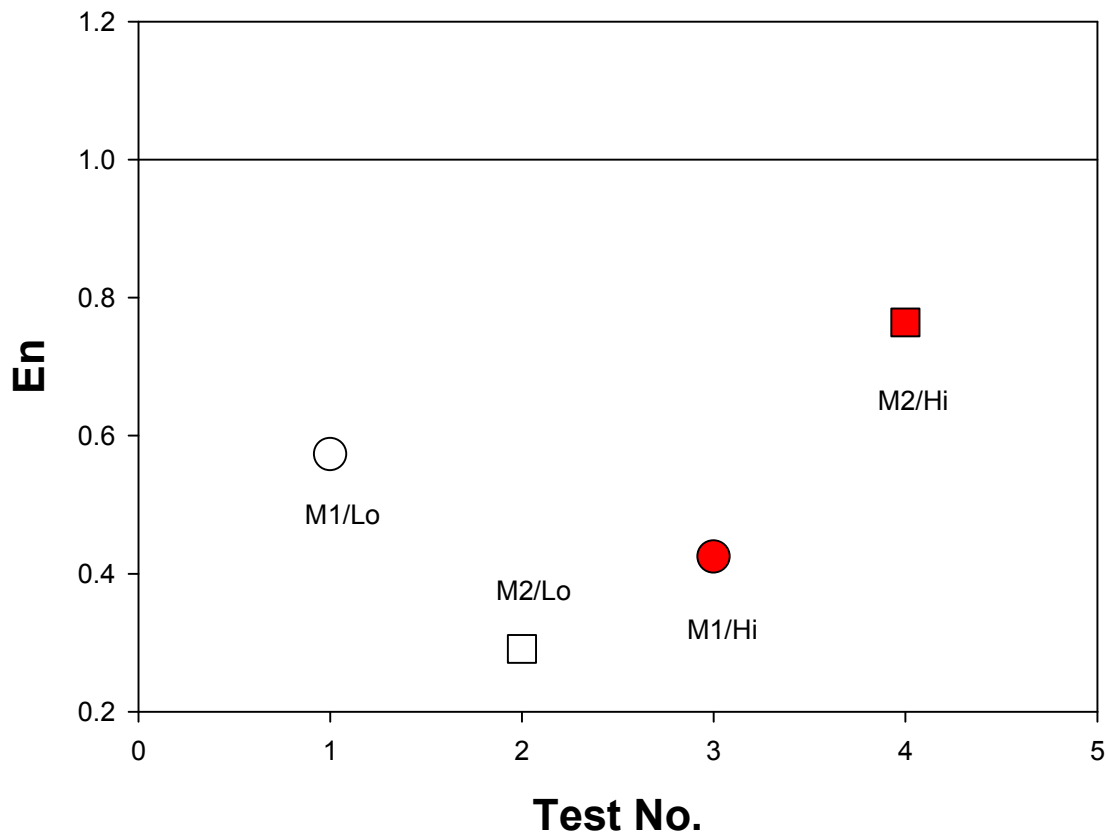
M1/Lo: Coriolis Meter @ Low flow rate, M2/Lo: Turbine Meter @ Low flow rate
 M1/Hi: Coriolis Meter @ High flow rate, M2/Hi: Turbine Meter @ High flow rate

Figure 42. Differences between KRISS and PTB.

Table 15. KRISS/PTB differences in %.

	d_{ij}	$U(d_{ij})$	En_i
cuphi ¹¹	-0.024	0.057	0.42
tuphi ¹²	0.059	0.077	0.76
cuplo ¹³	-0.025	0.044	0.57
tuplo ¹⁴	0.018	0.063	0.29
En_{total}			0.48

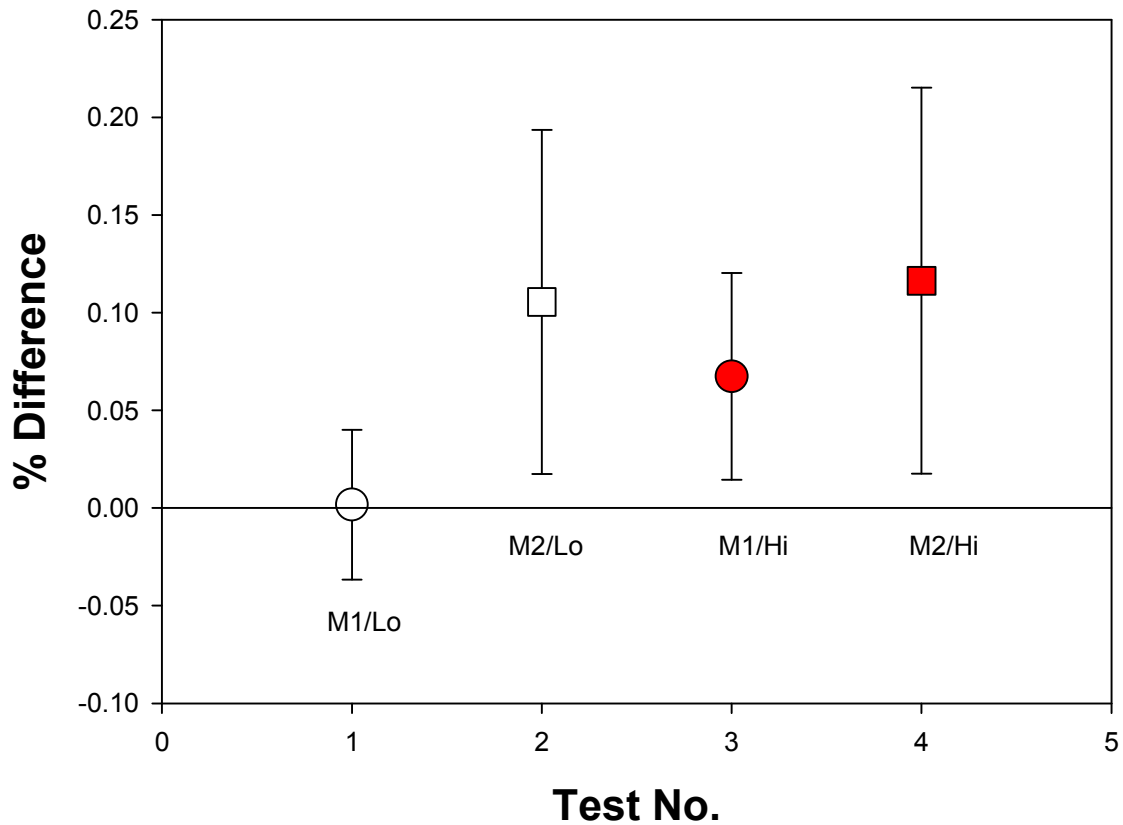
KRISS-to-PTB



M1/Lo: Coriolis Meter @ Low flow rate, M2/Lo: Turbine Meter @ Low flow rate
M1/Hi: Coriolis Meter @ High flow rate, M2/Hi: Turbine Meter @ High flow rate

Figure 43. En values of KRISS/PTB differences.

KRISS/CENAM Differences Meters Upstream



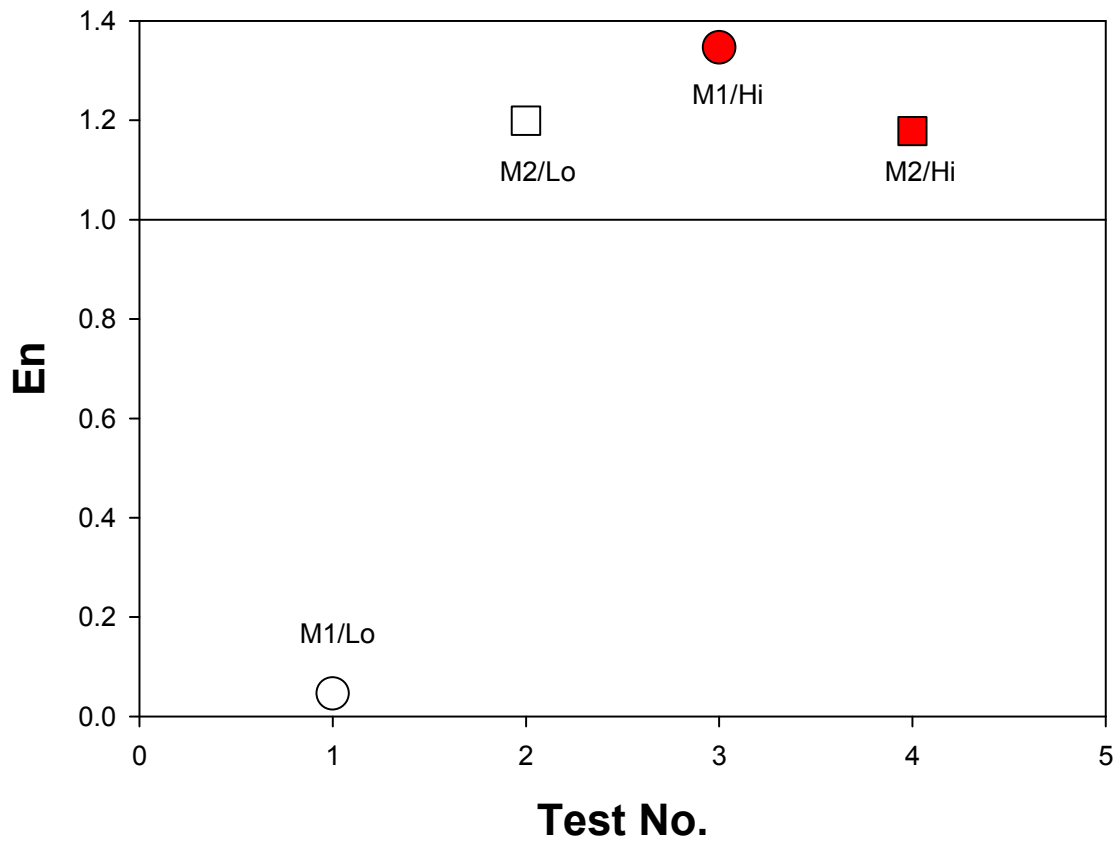
M1/Lo: Coriolis Meter @ Low flow rate, M2/Lo: Turbine Meter @ Low flow rate
 M1/Hi: Coriolis Meter @ High flow rate, M2/Hi: Turbine Meter @ High flow rate

Figure 44. Differences between KRISS and CENAM.

Table 16. KRISS/CENAM differences in %.

	d_{ij}	$U(d_{ij})$	En_i
cuphi ¹¹	0.067	0.053	1.27
tuphi ¹²	0.116	0.099	1.18
cuplo ¹³	0.002	0.038	0.04
tuplo ¹⁴	0.106	0.088	1.20
En_{total}			0.53

KRISS-to-CENAM

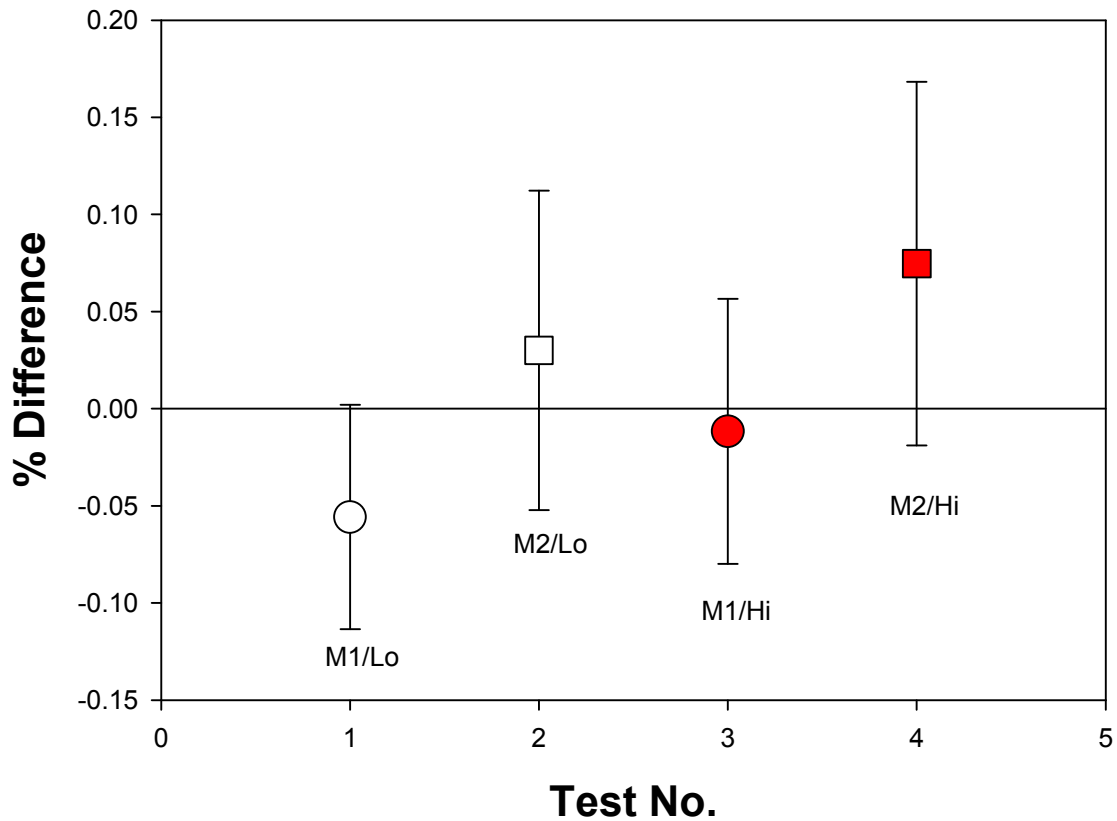


M1/Lo: Coriolis Meter @ Low flow rate, M2/Lo: Turbine Meter @ Low flow rate
M1/Hi: Coriolis Meter @ High flow rate, M2/Hi: Turbine Meter @ High flow rate

Figure 45. *En* values of KRISS/CENAM differences.

KRISS/NMIJ Differences

Meters Upstream



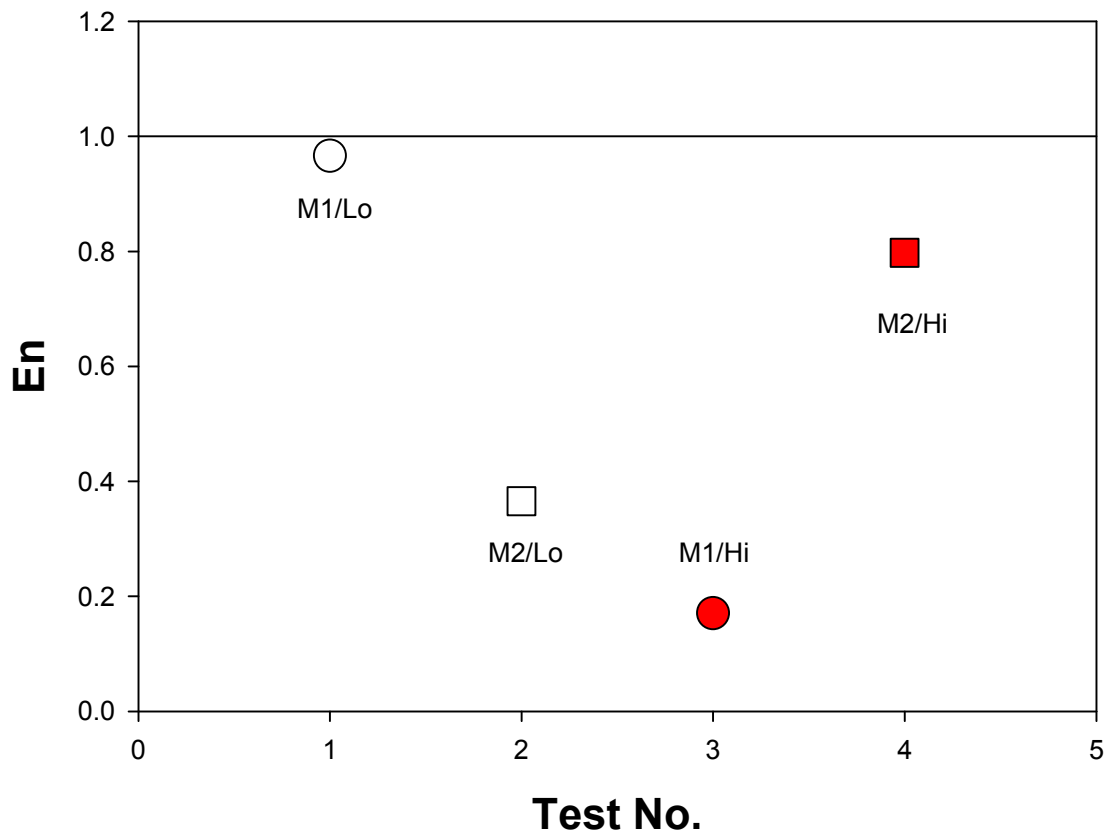
M1/Lo: Coriolis Meter @ Low flow rate, M2/Lo: Turbine Meter @ Low flow rate
M1/Hi: Coriolis Meter @ High flow rate, M2/Hi: Turbine Meter @ High flow rate

Figure 46. Differences between KRISS and NMIJ.

Table 17. KRISS/NMIJ differences in %.

	d_{ij}	$U(d_{ij})$	En_i
cuphi ¹¹	-0.012	0.068	0.17
tuphi ¹²	0.075	0.094	0.80
cuplo ¹³	-0.056	0.058	0.97
tuplo ¹⁴	0.030	0.082	0.37
En_{total}			0.47

KRISS-to-NMIJ

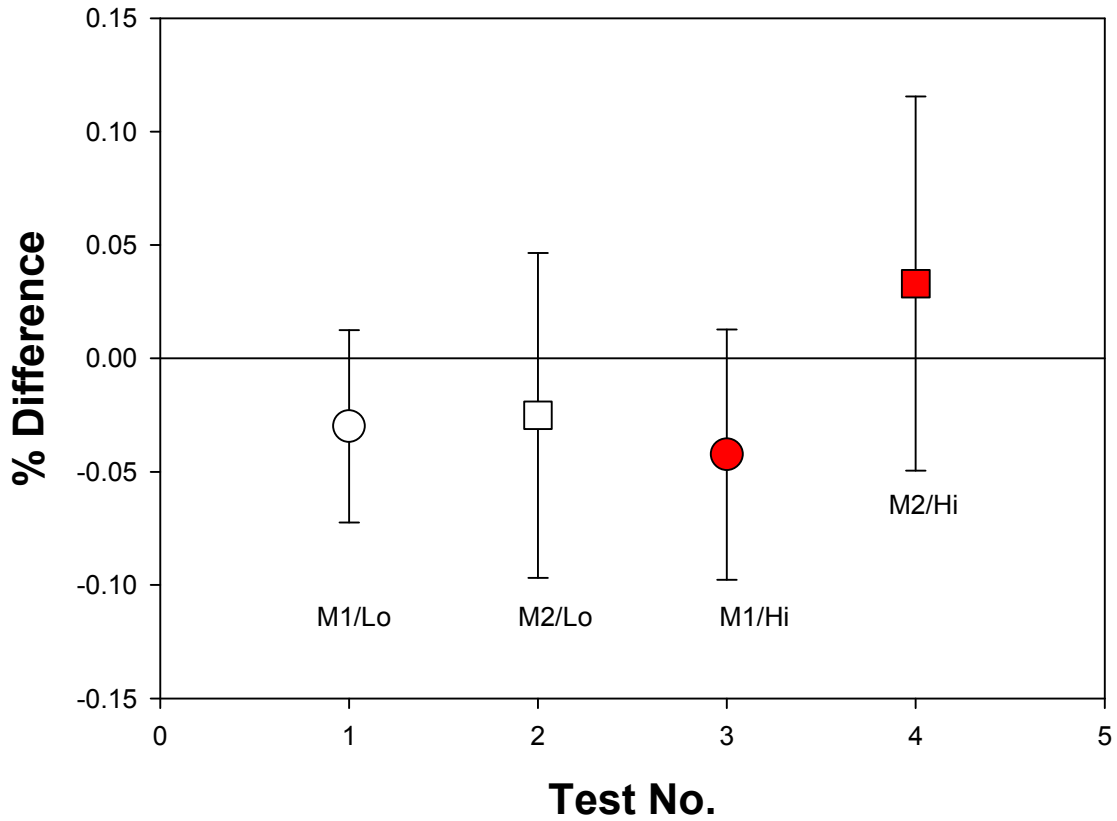


M1/Lo: Coriolis Meter @ Low flow rate, M2/Lo: Turbine Meter @ Low flow rate
M1/Hi: Coriolis Meter @ High flow rate, M2/Hi: Turbine Meter @ High flow rate

Figure 47. *En* values of KRISS/NMIJ differences.

KRISS/NEL Differences

Meters Upstream



M1/Lo: Coriolis Meter @ Low flow rate, M2/Lo: Turbine Meter @ Low flow rate
 M1/Hi: Coriolis Meter @ High flow rate, M2/Hi: Turbine Meter @ High flow rate

Figure 48. Differences between KRISS and NEL.

Table 18. KRISS/NEL differences in %.

	d_{ij}	$U(d_{ij})$	En_i
cuphi ¹¹	-0.042	0.055	0.77
tuphi ¹²	0.033	0.083	0.40
cuplo ¹³	-0.030	0.042	0.71
tuplo ¹⁴	-0.025	0.072	0.35
En_{total}			0.53

KRISS-to-NEL

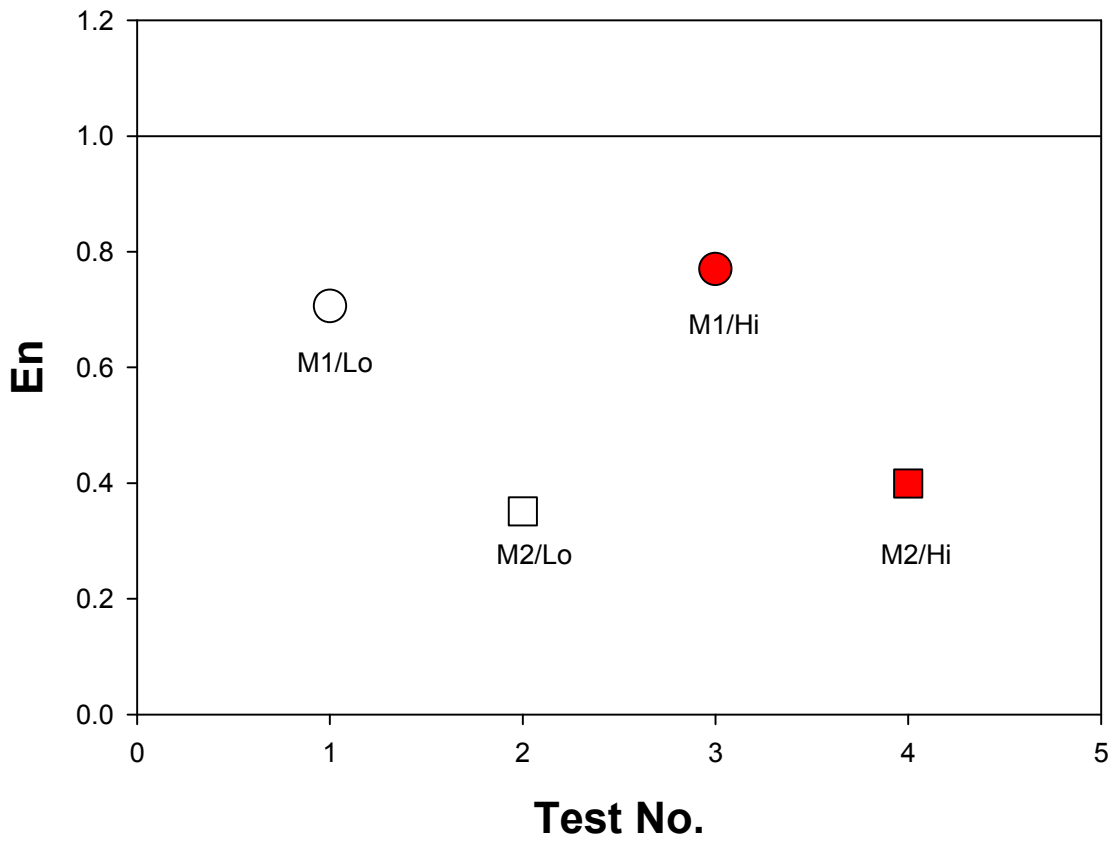
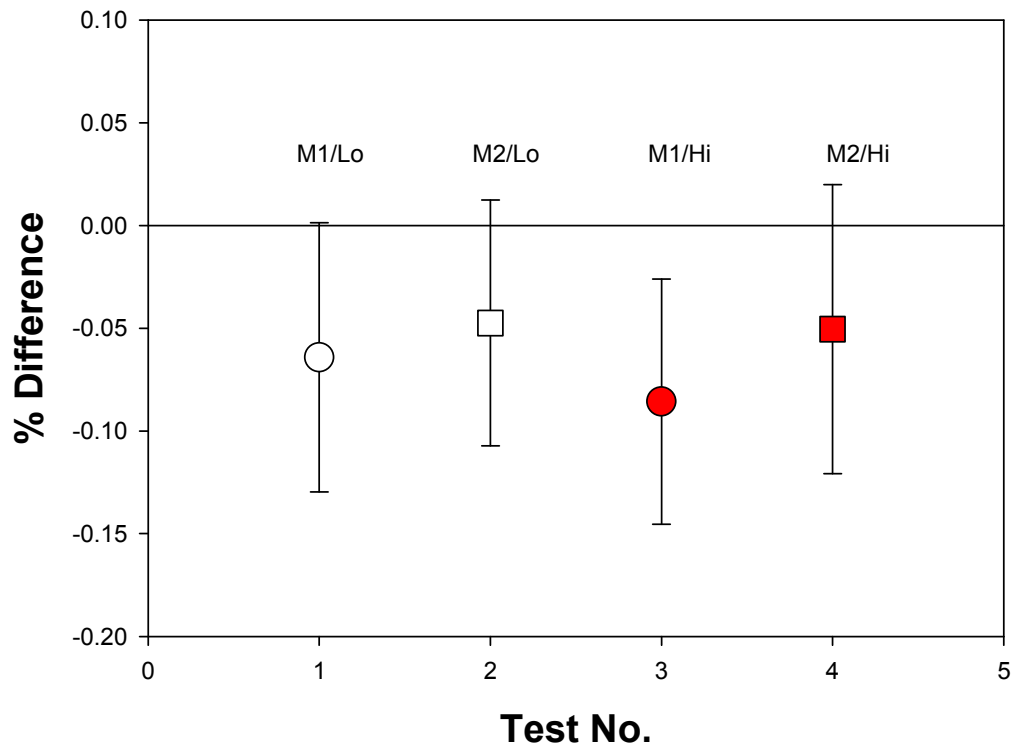


Figure 49. *En* values of KRISS/NEL differences.

SP/PTB Differences

Meters Upstream



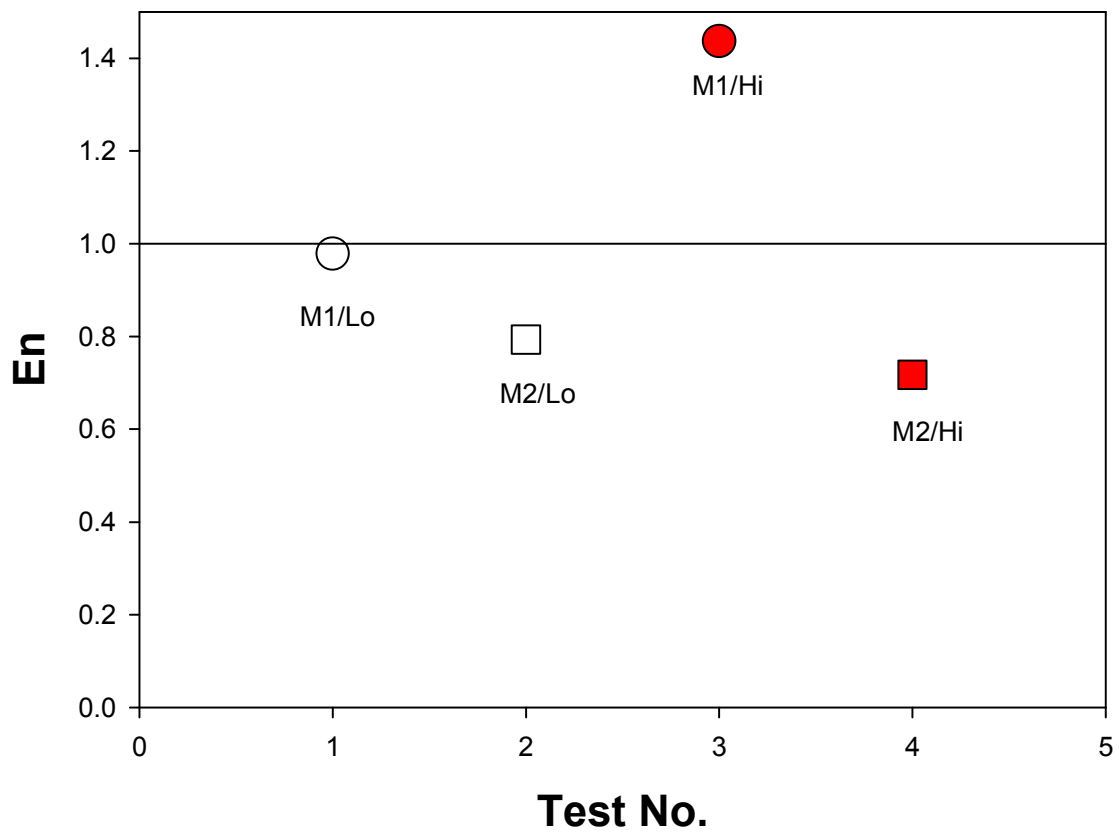
M1/Lo: Coriolis Meter @ Low flow rate, M2/Lo: Turbine Meter @ Low flow rate
 M1/Hi: Coriolis Meter @ High flow rate, M2/Hi: Turbine Meter @ High flow rate

Figure 50. Differences between SP and PTB.

Table 19. SP/PTB differences in %.

	d_{ij}	$U(d_{ij})$	En_i
cuphi ¹¹	-0.086	0.060	1.44
tuphi ¹²	-0.050	0.070	0.72
cuplo ¹³	-0.064	0.066	0.98
tuplo ¹⁴	-0.047	0.060	0.79
En_{total}			0.95

SP-to-PTB

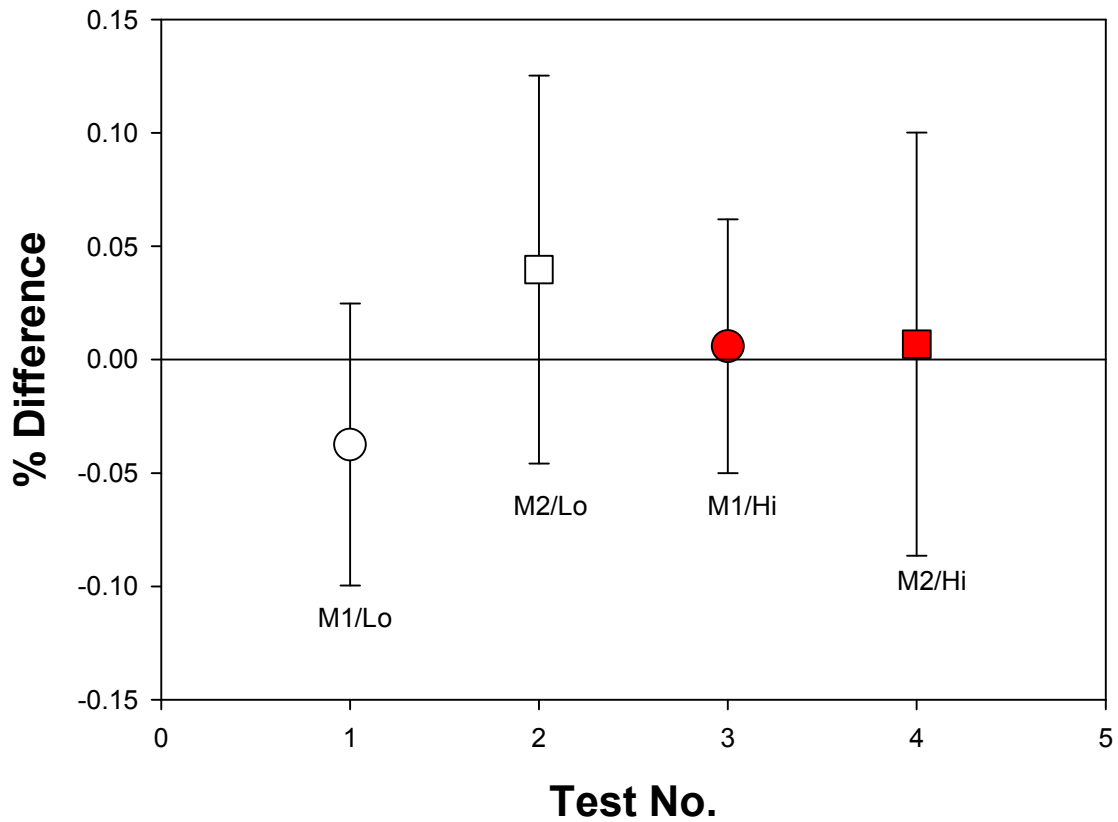


M1/Lo: Coriolis Meter @ Low flow rate, M2/Lo: Turbine Meter @ Low flow rate
M1/Hi: Coriolis Meter @ High flow rate, M2/Hi: Turbine Meter @ High flow rate

Figure 51. *En* values of SP/PTB differences.

SP/CENAM Differences

Meters Upstream



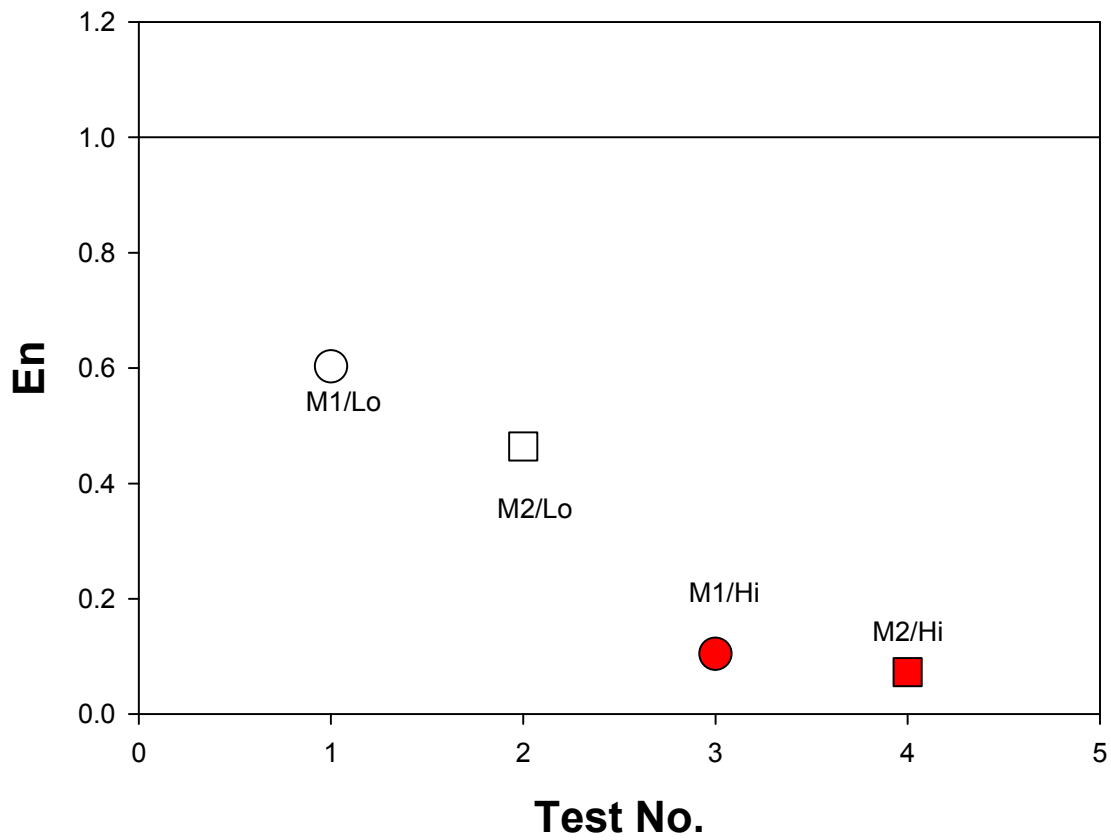
M1/Lo: Coriolis Meter @ Low flow rate, M2/Lo: Turbine Meter @ Low flow rate
 M1/Hi: Coriolis Meter @ High flow rate, M2/Hi: Turbine Meter @ High flow rate

Figure 52. Differences between SP and CENAM.

Table 20. SP/CENAM differences in %.

	d_{ij}	$U(d_{ij})$	En_i
cuphi ¹¹	0.006	0.056	0.10
tuphi ¹²	0.007	0.093	0.07
cuplo ¹³	-0.037	0.062	0.60
tuplo ¹⁴	0.040	0.086	0.46
En_{total}			0.21

SP-to-CENAM

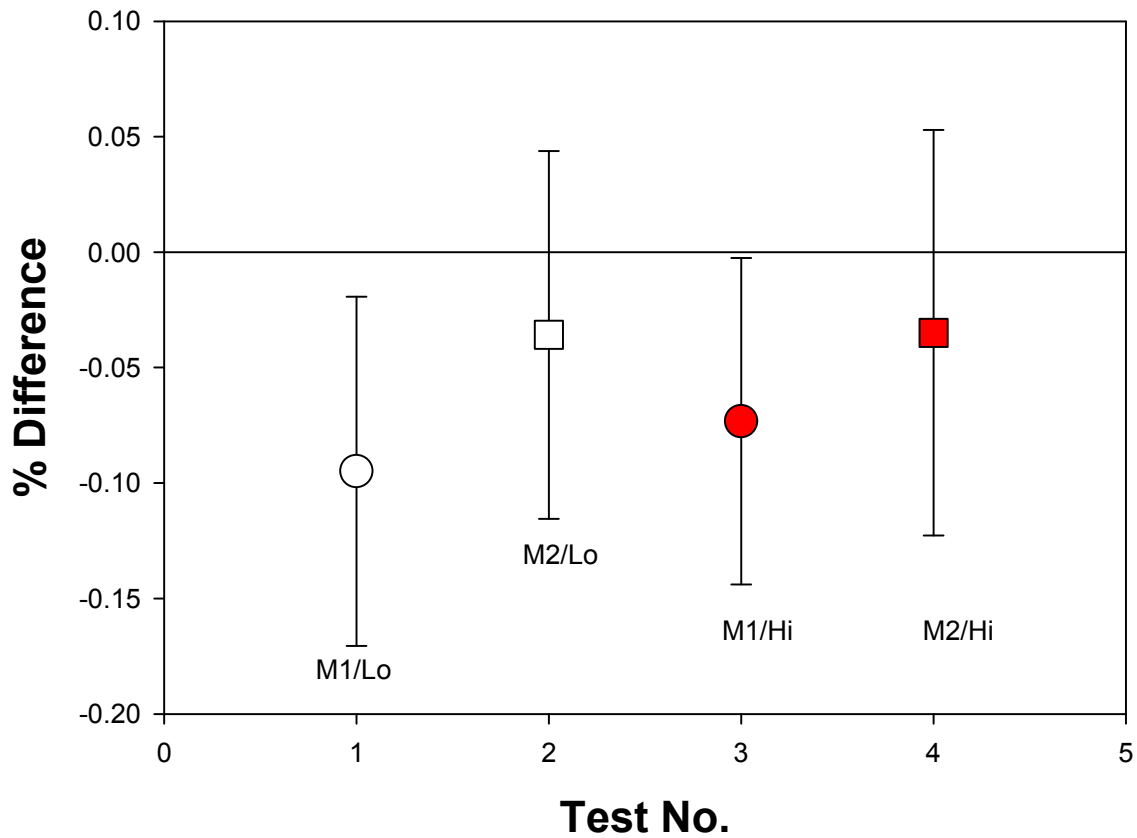


M1/Lo: Coriolis Meter @ Low flow rate, M2/Lo: Turbine Meter @ Low flow rate
M1/Hi: Coriolis Meter @ High flow rate, M2/Hi: Turbine Meter @ High flow rate

Figure 53. *En* values of SP/CENAM differences.

SP/NMIJ Differences

Meters Upstream



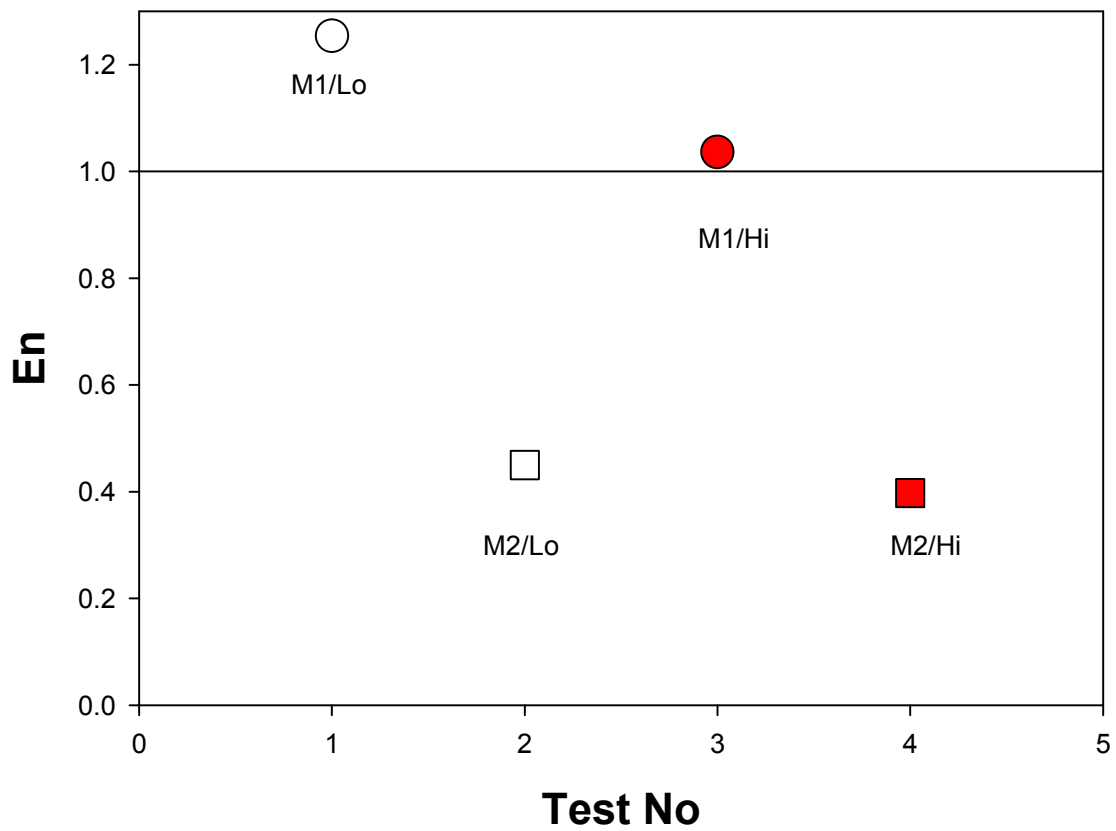
M1/Lo: Coriolis Meter @ Low flow rate, M2/Lo: Turbine Meter @ Low flow rate
M1/Hi: Coriolis Meter @ High flow rate, M2/Hi: Turbine Meter @ High flow rate

Figure 54. Differences between SP and NMIJ.

Table 21. SP/NMIJ differences in %.

	d_{ij}	$U(d_{ij})$	En_i
cuphi ¹¹	-0.073	0.071	1.04
tuphi ¹²	-0.035	0.088	0.40
cuplo ¹³	-0.095	0.076	1.25
tuplo ¹⁴	-0.036	0.080	0.45
En_{total}			0.69

SP-to-NMIJ

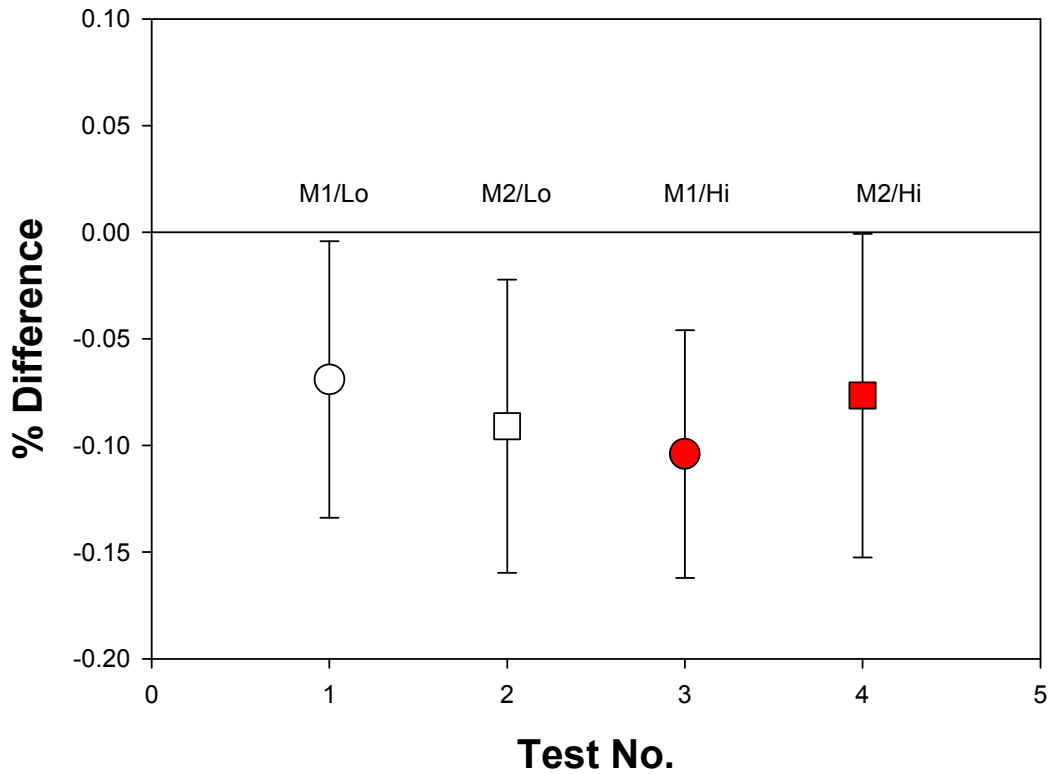


M1/Lo: Coriolis Meter @ Low flow rate, M2/Lo: Turbine Meter @ Low flow rate
M1/Hi: Coriolis Meter @ High flow rate, M2/Hi: Turbine Meter @ High flow rate

Figure 55. *En* values of SP/NMIJ differences.

SP/NEL Differences

Meters Upstream



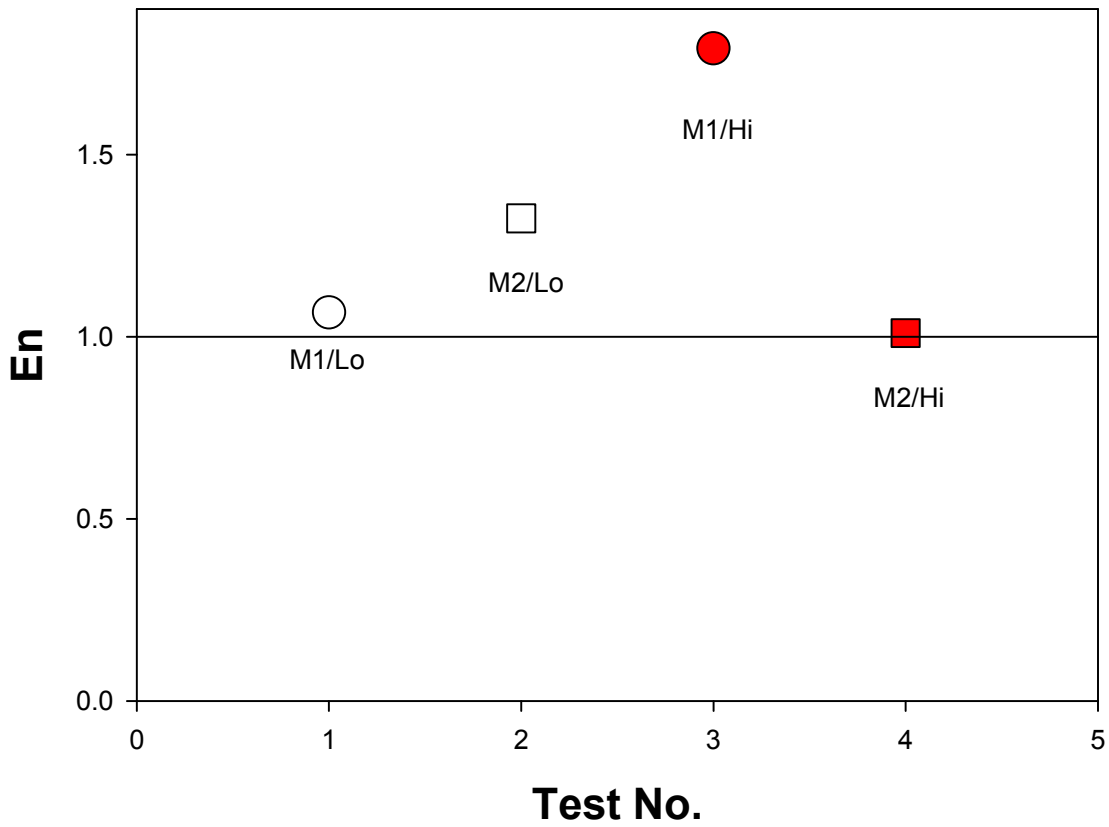
M1/Lo: Coriolis Meter @ Low flow rate, M2/Lo: Turbine Meter @ Low flow rate
 M1/Hi: Coriolis Meter @ High flow rate, M2/Hi: Turbine Meter @ High flow rate

Figure 56. Differences between SP and NEL.

Table 22. SP/NEL differences in %.

	d_{ij}	$U(d_{ij})$	En_i
cuphi ¹¹	-0.104	0.058	1.79
tuphi ¹²	-0.077	0.076	1.01
cuplo ¹³	-0.069	0.065	1.07
tuplo ¹⁴	-0.091	0.069	1.33
En_{total}			1.26

SP-to-NEL

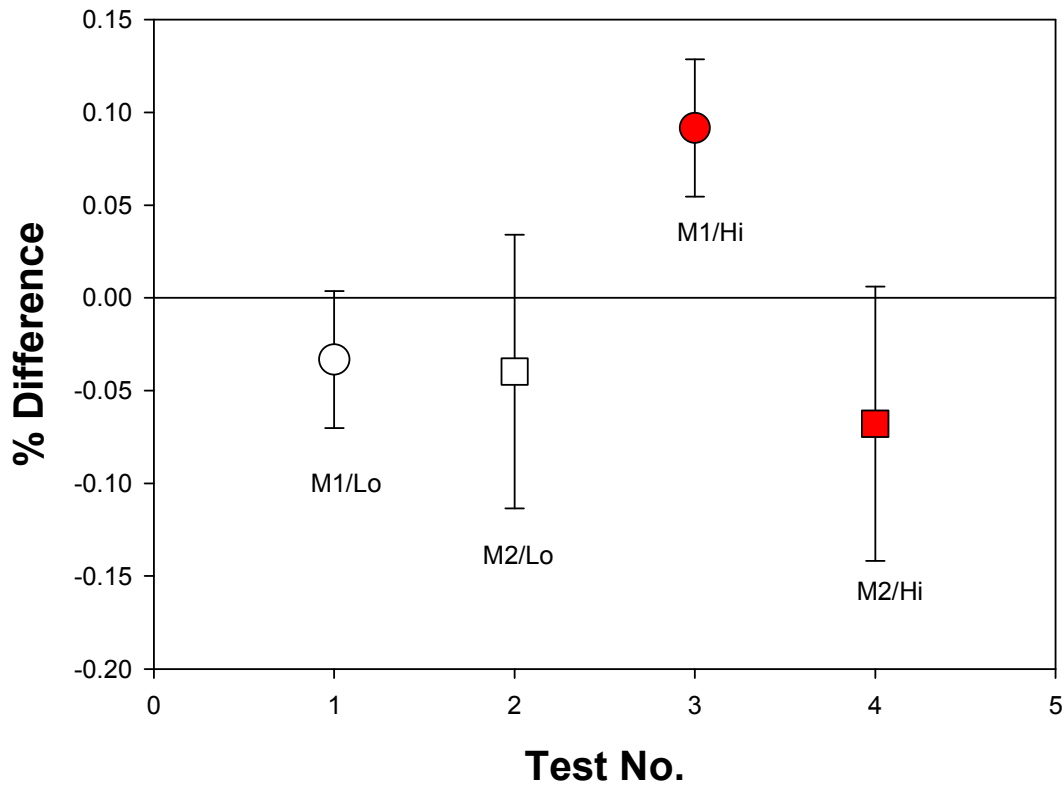


M1/Lo: Coriolis Meter @ Low flow rate, M2/Lo: Turbine Meter @ Low flow rate
M1/Hi: Coriolis Meter @ High flow rate, M2/Hi: Turbine Meter @ High flow rate

Figure 57. *En* values of SP/NEL differences.

PTB/CENAM Differences

Meters Upstream



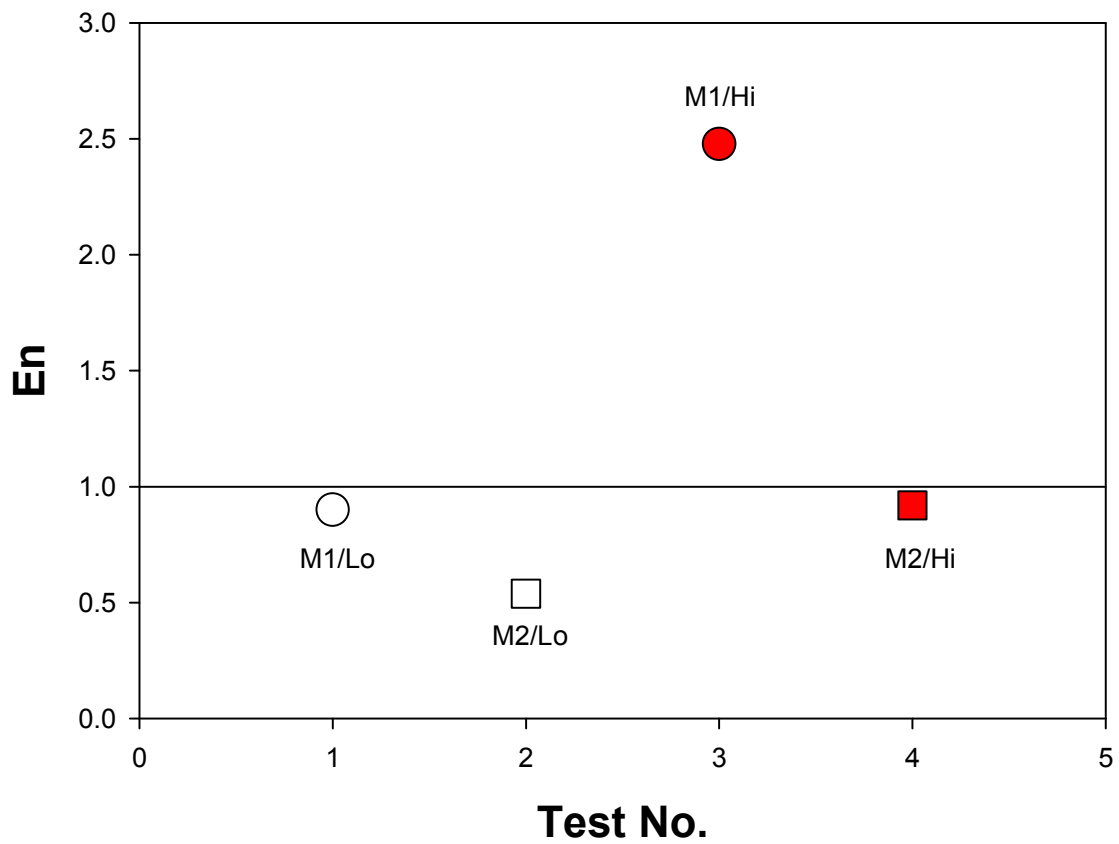
M1/Lo: Coriolis Meter @ Low flow rate, M2/Lo: Turbine Meter @ Low flow rate
M1/Hi: Coriolis Meter @ High flow rate, M2/Hi: Turbine Meter @ High flow rate

Figure 58. Differences between PTB and CENAM.

Table 23. PTB/CENAM differences in %.

	d_{ij}	$U(d_{ij})$	En_i
cuphi ¹¹	0.092	0.037	2.48
tuphi ¹²	-0.068	0.074	0.92
cuplo ¹³	-0.033	0.037	0.90
tuplo ¹⁴	-0.040	0.074	0.54
En_{total}			1.03

PTB-to-CENAM

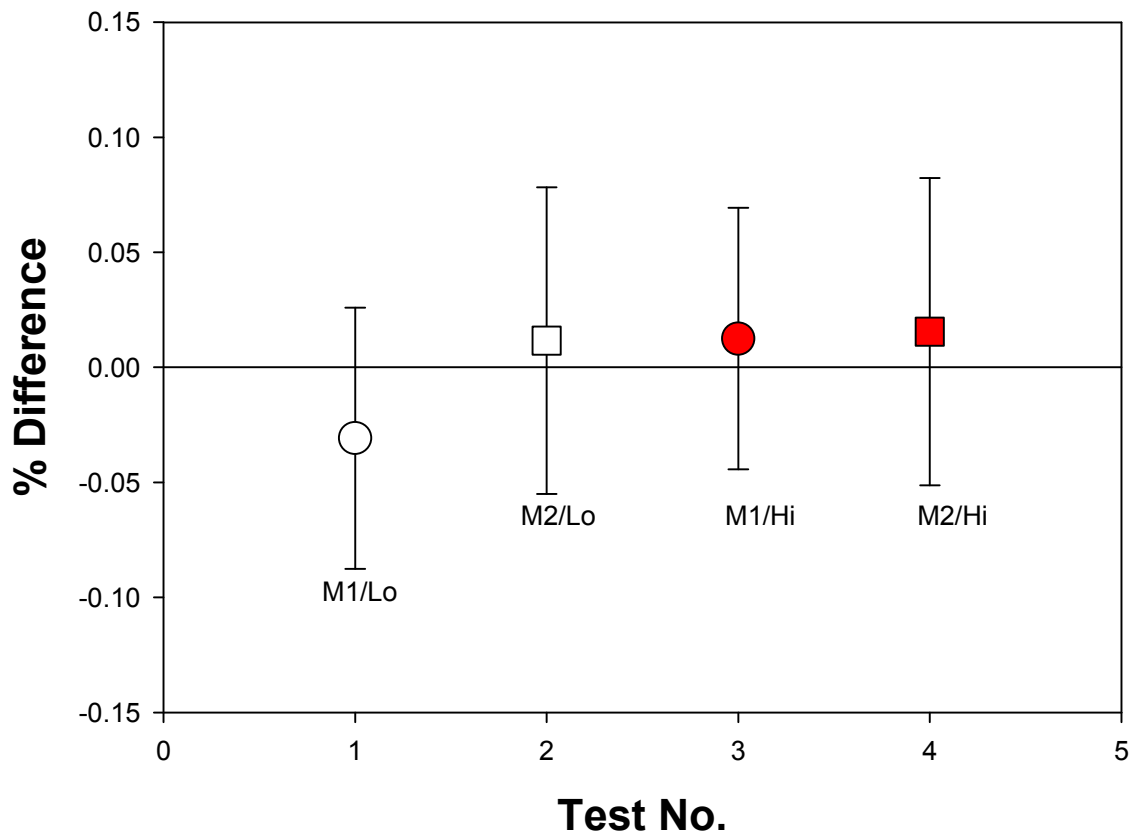


M1/Lo: Coriolis Meter @ Low flow rate, M2/Lo: Turbine Meter @ Low flow rate
M1/Hi: Coriolis Meter @ High flow rate, M2/Hi: Turbine Meter @ High flow rate

Figure 59. *En* values of PTB/CENAM differences.

PTB/NMIJ Differences

Meters Upstream



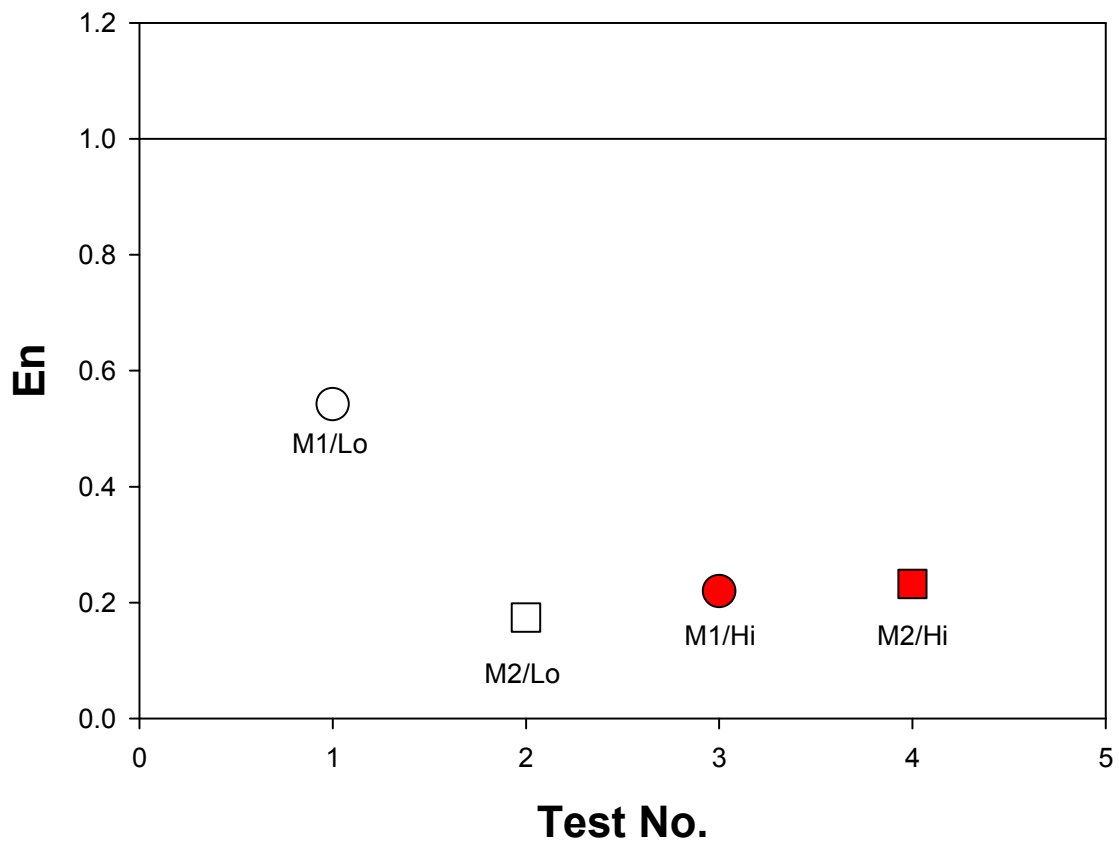
M1/Lo: Coriolis Meter @ Low flow rate, M2/Lo: Turbine Meter @ Low flow rate
 M1/Hi: Coriolis Meter @ High flow rate, M2/Hi: Turbine Meter @ High flow rate

Figure 60. Differences between PTB and NMIJ.

Table 24. PTB/NMIJ differences in %.

	d_{ij}	$U(d_{ij})$	En_i
cuphi ¹¹	0.012	0.057	0.22
tuphi ¹²	0.016	0.067	0.23
cuplo ¹³	-0.031	0.057	0.54
tuplo ¹⁴	0.012	0.067	0.17
En_{total}			0.26

PTB-to-NMIJ

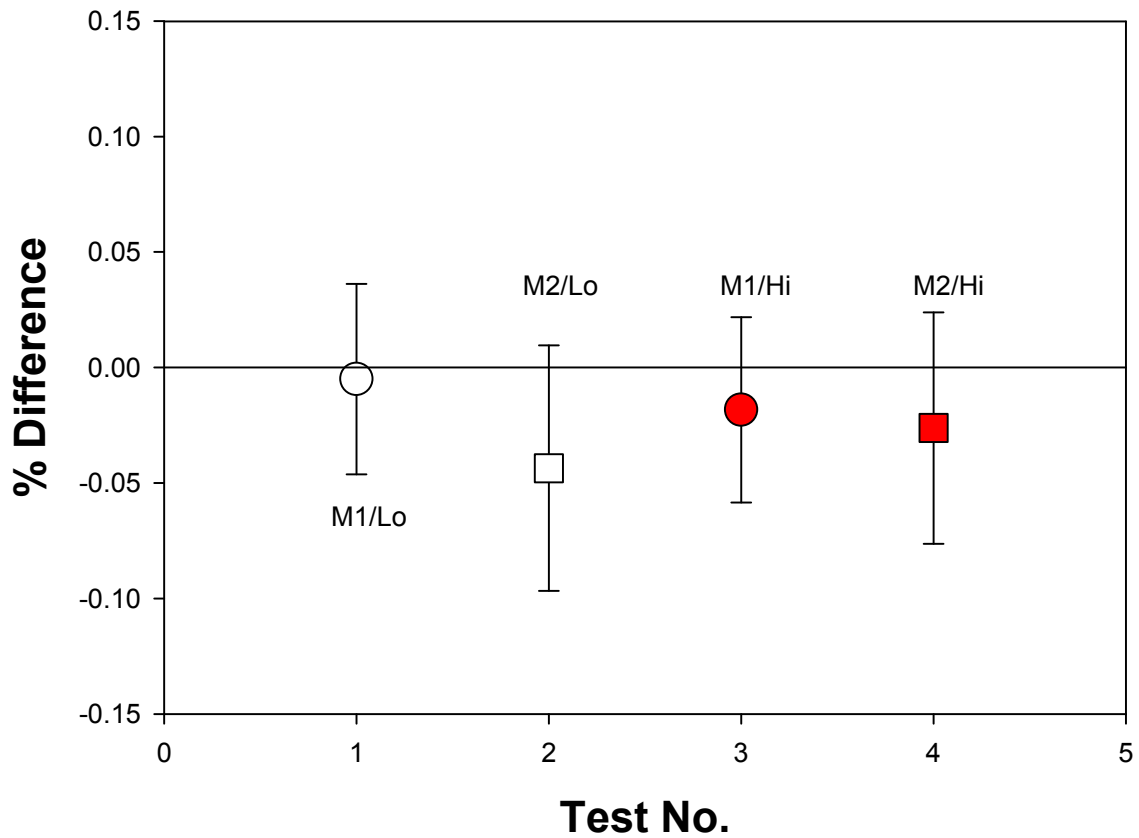


M1/Lo: Coriolis Meter @ Low flow rate, M2/Lo: Turbine Meter @ Low flow rate
M1/Hi: Coriolis Meter @ High flow rate, M2/Hi: Turbine Meter @ High flow rate

Figure 61. *En* values of PTB/NMIJ differences.

PTB/NEL Differences

Meters Upstream



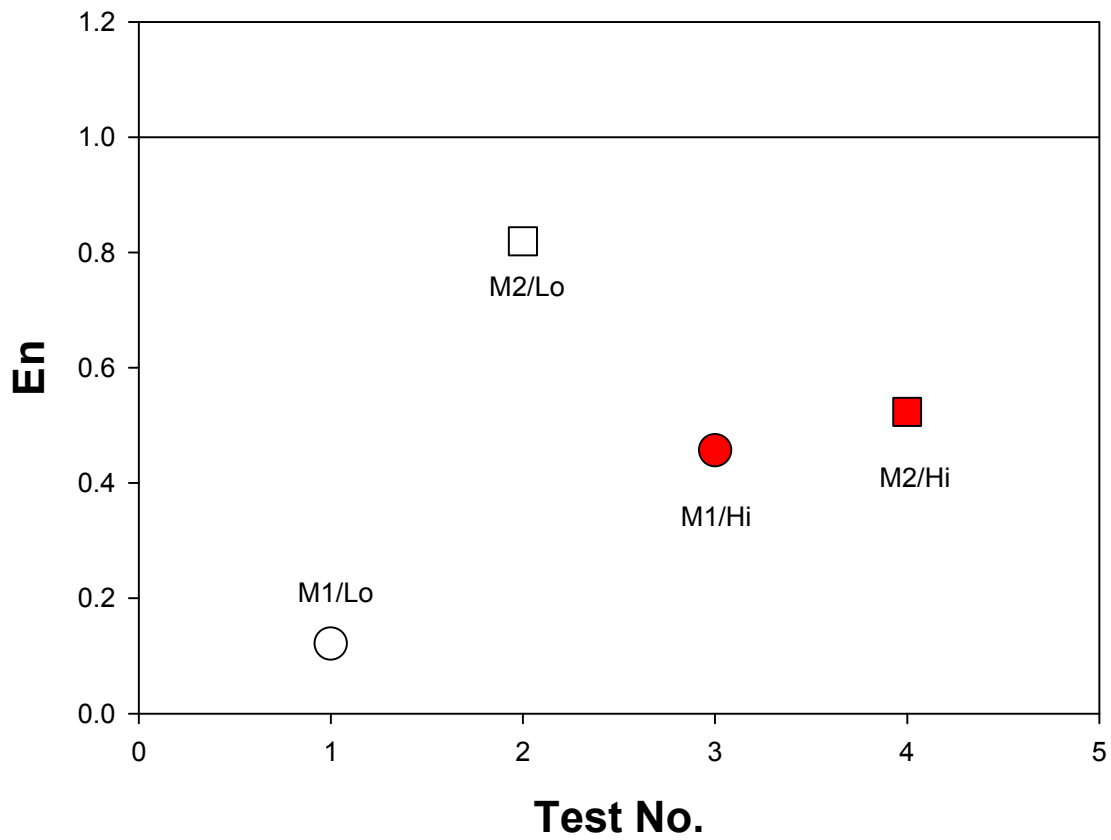
M1/Lo: Coriolis Meter @ Low flow rate, M2/Lo: Turbine Meter @ Low flow rate
 M1/Hi: Coriolis Meter @ High flow rate, M2/Hi: Turbine Meter @ High flow rate

Figure 62. Differences between PTB and NEL.

Table 25. PTB/NEL differences in %.

	d_{ij}	$U(d_{ij})$	En_i
cuphi ¹¹	-0.018	0.040	0.46
tuphi ¹²	-0.026	0.050	0.52
cuplo ¹³	-0.005	0.041	0.12
tuplo ¹⁴	-0.044	0.053	0.82
En_{total}			0.39

PTB-to-NEL

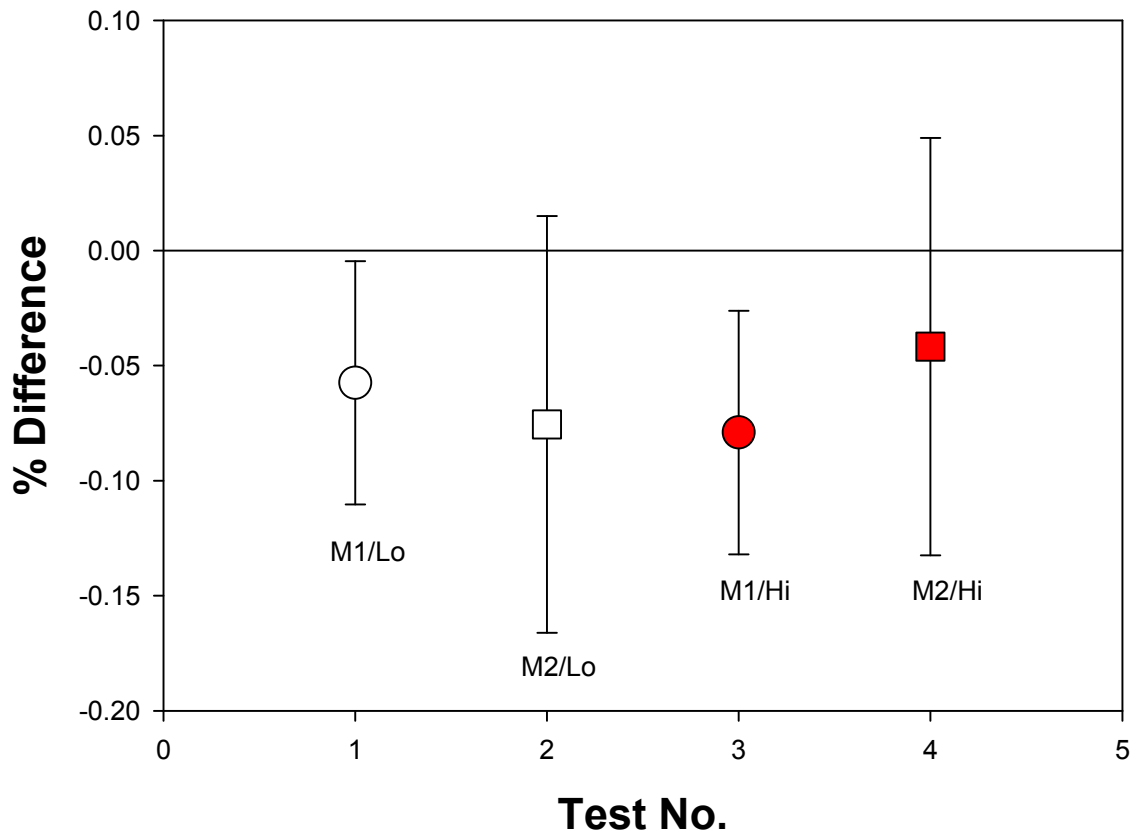


M1/Lo: Coriolis Meter @ Low flow rate, M2/Lo: Turbine Meter @ Low flow rate
M1/Hi: Coriolis Meter @ High flow rate, M2/Hi: Turbine Meter @ High flow rate

Figure 63. *En* values of PTB/NEL differences.

CENAM/NMIJ Differences

Meters Upstream



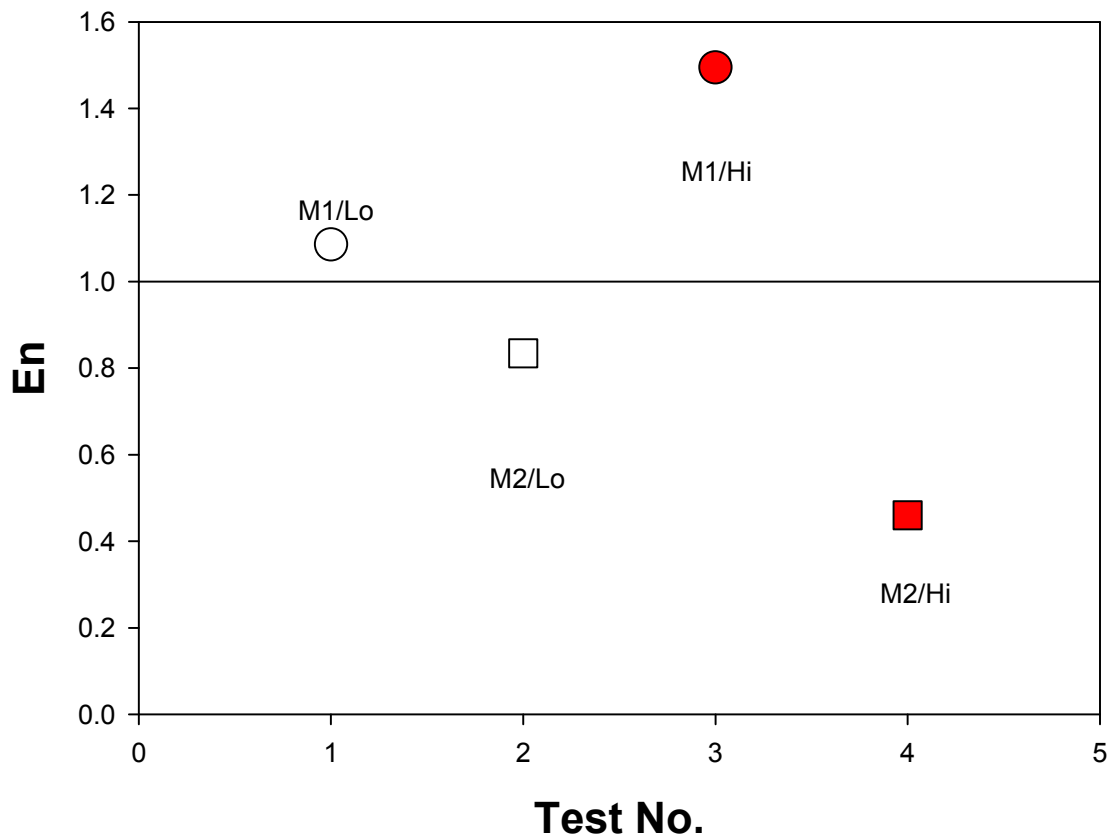
M1/Lo: Coriolis Meter @ Low flow rate, M2/Lo: Turbine Meter @ Low flow rate
M1/Hi: Coriolis Meter @ High flow rate, M2/Hi: Turbine Meter @ High flow rate

Figure 64. Differences between CENAM and NMIJ.

Table 26. CENAM/NMIJ differences in %.

	d_{ij}	$U(d_{ij})$	En_i
cuphi ¹¹	-0.079	0.053	1.49
tuphi ¹²	-0.042	0.091	0.46
cuplo ¹³	-0.057	0.053	1.09
tuplo ¹⁴	-0.076	0.091	0.83
En_{total}			0.89

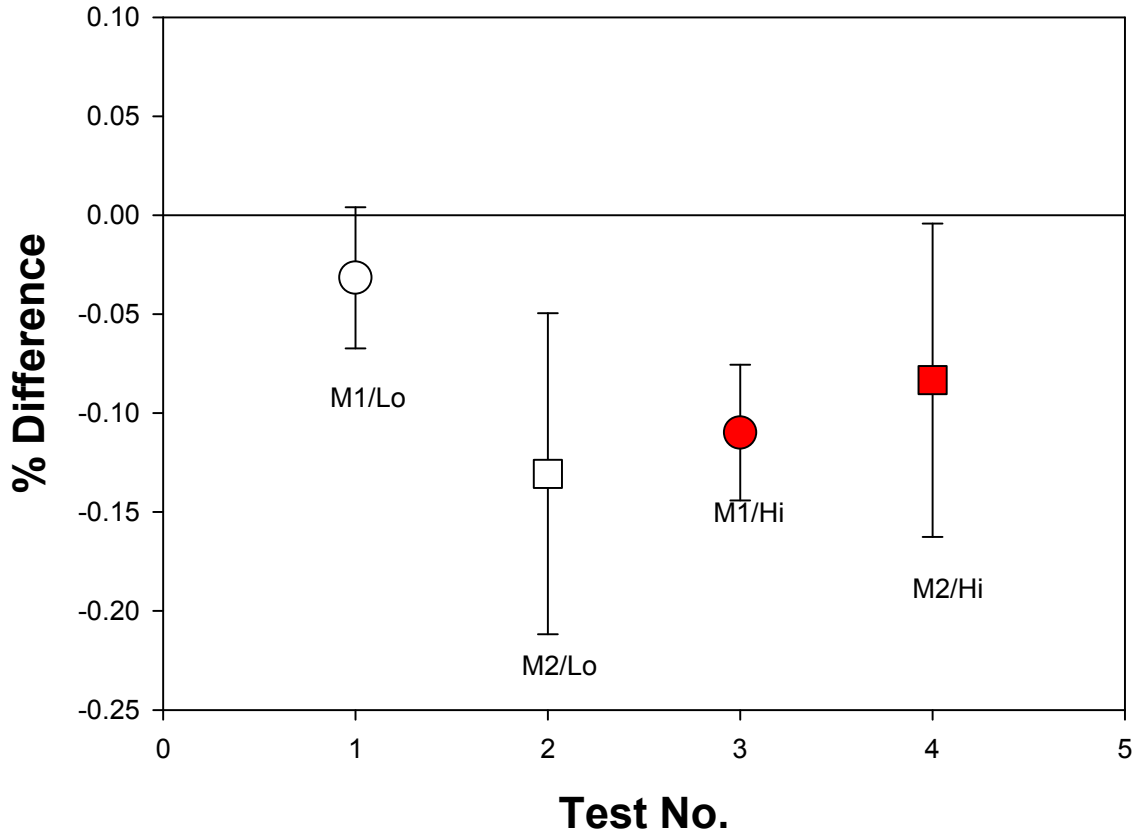
CENAM-to-NMIJ



M1/Lo: Coriolis Meter @ Low flow rate, M2/Lo: Turbine Meter @ Low flow rate
M1/Hi: Coriolis Meter @ High flow rate, M2/Hi: Turbine Meter @ High flow rate

Figure 65. *En* values of CENAM/NMIJ differences.

CENAM/NEL Differences Meters Upstream



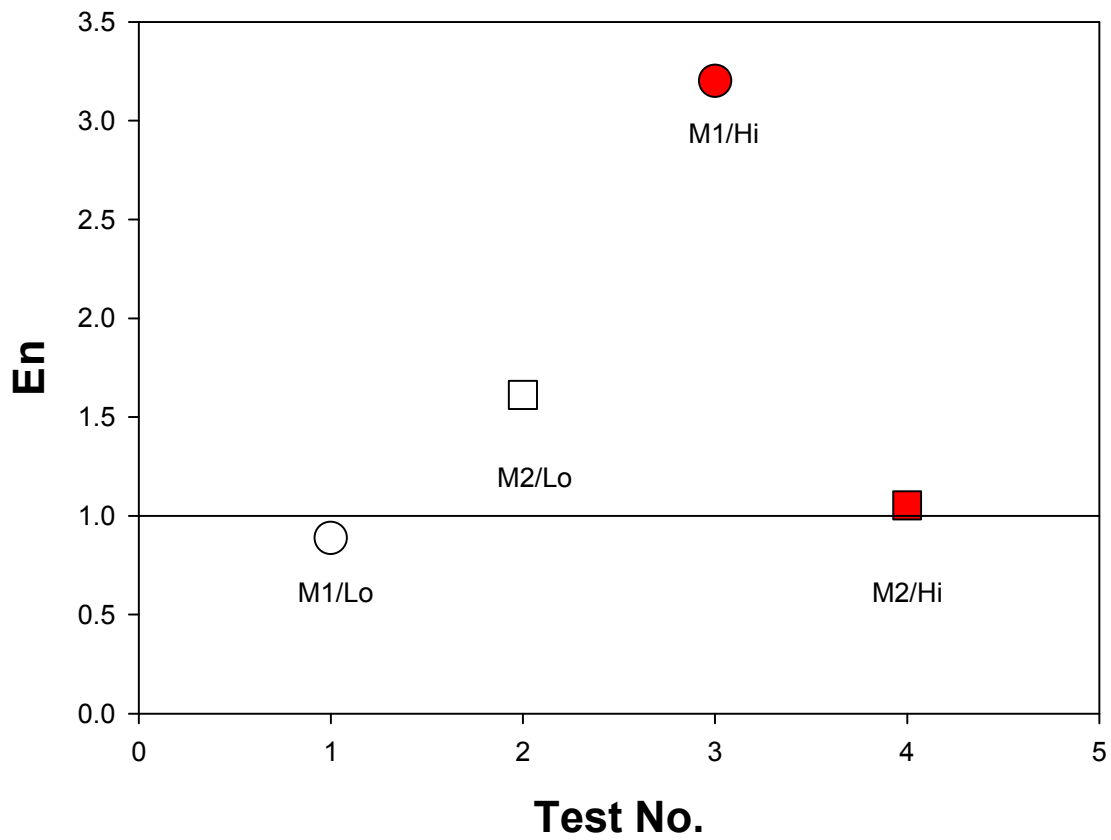
M1/Lo: Coriolis Meter @ Low flow rate, M2/Lo: Turbine Meter @ Low flow rate
 M1/Hi: Coriolis Meter @ High flow rate, M2/Hi: Turbine Meter @ High flow rate

Figure 66. Differences between CENAM and NEL.

Table 27. CENAM/NEL differences in %.

	d_{ij}	$U(d_{ij})$	En_i
cuphi ¹¹	-0.110	0.034	3.20
tuphi ¹²	-0.083	0.079	1.05
cuplo ¹³	-0.032	0.036	0.89
tuplo ¹⁴	-0.131	0.081	1.61
En_{total}			1.48

CENAM-to-NEL

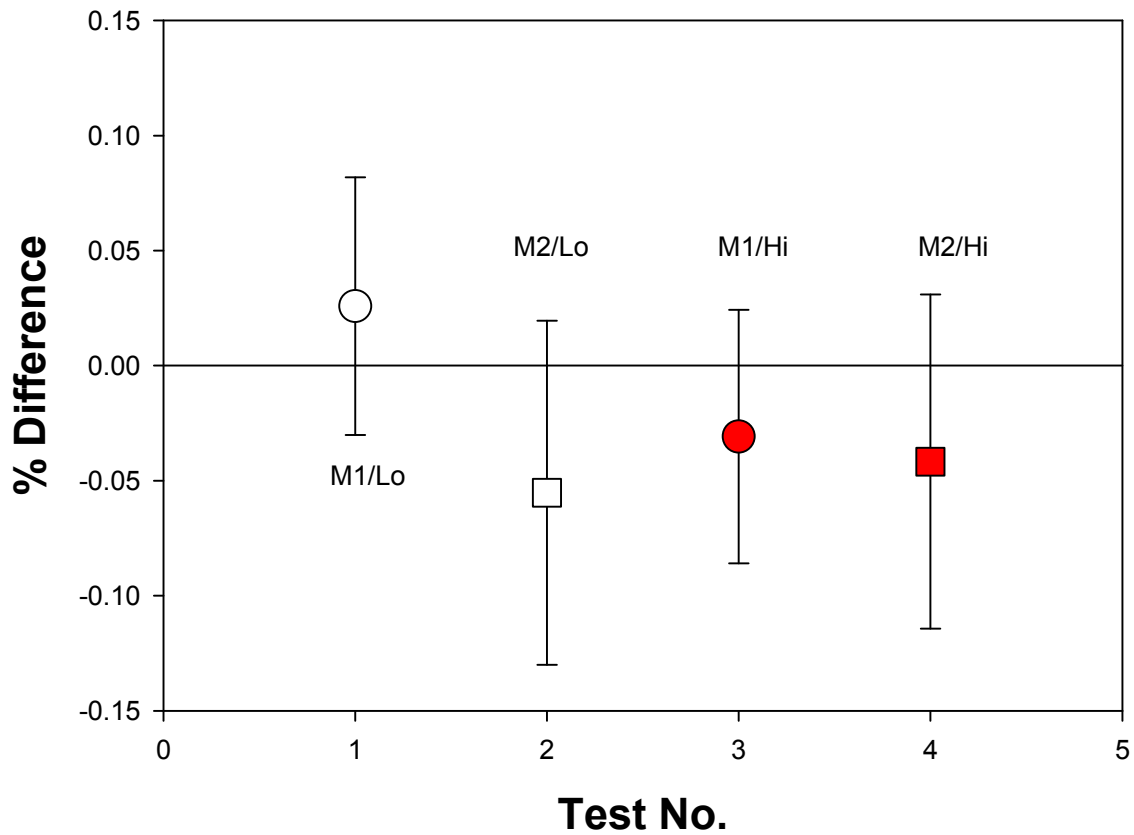


M1/Lo: Coriolis Meter @ Low flow rate, M2/Lo: Turbine Meter @ Low flow rate
M1/Hi: Coriolis Meter @ High flow rate, M2/Hi: Turbine Meter @ High flow rate

Figure 67. *En* values of CENAM/NEL differences.

NMIJ/NEL Differences

Meters Upstream



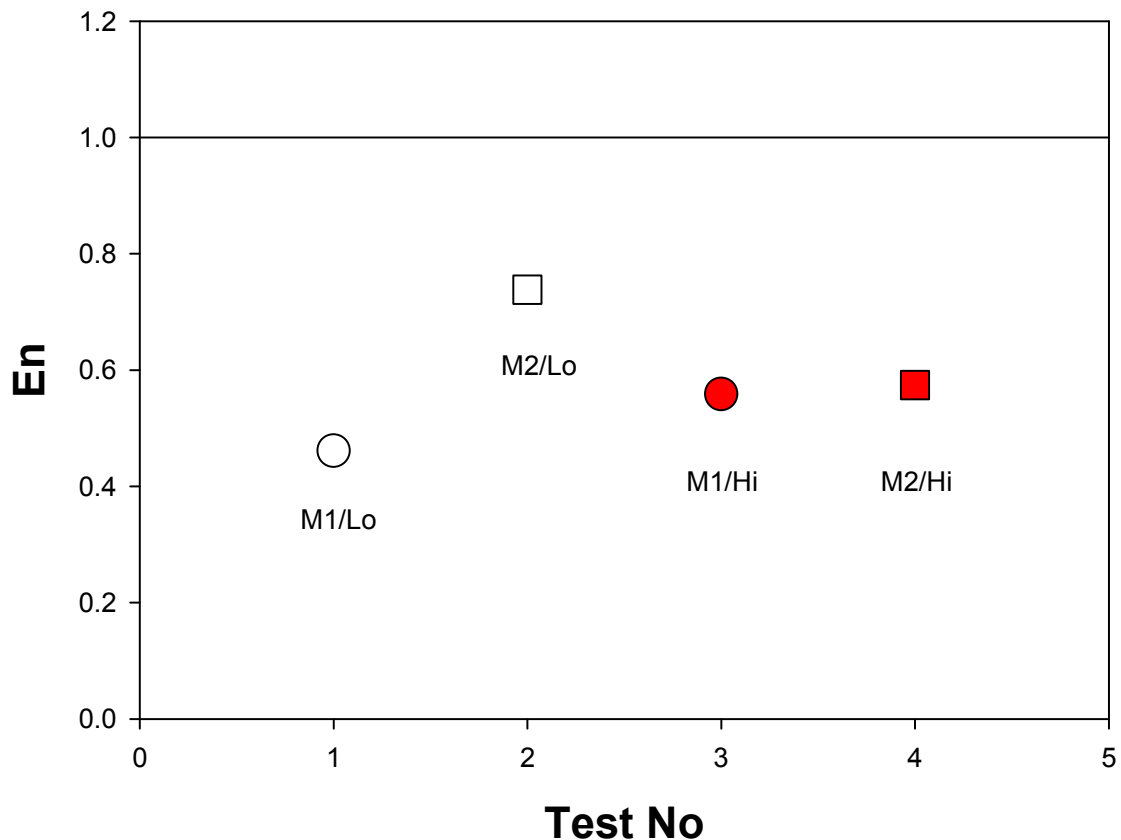
M1/Lo: Coriolis Meter @ Low flow rate, M2/Lo: Turbine Meter @ Low flow rate
M1/Hi: Coriolis Meter @ High flow rate, M2/Hi: Turbine Meter @ High flow rate

Figure 68. Differences between NMIJ and NEL.

Table 28. NMIJ/NEL differences in %.

	d_{ij}	$U(d_{ij})$	En_i
cuphi ¹¹	-0.031	0.055	0.56
tuphi ¹²	-0.042	0.073	0.57
cuplo ¹³	0.026	0.056	0.46
tuplo ¹⁴	-0.055	0.075	0.74
En_{total}			0.57

NMIJ-to-NEL



M1/Lo: Coriolis Meter @ Low flow rate, M2/Lo: Turbine Meter @ Low flow rate
 M1/Hi: Coriolis Meter @ High flow rate, M2/Hi: Turbine Meter @ High flow rate

Figure 69. En values of NMIJ/NEL differences.

9 Summary and Conclusions

A water flow key comparison, known as CCM.FF-K1, was performed successfully. From each participating NMI, test results from a Coriolis meter and a turbine meter at 4 different flow conditions were reported with corresponding uncertainty budgets. Uncertainties of the key comparison results were estimated based on the uncertainty budgets reported by the participating NMIs. KCRVs and medians from key comparison results for the Coriolis meter and turbine meter at four different flow conditions were estimated using Monte Carlo simulation; the final check test results at the Pilot Lab were excluded in these calculations.

In order to describe the degree of equivalence between key comparison results from each NMI, a En_{total} – describing the overall degree of equivalence between the NMIs

and KCRV – was estimated by using the geometric mean of En_i values for two flow meters at high and low Cardinal test points. En_{total} values are listed in Table 29 and are less than 1.0 for KRISS, SP, PTB, NMIJ, and NEL, while the results of CENAM yielded a value of 1.01. Nonetheless, the results from this key comparison from all participating NMIs support their CMC claimed uncertainties, which in all cases are larger than those reported in this key comparison.

Table 29. Overall degree of equivalence for the participating NMIs

Participating NMI	Entotal
KRISS	0.32
SP	0.84
PTB	0.35
CENAM	1.01
NMIJ	0.25
NEL	0.84

10 Acknowledgements

The authors thank K.A. Park and Y. R. Yoon from KRISS; D. Dopheide from PTB; and R. Paton from NEL who have contributed to this comparison either by analyzing and discussing the results as well as a critical reading of the manuscript, or by characterizing the transfer standard and carrying out flow measurement. We also thank M. Anklin from Endress+Hauser Flowtec Ag for donating three Coriolis meters for the key comparison. This document was edited by P.I. Espina from the BIPM.

11 References

- 1 Guidelines for CIPM key comparisons, 1999 with modification by CIPM, in October 2003.
- 2 M. Cox, “A discussion of approaches for determining a reference value in the analysis of key-comparison data”, in *Advanced Mathematical and Computational Tools in Metrology IV*, Edited by P. Ciarini, A.B. Forbes, F. Pavese, and D. Richter, pp45-65, 2000, World Scientific Publishing Com.
- 3 M. G. Cox, “The evaluation of key comparison data”, *Metrologia* 39, pp 589-595, 2002.